Supporting Information

Multidimensional optical encoding via light-promoted stereochemical editing

Mary C. Yenca,[1†] Antoine C. Gravet,[1] Taeseung Hwang,[2†] Jake L. Nicholson,[1†] Samuel J. Kempel, [1] Ting-Wei Hsu, [1] Amanda Foster,[1] Kaiwen Hsiao,[2]* Quentin Michaudel[1,2]*

[1] Department of Chemistry, Texas A&M University, College Station, Texas 77843, United States.

[2] Department of Materials Science and Engineering, Texas A&M University, College Station, Texas, 77843, United States.

†These authors contributed equally to this work.

Experimental Procedures

General Reagent Information S5

General Analytical Information S5

Monomer Synthesis S6

Monomer Precursors S6

Boronic Acid/Ester Preparation S7

Suzuki–Miyaura Cross-Coupling General Procedure S10

Monomers **M1**–**M6** S10

Monomers **M7** and **M8** S14

Polymer Synthesis S15

Stereoretentive ROMP of Arylated PCDs General Procedure S15

Table S1. Monomer concentration optimization for stereoretentive ROMP S15

Table S2. Stereoretentive ROMP of **M1**–**M6** S15

Synthesis of **P1**–**P6** S16

Synthesis of **P7** S18

Copolymer Synthesis S18

Synthesis of *cis*-**P1**-*b*-*cis*-**P7** S19

Figure S1. SEC traces showing chain extension S20

Figure S2. *cis*-**P1**, *cis*-**P7**, and *cis*-**P1**-*b*-*cis*-**P7** ^{1}H NMR spectra S20

Synthesis of *cis*-**P1**-*r*-*cis*-**P7** S21

Figure S3. SEC trace S22

Figure S4. *cis*-**P1**, *cis*-**P7**, and *cis*-**P1**-*r*-*cis*-**P7** ^{1}H NMR spectra S22

Synthesis of *cis*-**P1**-*b*-*cis*-**P8**-*b*-*cis*-**P7** S23

Figure S5. SEC traces showing chain extension S24

Figure S6. *cis*-**P1**, *cis*-**P7**, and *cis*-**P1**-*b*-*cis*-**P7** ^{1}H NMR spectra S25
Figure S7. Vacuum removal of solvent set-up S25
Solution-State Photoisomerization S26
Photoisomerization General Procedure S26
UV and Visible Light Photoisomerizations of all-*cis* **P1** S26
Figure S8. ^{1}H NMR spectra using UV light S27
Figure S9. ^{1}H NMR spectra using blue light S28
Figure S10. ^{1}H NMR spectra using green light S30
Figure S11. Overlayed *cis* content and kinetics plots S31
UV and Visible Light Photoisomerizations of all-*cis* **P7** S32
Figure S12. ^{1}H NMR spectra using UV light S32
Figure S13. ^{1}H NMR spectra using blue light S33
Figure S14. ^{1}H NMR spectra using green light S34
Figure S15. Overlayed *cis* content and kinetics plots S35
UV and Visible Light Photoisomerizations of Copolymers S36
Figure S16. Diblock copolymer ^{1}H NMR spectra using UV light S36
Figure S17. Diblock copolymer ^{1}H NMR spectra using green light S37
Figure S18. Diblock copolymer block-resolved *cis* content and kinetics plots S38
Figure S19. Random copolymer ^{1}H NMR spectra using UV light S39
Figure S20. Random copolymer ^{1}H NMR spectra using green light S40
Figure S21. Random copolymer block-resolved *cis* content and kinetics plots S41
Figure S22. Triblock copolymer ^{1}H NMR spectra using green light S42
Figure S23. Triblock copolymer ^{1}H NMR spectra using UV light S44
Figure S24. Block-resolved *cis* content plots for sequential green/UV irradiation S45
Figure S25. Stereoblock copolymer overlayed ^{1}H NMR spectra S46
Photophysical Characterization S47
UV–Visible Absorption Spectra S47
Figure S26. Absorption profiles of all-*cis* and all-*trans* **P1** S47
Figure S27. Absorption profiles of all-*cis* and all-*trans* **P2** S47
Figure S28. Absorption profiles of all-*cis* and all-*trans* **P3** S48
Figure S29. Absorption profiles of all-*cis* and all-*trans* **P4** S48
Figure S30. Absorption profiles of all-*cis* and all-*trans* **P5** S49
Figure S31. Absorption profiles of all-*cis* and all-*trans* **P6** S49
Figure S32. Absorption profiles of all-*cis* and all-*trans* **P7** S50

Figure S33. Absorption profiles of all-*trans* **P1**–**P6** S50
Figure S34. Absorption profiles of *cis*-**P7**-*b*-*cis*-**P1** and *trans*-**P7**-*b*-*trans*-**P1** S51
Figure S35. Absorption profiles of *cis*-**P7**-*r*-*cis*-**P1** and *trans*-**P7**-*r*-*trans*-**P1** S51
Figure S36. Absorption profiles of all-*cis* **P7**/**P1** homo- and copolymers S52
Figure S37. Absorption profiles of all-*trans* **P7**/**P1** homo- and copolymers S52
Figure S38. Absorption profiles of stereoblock copolymers S53
Figure S39. Absorption profiles of stereoblock copolymers and all-*cis* **P7**/**P1** S53
Figure S40. Absorption profiles of stereoblock copolymers and all-*trans* **P7**/**P1** S54
Fluorescence Emission Spectra S55
Figure S41. Emission profiles of all-*cis* and all-*trans* **P1** S55
Figure S42. Emission profiles of all-*cis* and all-*trans* **P2** S55
Figure S43. Emission profiles of all-*cis* and all-*trans* **P3** S56
Figure S44. Emission profiles of all-*cis* and all-*trans* **P4** S56
Figure S45. Emission profiles of all-*cis* and all-*trans* **P5** S57
Figure S46. Emission profiles of all-*cis* and all-*trans* **P6** S57
Figure S47. Emission profiles of all-*cis* and all-*trans* **P7** S58
Figure S48. Emission profiles of all-*cis* **P1**–**P6** S58
Figure S49. Emission profiles of all-*trans* **P1**–**P6** S59
Figure S50. Emission profiles of *cis*-**P7**-*b*-*cis*-**P1** and *trans*-**P7**-*b*-*trans*-**P1** S59
Figure S51. Emission profiles of *cis*-**P7**-*r*-*cis*-**P1** and *trans*-**P7**-*r*-*trans*-**P1** S60
Figure S52. Emission profiles of stereoblock copolymers S60
Figure S53. Emission profiles of stereoblock copolymers and all-*cis* **P7**/**P1** S61
Figure S54. Emission profiles of stereoblock copolymers and all-*trans* **P7**/**P1** S61
Visual Appearance of Polymer Solutions under Irradiation S62
Figure S55. Photographs of all-*cis* and all-*trans* **P1** solution fluorescence S62
Figure S56. Photographs of all-*cis* and all-*trans* **P7** solution fluorescence S62
Figure S57. Photograph of *cis*-**P7**-*b*-*cis*-**P8**-*b*-*cis*-**P1** solution fluorescence S62
Figure S58. Photograph of *cis*-**P7**-*b*-*cis*-**P8**-*b*-*trans*-**P1** solution fluorescence S63
Figure S59. Photograph of *trans*-**P7**-*b*-*cis*-**P8**-*b*-*trans*-**P1** solution fluorescence S63
Digital-Light Projection (DLP) Details S64
Thin Film Preparation Procedure S64
DLP on Thin Film Procedure S64
DLP Pattern Designs and Dimensions S65
Figure S60. Hexagon DLP pattern S65

Figure S61. Grayscale bars DLP pattern S65
Figure S62. Grayscale 3x3 grid DLP pattern..... S66
Figure S63. Grayscale bluebonnet DLP pattern S66
Figure S64. Inverse Texas DLP pattern S67
Figure S65. Widefield illumination DLP pattern..... S67
Figure S66. Photopatterning photo and schematic S68
Figure S67. Full DLP platform schematic S69
Figure S68. CIE 1931 chromaticity diagrams with extraction points S70
Supporting NMR Data S71
References..... S109

General Reagent Information: All reactions were carried out under an inert nitrogen atmosphere with dry solvents under anhydrous conditions unless otherwise stated. Dry dichloromethane (DCM), diethyl ether (Et_2O), tetrahydrofuran (THF), and toluene (PhMe) were obtained by passing the previously degassed solvents through activated alumina columns. Anhydrous and degassed 1,4-dioxane was purchased from Thermo Scientific Chemicals as acroseal bottle. Anhydrous THF was degassed via "freeze-pump-thaw" before being brought into a nitrogen-filled glove box. Synthesis of polymers using stereoselective ruthenium catalysts were carried out in a nitrogen-filled glove box (SG1800/750TS-F, VIGOR). Reagents were purchased at the highest commercial quality and used without further purification, unless otherwise stated. Catalyst **Ru-St** was generously donated by Umicore. Yields refer to chromatographically and spectroscopically (^{1}H NMR) homogeneous material, unless otherwise stated. Reactions were monitored by thin layer chromatography (TLC) carried out on 250 μm SiliCycle SiliaPlate™ silica plates (F254), using UV light as the visualizing agent. Flash silica gel chromatography was performed using SiliCycle SiliaFlash® Irregular Silica Gel (60 Å, particle size 40–63 μm). The polymer was isolated after precipitation using an Eppendorf 5804 centrifuge. Visible light photoisomerization was carried out using Kessil lamp models PR160L-456 nm (55W) and PR160L-525 nm (45W). Thin film spin coating was carried out using a spin coater(WS-400BZ-6NPP/LITE, Laurell).

General Analytical Information: All polymer samples were analyzed using a Tosoh EcoSec HLC 8320GPC system with a TSKgel SuperHM-M column and a TSKgel SuperH-RC column at a flow rate of 0.40 mL/min at 40 °C. THF stabilized with BHT was used as the eluent and the number-average molecular weight (M_n), weight-average molecular weight (M_w), and dispersity ($Đ$) for the polymer were calculated from an RI chromatogram against a TSKgel polystyrene standard. NMR spectra were recorded on Bruker Avance Neo 400 and Bruker Avance 500 instruments and were calibrated using residual undeuterated solvent as an internal reference ($CHCl_3$ @ 7.26 ppm ^{1}H NMR, 77.16 ppm ^{13}C NMR). The following abbreviations were used to explain NMR peak multiplicities: s = singlet, d = doublet, dd = doublet of doublets, t = triplet, q = quartet, quin. = quintet, hep. = heptet m = multiplet, br = broad. High-resolution mass spectra (HRMS) were recorded on an Agilent LC/MSD TOF mass spectrometer by Atmospheric pressure chemical ionization (APCI) or electrospray ionization (ESI). The absorption and emission measurements were carried out in dilute chloroform solutions. Absorption spectra were collected on a Shimadzu UV-2600 UV–visible spectrophotometer using 1.0 cm path length quartz cuvettes. Fluorescence measurements were collected on a Horiba FluoroMax 4 spectrofluorometer with entrance and exit slits set to 5.0 nm and an integration time of 0.1 s.

Monomer Synthesis:

Monomer Precursors

Compound **S1**

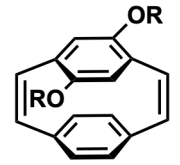

R = 2-ethylhexyl

S1

Monomer **S1** and its precursors were synthesized following a route previously reported by our group. [1]

Compound **S2**

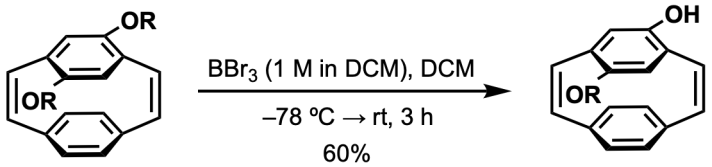

S1 **S2**

Compound **S2** was synthesized using a procedure adapted from literature. [2] To a flame-dried round bottom flask equipped with a stir bar and **S1** (0.535 g, 1.16 mmol, 1.0 equiv), anhydrous DCM (44 mL) was added and cooled to –78 °C. Following this, BBr_3 (1 M in DCM, 3.5 mL, 3.5 mmol, 3.0 equiv) was added dropwise and the solution was allowed to warm to room temperature and react for 3 h. The reaction mixture was then cooled to 0 °C before quenching with water (30 mL). The mixture was washed with water (3 x 30 mL), and the combined aqueous layers were then extracted using DCM (3 x 30 mL). The combined organic layers were dried using Na_2SO_4 before concentrating under reduced pressure. Purification via column chromatography (SiO_2, hexanes, 3:1 hexanes:DCM, 1:1 hexanes:DCM, then 1:2 hexanes:DCM) afforded the desired compound **S2** as a yellow semisolid (0.405 g, 60%).

^{1}H NMR (500 MHz, $CDCl_3$) δ 7.36–7.28 (m, 1 H), 7.12 (d, *J* = 10.1 Hz, 1 H), 7.02 (dt, *J* = 7.9, 1.2 Hz, 1 H), 6.89 (d, *J* = 10.2 Hz, 1 H), 6.83 (d, *J* = 9.9 Hz, 1 H), 6.80–6.75 (m, 1 H), 6.58 (dt, *J* = 7.9, 1.4 Hz, 1 H), 6.44 (dt, *J* = 7.9, 1.4 Hz, 1 H), 5.76 (s, 1 H), 5.69 (s, 1 H), 4.23 (s, 1 H), 3.75–3.56 (m, 2 H), 1.74–1.65 (m, 1 H), 1.59–1.23 (m, 9 H), 0.99–0.90 (m, 7 H) ppm.

^{13}C NMR (126 MHz, $CDCl_3$) δ 152.9, 148.0, 139.9, 138.8, 137.5, 135.6, 134.6, 132.4, 131.7, 131.4, 128.5, 128.5, 128.2, 126.3, 124.4, 124.2, 118.7, 118.6, 71.6, 71.6, 39.9, 39.8, 30.8, 30.7, 29.3, 29.3, 24.2, 24.1, 23.2, 14.27, 11.4, 11.3 ppm.

HRMS-(+)APCI: calc'd. for $C_{24}H_{29}O_2$ $[M + H]^+$ 349.2162, found 349.2153

Compound **1**

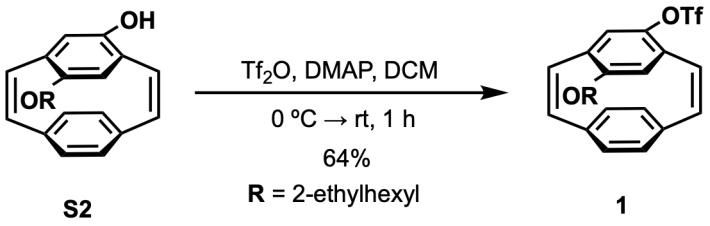

S2 **1**

To a flame-dried reaction tube equipped with a stir bar and **S2** (256 mg, 0.73 mmol, 1.0 equiv), DMAP (269 mg, 2.20 mmol, 3.0 equiv) was added followed by three vacuum/nitrogen cycles. Next, anhydrous DCM (7.3 mL) was added and the mixture was cooled to 0 °C. Trifluoromethanesulfonic anhydride (0.25 mL, 1.46 mmol, 2 equiv) was added dropwise under nitrogen, and the reaction was allowed to warm to room temperature and stir for 1 h. The solution was then diluted using DCM (8 mL) and washed with water (5 mL) before drying over Na_2SO_4 and concentrating under reduced pressure. Purification via column chromatography (SiO_2, hexanes, then 1:1 hexanes:DCM) afforded the desired compound **1** as a yellow semisolid (226 mg, 64%).

^{1}H NMR (500 MHz, $CDCl_3$) δ 7.28 (d, *J* = 10.9 Hz, 1 H), 7.18 (d, *J* = 10.2 Hz, 1 H), 6.91 (dt, *J* = 8.0, 1.3 Hz, 1 H), 6.86 (dd, *J* = 10.2, 4.3 Hz, 2 H), 6.76 (d, *J* = 8.0 Hz, 1 H), 6.56 (d, *J* = 7.7 Hz, 1 H), 6.49 (dd, *J* = 8.0, 1.8 Hz, 1 H), 6.14 (s, 1 H), 5.88 (s, 1 H), 3.75–3.64 (m, 2 H), 1.74–1.61 (m, 1 H), 1.52–1.31 (m, 10 H), 0.98–0.90 (m, 7 H) ppm.

^{13}C NMR (126 MHz, $CDCl_3$) δ 157.7, 157.7, 141.5, 138.4, 138.3, 137.7, 136.5, 133.5, 133.3, 133.3, 131.9, 131.8, 131.2, 128.2, 127.9, 127.7, 127.6, 122.7, 120.2, 119.1, 117.6, 115.1, 71.3, 71.2, 39.8, 39.7, 30.8, 30.7, 29.3, 29.2, 24.2, 23.2, 23.2, 14.2, 11.5, 11.3 ppm.

^{19}F NMR (376 MHz, $CDCl_3$) δ 72.94 ppm.

HRMS-(+)APCI: calc'd. for $C_{25}H_{28}F_3O_4S$ $[M + H]^+$ 481.1655, found 481.1646

Boronic Esters/Acids Preparation

Compound **S3**

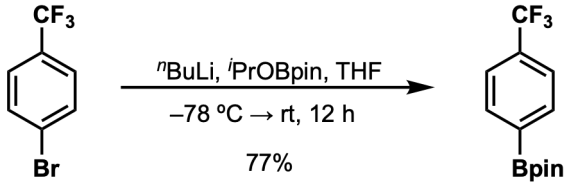

S3

Compound **S3** was synthesized using a procedure adapted from literature with minor modifications.[3] To a flame-dried round-bottom flask under inert atmosphere, equipped with a stir bar, was added 4-bromobenzotrifluoride (225 mg, 1.0 mmol, 1 equiv), followed by anhydrous THF (2.3 mL). The solution was cooled to –78 ºC then *n*-BuLi (1.6 M in hexane, 0.75 mL, 1.2 mmol, 1.2 equiv) was added dropwise. After stirring for 1 h at –78 ºC, 2-isopropoxy-4,4,5,5-tetramethyl-1,3,2-dioxaborolane (0.25 mL, 1.2 mmol, 1.2 equiv) was slowly added to the reaction mixture

at –78 ºC. The reaction mixture was warmed to room temperature and allowed to stir for 12 h. The reaction was quenched with deionized water (5 mL) slowly, then the reaction mixture was extracted with ethyl acetate (3 x 5 mL). The combined organic layers were washed with brine (1 x 15 mL), then dried over Na_2SO_4 and concentrated *in vacuo*. A 1:1 mixture of dichloromethane and hexanes was used to recrystallize the crude product, affording **S3** as an off-white crystalline solid (211 mg, 77%). The spectroscopic data were identical to those reported in the literature.

^{1}H NMR (400 MHz, $CDCl_3$) δ 7.91 (d, J = 7.5 Hz, 1 H), 7.61 (d, J = 8.3 Hz, 1 H), 1.36 (s, 6 H) ppm.

Compound **S4**

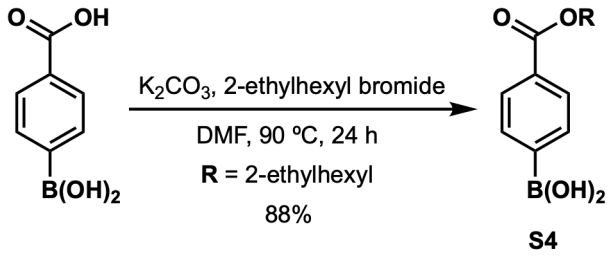

S4

Compound **S4** was synthesized following literature procedure. [4] Analysis via ^{1}H NMR showed that the obtained product was comprised of 88% boronic acid **S4** and 12% of the boroxine derivative (distinct signals in brackets).

^{1}H NMR (500 MHz, $CDCl_3$) δ 8.31 (d, J = 8.1 Hz, 2 H), 8.17 (d, J = 8.1 Hz, 2 H), [8.05 (d, J = 8.1 Hz, 1 H)], [7.82 (d, J = 8.1 Hz, 1 H)], 4.30 (dd, J = 5.8, 4.5 Hz, 2 H), [4.26 (dd, J = 5.9, 4.1 Hz, 1 H)], 1.76 (m, J = 12.1, 6.1 Hz, 1 H), 1.53–1.32 (m, 12 H), 1.00–0.89 (m, 9 H) ppm.

Compound **S5**

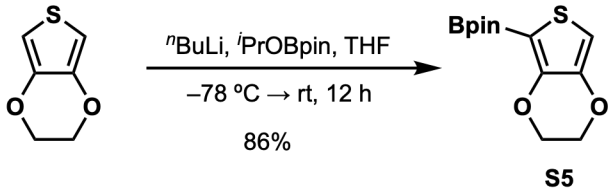

S5

Compound **S5** was synthesized following a literature procedure. [5]

Compound **S6**

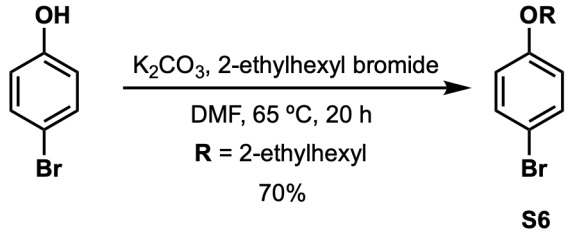

S6

Compound **S6** was synthesized following a literature procedure. [6]

Compound **S7**

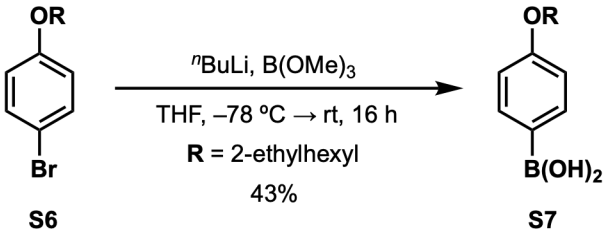

Compound **S7** was synthesized following a literature procedure with slight modification and the spectroscopic data were identical to those reported in the literature. [6] The crude residue was purified via column chromatography (SiO_2, 4:1 hexanes:Et_2O, then 2:1 hexanes:Et_2O, then 1:1 hexanes:Et_2O) afforded the desired compound **S7** as a viscous orange oil. The purified material was stored in the fridge (~4ºC) under inert atmosphere to prevent degradation.

^{1}H NMR (400 MHz, $CDCl_3$) δ 8.15 (d, *J* = 8.6 Hz, 2 H), 7.00 (d, *J* = 8.6 Hz, 2 H), 3.93 (dd, *J* = 5.8, 1.3 Hz, 2 H), 1.84–1.68 (m, 1 H), 1.52–1.31 (m, 8 H), 0.99–0.88 (m, 6 H) ppm.

Suzuki–Miyaura Cross-Coupling reaction: **General Procedure A**

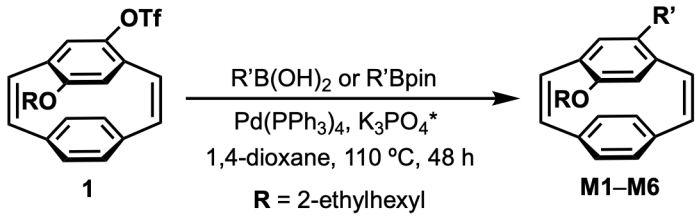

To a flame-dried reaction tube equipped with a stir bar, **1**, $Pd(PPh_3)_4$, K_3PO_4*, and the desired boronic ester or acid were added under nitrogen, followed by three vacuum/nitrogen cycles. The mixture was then dissolved in anhydrous and degassed 1,4-dioxane under nitrogen. The reaction tube was sealed with electrical tape, and the reaction was left to stir at 110 ºC for 48 h. After cooling to room temperature, the reaction was concentrated under reduced pressure. The crude residues were purified by silica chromatography. *CsF was used in place of K_3PO_4 in the synthesis of **M5**.

Monomer **M1**

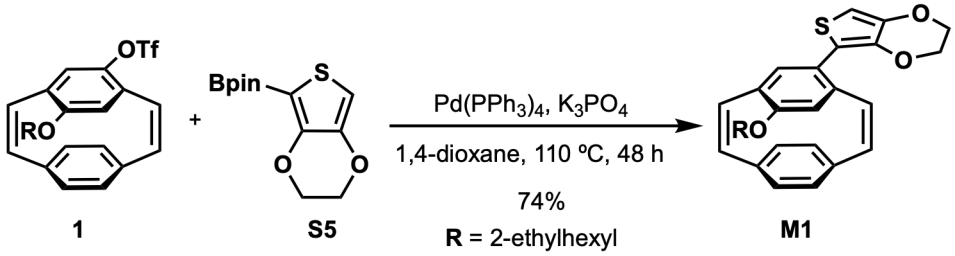

M1 was prepared from **1** (10 mg, 0.02 mmol, 1.0 equiv) following **general procedure A** using **S5** (33 mg, 0.12 mmol, 6.0 equiv), $Pd(PPh_3)_4$ (2 mg, 0.002 mmol, 0.1 equiv), K_3PO_4 (20 mg, 0.09 mmol, 4.5 equiv), and anhydrous 1,4-dioxane (0.40 mL). Column chromatography (SiO_2, hexanes, 95:5 hexanes:DCM, 90:10 hexanes:DCM, 80:20 hexanes:DCM, then 70:30 hexanes:DCM) afforded the desired monomer **M1** as a clear semisolid (7 mg, 74%).

^{1}H NMR (500 MHz, $CDCl_3$) δ 7.17 (d, *J* = 10.4 Hz, 1 H), 7.14 (d, *J* = 10.2 Hz, 1 H), 7.00 (d, *J* = 10.3 Hz, 1 H), 6.91 (d, *J* = 10.1 Hz, 1 H), 6.82 (dd, *J* = 7.9, 1.6 Hz, 1 H), 6.72 (dt, *J* = 8.0, 1.3 Hz, 1 H), 6.56–6.50 (m, 3H), 6.32 (s, 1 H), 5.91 (s, 1 H), 4.38–4.19 (m, 4 H), 3.70 (d, *J* = 5.7 Hz, 2 H), 1.75–1.65 (m, 1 H), 1.59–1.43 (m, 3 H), 1.39–1.31 (m, 4 H), 1.29–1.24 (m, 1 H), 0.99–0.90 (m, 6 H) ppm.

^{13}C NMR (126 MHz, $CDCl_3$) δ 155.9, 141.0, 137.6, 137.4, 136.8, 136.7, 135.5, 134.6, 134.1, 132.8, 130.9, 130.7, 129.6, 127.7, 125.8, 124.7, 123.8, 118.6, 116.9, 96.6, 69.6, 63.7, 38.6, 29.7, 28.2, 23.0, 22.0, 13.1, 10.2 ppm.

HRMS-(+)APCI: calc'd. for $C_{30}H_{33}O_3S$ $[M + H]^+$ 473.2145, found 473.2140

Monomer **M2**

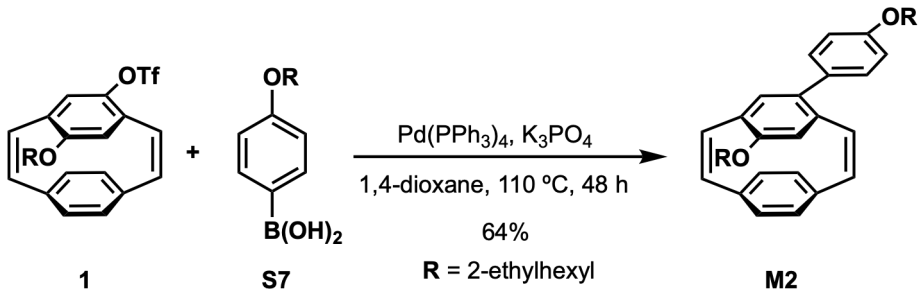

1 S7 M2

M2 was prepared from **1** (20 mg, 0.04 mmol, 1.0 equiv) following **general procedure A** using **S7** (42 mg, 0.16 mmol, 4.0 equiv), $Pd(PPh_3)_4$ (3 mg, 0.002 mmol, 0.06 equiv), K_3PO_4 (27 mg, 0.12 mmol, 3.0 equiv), and anhydrous 1,4-dioxane (0.40 mL). Column chromatography (SiO_2, hexanes, 9:1 hexanes:DCM, then 4:1 hexanes:DCM) afforded the desired monomer **M2** as a clear, colorless semisolid (14 mg, 64%).

^{1}H NMR (500 MHz, $CDCl_3$) δ 7.39–7.32 (m, 2 H), 7.16 (d, *J* = 10.2 Hz, 2 H), 6.98–6.93 (m, 3 H), 6.91 (d, *J* = 10.3 Hz, 1 H), 6.85 (d, *J* = 7.9 Hz, 1 H), 6.57–6.50 (m, 4 H), 5.95 (s, 1 H), 3.89 (dd, *J* = 5.7, 1.5 Hz, 2 H), 3.75–3.67 (m, 2 H), 1.73 (m, 2 H), 1.59–1.54 (m, 1 H), 1.51–1.39 (m, 7 H), 1.38–1.33 (m, 8 H), 0.99–0.92 (m, 12 H) ppm.

^{13}C NMR (126 MHz, $CDCl_3$) δ 158.6, 156.7, 138.6, 138.5, 138.0, 137.7, 135.7, 134.9, 134.8, 134.3, 132.9, 131.2, 131.0, 130.9, 130.0, 128.0, 127.1, 125.8, 120.5, 114.7, (70.9, 70.8), 70.7, (39.89, 39.8), 39.7, (30.9, 30.8), 30.7, (29.4, 29.3), 29.2, (24.2, 24.1), 23.2, 14.3, 14.2, (11.5, 11.4), 11.3 ppm.

HRMS-(+)ESI: calc'd. for $C_{38}H_{49}O_2$ $[M + H]^+$ 537.3727, found 537.3722

Monomer **M3**

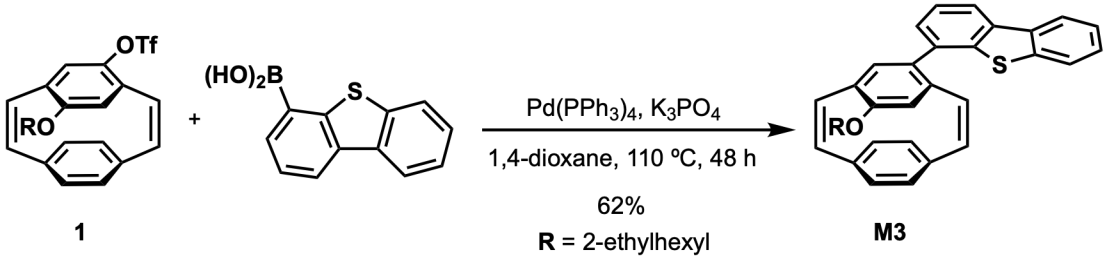

1 M3

M3 was prepared from **1** (38 mg, 0.08 mmol, 1.0 equiv) following **general procedure A** using 4-dibenzothienylboronic acid (109 mg, 0.47 mmol, 6.0 equiv), $Pd(PPh_3)_4$ (11 mg, 0.009 mmol, 0.12 equiv), K_3PO_4 (89 mg, 0.42 mmol, 4.5 equiv), and anhydrous 1,4-dioxane (1.6 mL). Column chromatography (SiO_2, hexanes, 9:1 hexanes:DCM, 7:1 hexanes:DCM, 5:1 hexanes:DCM, 3:1 hexanes:DCM, then 1:1 hexanes:DCM) afforded the desired monomer **M3** as a clear, colorless semisolid (25 mg, 62%).

^{1}H NMR (400 MHz, $CDCl_3$) δ 8.31–8.08 (m, 2 H), 7.92–7.80 (m, 1 H), 7.67 (d, *J* = 7.4 Hz, 1 H), 7.62 (t, *J* = 7.5 Hz, 1 H), 7.56–7.43 (m, 2 H), 7.23 (dd, *J* = 10.3, 3.8 Hz, 2 H), 6.99 (d, *J* = 10.2 Hz, 1 H), 6.93 (d, *J* = 8.0 Hz, 1 H), 6.85 (d, *J* = 10.4 Hz, 1 H), 6.70–6.76 (m, 3 H), 6.61 (d, *J* = 8.0 Hz, 1 H), 6.08 (s, 1 H), 3.80 (d, *J* = 5.5 Hz, 2 H), 1.83–1.72 (m, 1 H), 1.69–1.46 (m, 3 H), 1.48–1.34 (m, 3 H), 1.28 (s, 1 H) 1.20–0.88 (m, 6 H) ppm.

^{13}C NMR (126 MHz, $CDCl_3$) δ 157.7, 140.2, 139.8, 138.8, 138.6, 138.0, 137.7, 136.3, 136.2, 136.0, 135.7, 134.1, 132.5, 132.2, 131.3, 130.9, 128.1, 127.1, 126.8, 126.6, 126.1, 125.0, 124.4, 122.7, 121.8, 120.5, 120.2, 70.7, 39.8, 30.8, 29.3, 24.2, 23.2, 14.3, 11.5 ppm.

HRMS-(+)ESI: calc'd. for $C_{36}H_{35}OS$ $[M + H]^+$ 515.2403, found 515.2402

Monomer **M4**

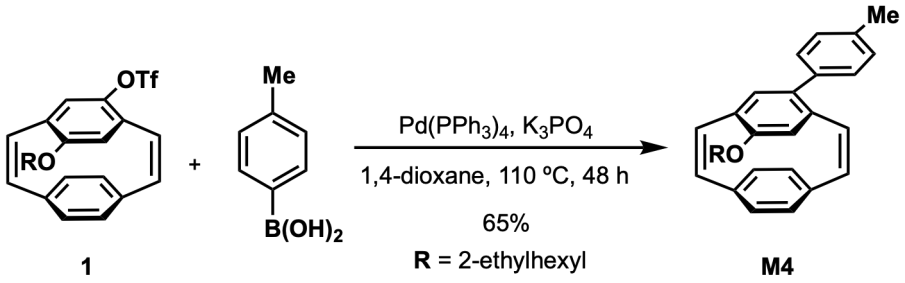

1 M4

M4 was prepared from **1** (54 mg, 0.11 mmol, 1.0 equiv) following **general procedure A** using p-tolueneboronic acid (138 mg, 1.0 mmol, 9.0 equiv), $Pd(PPh_3)_4$ (13 mg, 0.01 mmol, 0.1 equiv), K_3PO_4 (108 mg, 0.5 mmol, 4.5 equiv), and anhydrous 1,4-dioxane (2.3 mL). Column chromatography (SiO_2, hexanes, 9:1 hexanes:DCM, then 4:1 hexanes:DCM) afforded the desired monomer **M4** as a clear, colorless semisolid (30.9 mg, 65%).

^{1}H NMR (500 MHz, $CDCl_3$) δ 7.36 (d, *J* = 7.8 Hz, 2 H), 7.24 (d, *J* = 7.7 Hz, 2 H), 7.19 (d, *J* = 7.7 Hz, 1 H), 7.17 (d, *J* = 7.5 Hz, 1 H), 6.96 (d, *J* = 10.1 Hz, 1 H), 6.92 (d, *J* = 10.3 Hz, 1 H), 6.86 (d, *J* = 7.9 Hz, 1 H), 6.60 (s, 1 H), 6.57 (d, *J* = 5.1 Hz, 2 H), 6.54 (d, *J* = 8.4 Hz, 1 H), 5.97 (s, 1 H), 3.73 (d, *J* = 5.2 Hz, 2 H), 2.41 (s, 3 H), 1.75–1.69 (m, 1 H), 1.63–1.42 (m, 3 H), 1.41–1.34 (m, 4 H), 1.28 (s, 1 H), 1.02–0.97 (m, 6 H) ppm.

^{13}C NMR (126 MHz, $CDCl_3$) δ 156.93, 138.61, 138.40, 138.00, 137.86, 137.69, 136.40, 135.70, 135.00, 134.92, 134.27, 131.27, 131.18, 130.92, 129.40, 128.95, 128.10, 127.03, 125.80, 120.54, 70.84, 39.85, 30.83, 29.33, 24.23, 23.23, 21.29, 14.26, 11.48 ppm.

HRMS-(+)APCI: calc'd. for $C_{31}H_{35}O$ $[M + H]^+$ 423.2682, found 423.2675

Monomer **M5**

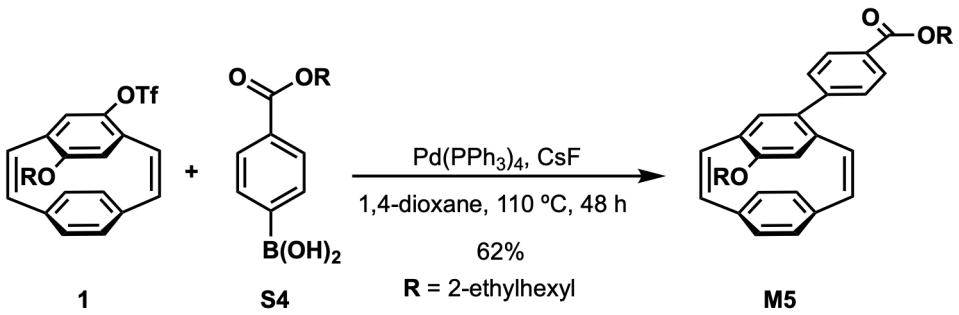

1 S4 M5

M5 was prepared from **1** (13 mg, 0.03 mmol, 1.0 equiv) following **general procedure A** using **S4** (45 mg, 0.20 mmol, 6.0 equiv), $Pd(PPh_3)_4$ (2 mg, 0.001 mmol, 0.05 equiv), CsF (25 mg, 0.20 mmol, 6.0 equiv), and anhydrous 1,4-dioxane (0.54 mL). Column chromatography (SiO_2, hexanes, 98:2 hexanes:diethyl ether, then 95:5 hexanes:diethyl ether) afforded the desired monomer **M5** as a clear yellow semisolid (9 mg, 62%).

^{1}H NMR (500 MHz, $CDCl_3$) δ 8.08 (d, J = 8.3 Hz, 2 H), 7.53 (d, J = 8.4 Hz, 2 H), 7.18 (d, J = 10.3 Hz, 2 H), 6.95 (d, J = 10.1 Hz, 1 H), 6.92 (d, J = 10.4 Hz, 1 H), 6.85 (dt, J = 7.9, 1.4 Hz, 1 H), 6.65 (s, 1 H), 6.58 (dt, J = 7.8, 1.3 Hz, 1 H), 6.53 (dd, J = 7.9, 1.8 Hz, 1 H), 6.48 (dd, J = 8.3, 1.7 Hz, 1 H), 6.00 (s, 1 H), 4.31–4.22 (m, 2 H), 3.74 (dd, J = 5.9, 1.8 Hz, 2 H), 1.74 (m, 2 H), 1.64–1.25 (m, 16 H), 1.00–0.87 (m, 12 H) ppm.

^{13}C NMR (126 MHz, $CDCl_3$) δ 166.9, 157.7, 144.8, 138.6, 138.4, 137.9, 137.8, 135.9, 135.5, 134.0, 133.9, 131.5, 131.1, 130.9, 129.9, 128.9, 128.7, 127.9, 127.2, 126.0, 120.7, (70.9, 70.9), 67.4, (39.9, 39.8), 39.2, (30.9, 30.8), 30.8, (29.4, 29.3), 29.2, 24.2, (23.2, 23.2), 23.2, 14.3, 14.2, (11.5, 11.4), 11.3 ppm.

HRMS-(+)ESI: calc'd. for $C_{39}H_{49}O_3$ $[M + H]^+$ 565.3676, found 565.3671

Monomer **M6**

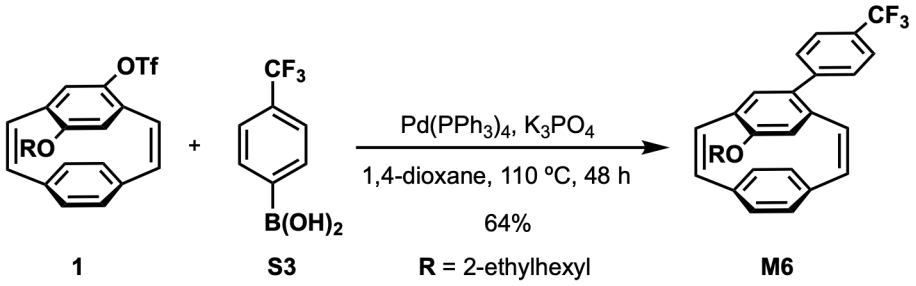

1 S3 M6

M6 was prepared from **1** (21 mg, 0.04 mmol, 1.0 equiv) following **general procedure A** using **S3** (109 mg, 0.4 mmol, 9.0 equiv), $Pd(PPh_3)_4$ (6 mg, 0.005 mmol, 0.12 equiv), K_3PO_4 (42 mg, 0.2 mmol, 4.5 equiv), and anhydrous 1,4-dioxane (0.90 mL). Column chromatography (SiO_2, hexanes, 90:10 hexanes:DCM, then 80:20 hexanes:DCM) afforded the desired monomer **M6** as a clear semisolid (13 mg, 64%).

^{1}H NMR (500 MHz, $CDCl_3$) δ 7.66 (d, *J* = 8.1 Hz, 2 H), 7.56 (d, *J* = 8.1 Hz, 2 H), 7.17 (t, *J* = 11.0 Hz, 2 H), 6.95 (dd, *J* = 10.2, 7.5 Hz, 2 H), 6.86 (d, *J* = 8.0 Hz, 1 H), 6.62 (s, 1 H), 6.57 (d, *J* = 7.9 Hz, 1 H), 6.53 (d, *J* = 7.9 Hz, 1 H), 6.47 (d, *J* = 7.9 Hz, 1 H), 6.00 (s, 1 H), 3.74 (d, *J* = 5.5 Hz, 2 H), 1.71 (hep, *J* = 6.1 Hz, 1 H), 1.62–1.42 (m, 2 H), 1.41–1.31 (m, 4 H), 1.26 (s, 4 H), 1.01–0.91 (m, 6 H) ppm.

^{13}C NMR (126 MHz, $CDCl_3$) δ 157.7, 143.9, 138.7, 138.3, 137.8, 137.7, 136.0, 135.7, 134.0, 133.4, 131.4, 131.1, 131.0, 129.2, 127.8, 127.2, 126.1, 125.6, 125.6, 125.5, 120.8, 39.6, 30.56, 29.6, 29.1, 24.0, 23.0, 14.0, 11.2 ppm.

^{19}F NMR (376 MHz, $CDCl_3$) δ –62.24 ppm.

HRMS-(+)APCI: calc'd. for $C_{31}H_{32}F_3O$ $[M + H]^+$ 477.2400, found 477.2395

Monomer **M7**

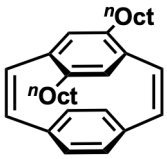

M7

Monomer **M7** was synthesized following literature procedures reported by our group. [7]

Monomer **M8**

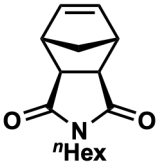

M8

Compound **M8** was synthesized following literature procedure. [8]

Polymer Synthesis

Stereoretentive ROMP of Arylated PCDs: **General procedure B**

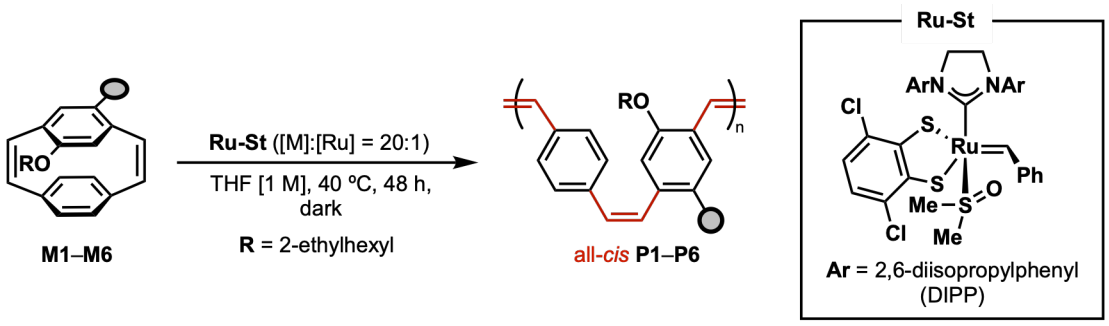

Inside a nitrogen-filled glovebox, **Ru-St** (5 mol%) was weighed into a vial and dissolved in deoxygenated anhydrous THF. Next, the solution of **Ru-St** was added into a reaction vial containing the desired monomer (**M1**–**M6**) and a stir bar. The vial was hermetically sealed with a cap and stirred at 40 °C for 48 h inside the nitrogen-filled glovebox. Once cooled to room temperature, the reaction was quenched inside the glovebox using excess ethyl vinyl ether (0.1 mL) and stirred for an additional 30 min at room temperature. The mixture was then taken outside the glovebox and two cycles of precipation with addition of methanol, centrifugation (9500 rpm for 10 min), and decantation afforded the corresponding isolated polymers **P1**–**P6** with residual solvent. All polymers vials were wrapped in aluminum foil, concentrated under reduced pressure at room temperature, and stored in the dark under a nitrogen atmosphere at –20 °C to prevent any undesired photoisomerization.

Table S1. Optimization of monomer concentration in THF for stereoretentive ROMP of **M2**.

Entry	Conc. (M)	% Conv.	M_n^{theo} (kg/mol)	M_n^{exp} (kg/mol)[a]	$Đ$ [a]	%*cis*
1	0.1	61	6.6	5.9	1.25	>99
2	0.8	>99	10.8	5.5	1.19	>99
3	1.0	>99	10.8	9.5	1.18	>99

[a]Determined by SEC analysis in THF against polystyrene standards.

Table S2. Stereoretentive ROMP of monomers **M1–M6** under optimized conditions.

Entry	Monomer	% Conv.	M_n^{theo} (kg/mol)	M_n^{exp} (kg/mol)[a]	$Đ$ [a]	%*cis*
1	**M1**	88	8.6	9.5	1.22	>99
2	**M2**	>99	10.8	9.5	1.18	>99
3	**M3**	>99	10.4	11.5	1.12	>99
4	**M4**	>99	8.5	10.0	1.18	>99
5	**M5**	>99	11.3	7.3	1.09	>99
6	**M6**	>99	9.6	9.3	1.22	>99

[a]Determined by SEC analysis in THF against polystyrene standards.

all-*cis* **P1**

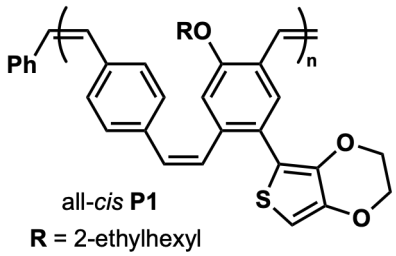

All-*cis* **P1** was prepared from **M1** (16 mg, 0.034 mmol, 20 equiv) following **general procedure B** using **Ru-St** (2 mg, 0.0017 mmol, 1 equiv), and deoxygenated anhydrous THF (0.03 mL). 88% of **M1** was consumed after 48 h.

M_n^{theo} = 8.6 kg/mol, M_n^{exp} = 9.5 kg/mol, $Đ$ = 1.22

^{1}H NMR (400 MHz, $CDCl_3$) δ 7.35–7.25 (m, 1 H), 7.18–6.97 (m, 4 H), 6.75–6.63 (m, 1 H), 6.62–6.49 (m, 1 H), 6.48–6.35 (m, 3 H), 6.19–6.07 (m, 1 H), 4.05–3.80 (m, 4 H), 3.37 (m, 2 H), 1.49–1.33 (m, 2 H), 1.25–1.06 (m, 8 H), 0.81–0.75 (m, 3 H), 0.74–0.64 (m, 3 H) ppm.

^{13}C NMR (126 MHz, $CDCl_3$) δ 156.1, 141.4, 138.0, 137.9, 137.3, 137.2, 136.2, 136.0, 132.3, 130.1, 129.8, 129.1, 128.9, 125.7, 125.0, 123.2, 115.8, 115.6, 113.2, 98.5, 70.6, 64.6, 64.4, 39.2, 30.6, 29.0, 24.0, 23.2, 14.2, 11.1 ppm.

all-*cis* **P2**

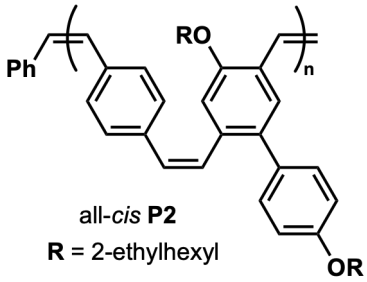

All-*cis* **P2** was prepared from **M2** (22 mg, 0.04 mmol, 20 equiv) following **general procedure B** using **Ru-St** (2 mg, 0.002 mmol, 1 equiv), and deoxygenated anhydrous THF (0.04 mL). >99% of **M2** was consumed after 48 h.

M_n^{theo} = 10.8 kg/mol, M_n^{exp} = 9.5 kg/mol, $Đ$ = 1.18

^{1}H NMR (400 MHz, $CDCl_3$) δ 7.34–7.26 (m, 2 H, *overlaps with $CDCl_3$*), 7.25–7.14 (m, 3 H, *overlaps with $CDCl_3$*), 7.14–7.00 (m, 2 H), 6.89–6.72 (m, 3 H), 6.67 (m, 1 H), 6.56–6.42 (m, 2 H), 6.36 (dd, J = 13.4, 6.1 Hz, 1 H), 3.84–3.69 (m, 2 H), 3.53–3.31 (m, 2 H), 1.75–1.62 (m, 1 H), 1.50–1.07 (m, 17 H), 0.95–0.68 (m, 12 H) ppm.

^{13}C NMR (126 MHz, $CDCl_3$) δ 158.5, 155.5, 136.8, 136.1, 135.4, 132.9, 132.7, 131.5, 130.7, 130.7, 129.6, 129.0, 128.9, 125.7, 114.1, 113.2, 70.6, 39.6, 39.3, 30.7, 30.6, 29.3, 29.1, 24.0, 23.9, 23.2, 23.2, 14.2, 11.3, 11.2 ppm.

all-*cis* **P3**

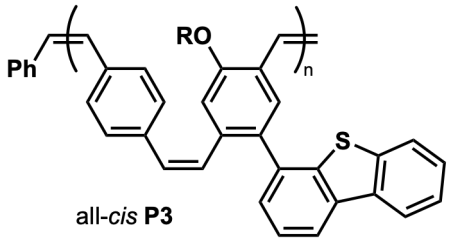

all-*cis* **P3**
R = 2-ethylhexyl

All-*cis* **P3** was prepared from **M3** (20 mg, 0.038 mmol, 20 equiv) following **general procedure B** using **Ru-St** (2 mg, 0.0019 mmol, 1 equiv), and deoxygenated anhydrous THF (0.04 mL). >99% of **M3** was consumed after 48 h.

M_n^{theo} = 10.4 kg/mol, M_n^{exp} = 11.5 kg/mol, $Đ$ = 1.12

^{1}H NMR (400 MHz, $CDCl_3$) δ 8.15–7.88 (m, 1 H), 7.85–7.57 (m, 2 H), 7.47–7.28 (m, 3 H), 7.25–6.99 (m, 5 H), 6.98–6.75 (m, 2 H), 6.75–6.42 (m, 2 H), 6.41–6.10 (m, 2 H), 3.75–3.00 (m, 2 H), 1.65–1.47 (m, 1 H), 1.43–0.97 (m, 10 H), 0.92–0.69 (m, 6 H), 0.68–0.51 (m, 1 H) ppm.

^{13}C NMR (126 MHz, $CDCl_3$) δ 156.4, 156.3, 140.5, 140.4, 140.2, 139.9, 139.8, 132.0, 131.4, 130.2, 129.3, 129.2, 129.1, 128.4, 128.1, 126.7, 126.4, 126.2, 124.5, 124.3, 124.1, 122.9, 121.7, 120.3, 119.0, 112.99, 39.2, 30.7, 29.1, 24.0, 23.8, 23.2, 23.1, 14.2, 11.1 ppm.

all-*cis* **P4**

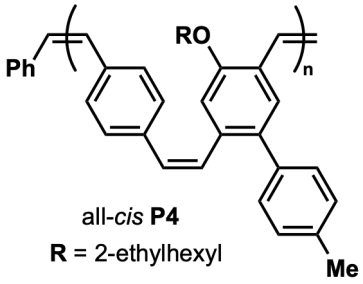

all-*cis* **P4**
R = 2-ethylhexyl

All-*cis* **P4** was prepared from **M4** (15 mg, 0.036 mmol, 20 equiv) following **general procedure B** using **Ru-St** (2 mg, 0.0018 mmol, 1 equiv), and deoxygenated anhydrous THF (0.04 mL). >99% of **M4** was consumed after 48 h.

M_n^{theo} = 8.5 kg/mol, M_n^{exp} = 10.0 kg/mol, $Đ$ = 1.18

^{1}H NMR (400 MHz, $CDCl_3$) δ 7.42–7.19 (m, 5 H), 7.17–6.98 (m, 4 H), 6.97–6.80 (m, 1 H), 6.78–6.65 (m, 1 H), 6.66–6.46 (m, 2 H), 6.44–6.33 (m, 1 H), 3.76–3.35 (m, 2 H), 2.49–2.18 (m, 3 H), 1.63–1.53 (m, 1 H), 1.50–1.06 (m, 10 H), 0.94–0.81 (m, 5 H), 0.79–0.73 (m, 2 H) ppm.

^{13}C NMR (126 MHz, $CDCl_3$) δ 155.7, 137.8, 136.8, 136.4, 136.1, 135.6, 132.9, 131.6, 130.7, 129.7, 129.6, 129.4, 129.1, 129.1, 129.0, 128.8, 125.7, 125.6, 113.4, 113.2, 70.6, 39.3, 30.6, 29.1, 24.0, 23.2, 21.3, 14.2, 11.2 ppm.

all-*cis* **P5**

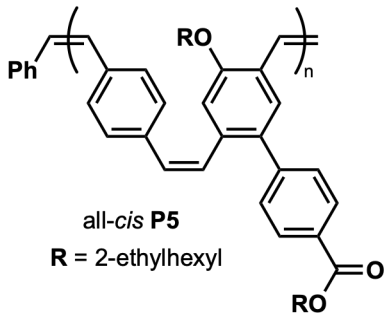

all-*cis* **P5**
R = 2-ethylhexyl

All-*cis* **P5** was prepared from **M5** (7 mg, 0.01 mmol, 20 equiv) following **general procedure B** using **Ru-St** (1 mg, 0.0006 mmol, 1 equiv), and deoxygenated anhydrous THF (0.01 mL). >99% of **M5** was consumed after 48 h.

M_n^{theo} = 11.3 kg/mol, M_n^{exp} = 7.3 kg/mol, $Đ$ = 1.09

^{1}H NMR (500 MHz, $CDCl_3$) δ 8.01–7.86 (m, 2 H), 7.34–7.27 (m, 1 H), 7.25–7.19 (m, 5 H), 7.19–7.13 (m, 1 H), 6.87–6.79 (m, 1 H), 6.70–6.59 (m, 1 H), 6.59–6.43 (m, 2 H), 6.41–6.27 (m, 1 H), 4.27–4.14 (m, 2 H), 3.57–3.27 (m, 2 H), 1.68 (m, 1 H), 1.45–1.12 (m, 17 H), 0.93–0.71 (m, 12 H) ppm.

^{13}C NMR (126 MHz, $CDCl_3$) δ 166.72, 156.26, 145.37, 136.76, 135.95, 135.69, 131.73, 131.66, 130.45, 130.12, 129.85, 129.61, 129.30, 129.07, 128.93, 128.79, 125.27, 113.31, 70.42, 67.34, 39.19, 39.06, 30.69, 30.51, 29.13, 29.08, 24.10, 23.86, 23.12, 14.23, 14.21, 11.20, 11.10 ppm.

all-*cis* **P6**

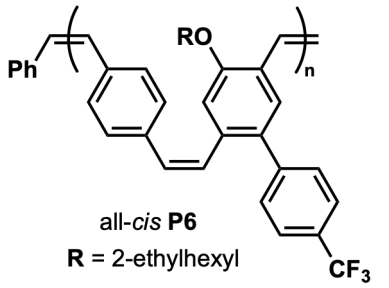

all-*cis* **P6**
R = 2-ethylhexyl

All-*cis* **P6** was prepared from **M6** (18 mg, 0.037 mmol, 20 equiv) following **general procedure B** using **Ru-St** (2 mg, 0.019 mmol, 1 equiv), and deoxygenated anhydrous THF (0.04 mL). >99% of **M6** was consumed after 48 h.

M_n^{theo} = 9.6 kg/mol, M_n^{exp} = 9.3 kg/mol, $Đ$ = 1.22

^{1}H NMR (400 MHz, $CDCl_3$) δ 7.65–7.41 (m, 2 H), 7.26–7.00 (m, 7 H), 6.87–6.79 (m, 1 H), 6.77–6.60 (m, 1 H), 6.59–6.43 (m, 2 H), 6.41–6.25 (m, 1 H), 3.62–3.38 (m, 2 H), 1.63–1.49 (m, 2 H), 1.48–1.00 (m, 10 H), 0.97–0.78 (m, 4 H), 0.78–0.64 (m, 2 H) ppm.

^{13}C NMR (126 MHz, $CDCl_3$) δ 156.4, 144.4, 136.9, 135.9, 135.8, 131.7, 131.3, 130.6, 130.0, 129.9, 129.8, 129.7, 129.6, 129.0, 126.0, 125.5, 124.9, 123.3, 113.3, 70.7, 39.2, 30.6, 29.1, 23.9, 23.1, 14.2, 11.1 ppm.

all-*cis* **P7**

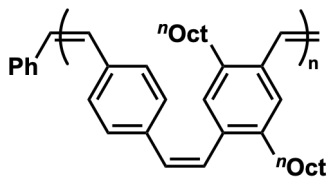

all-*cis* **P7**

All-*cis* **P7** was synthesized following literature procedures reported by our group. [7]

Copolymer Synthesis

*Diblock Copolymer Synthesis of cis-**P7**-b-cis-**P1***

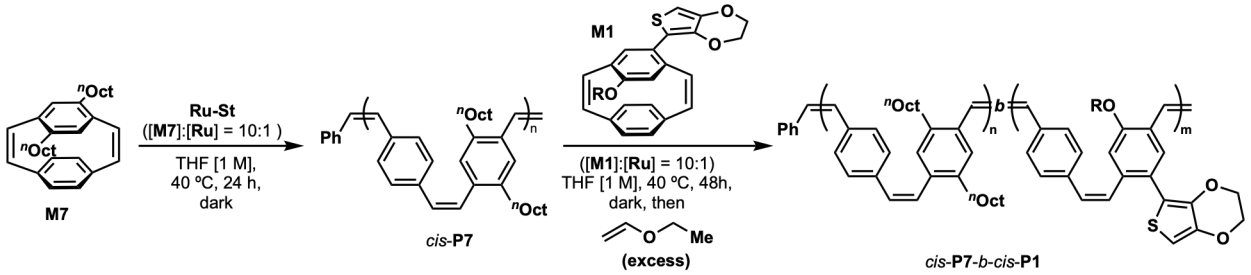

Inside a nitrogen-filled glovebox, **Ru-St** (2 mg, 0.0028 mmol) was weighed into a vial. **Ru-St** was dissolved in THF (0.03 mL). The catalyst solution was transferred to the vial containing the measured **M7** (12 mg, 0.028 mmol). The reaction was stirred at 40 °C for 24 h. After full conversion of **M7**, a 0.01 mL aliquot was removed and quenched using excess ethyl vinyl ether (0.1 mL) for SEC analysis. THF (0.02 mL) was added to the polymer solution and transferred into to the vial containing **M1** (9 mg, 0.019 mmol). The reaction was stirred at 40 °C for 48 h and 90% of **M1** was consumed. Once cooled to room temperature, the reaction was quenched inside the glovebox using excess ethyl vinyl ether (0.1 mL) and stirred for an additional 30 min at room temperature. The mixture was then taken outside the glovebox and two cycles of precipation with addition of methanol, centrifugation (9500 rpm for 10 min), and decantation afforded the corresponding isolated polymer *cis*-**P7**-*b*-*cis*-**P1**. The polymer was wrapped in aluminum foil, concentrated under reduced pressure at room temperature, and stored under a nitrogen atmosphere at –20 °C to prevent any undesired photoisomerization.

First Block: M_n^{theo} = 4.3 kg/mol, M_n^{exp} = 6.9 kg/mol, $Đ$ = 1.07
Full polymer: M_n^{theo} = 8.7 kg/mol, M_n^{exp} = 11.0 kg/mol, $Đ$ = 1.12

^{1}H NMR (400 MHz, $CDCl_3$) δ 7.32 (d, J = 18.1 Hz, 1 H), 7.18–7.04 (m, 5 H), 7.03–6.92 (m, 1 H), 6.89 (d, J = 5.5 Hz, 6 H), 6.70 (d, J = 18.5 Hz, 1 H), 6.60–6.49 (m, 3 H), 6.46–6.36 (m, 5 H), 6.18–6.08 (m, 1 H), 4.05–3.83 (m, 4 H), 3.44–3.30 (m, 2 H), 2.41–2.30 (m, 4 H), 1.38–1.27 (m, 5 H), 1.26–1.04 (m, 37 H), 0.86–0.64 (m, 16 H) ppm.

^{13}C NMR (126 MHz, $CDCl_3$) δ 156.1, 141.4, 138.4, 138.0, 137.9, 137.4, 137.2, 136.3, 136.0, 135.9, 135.7, 132.3, 130.4, 130.2, 130.1 129.7, 129.6, 129.1, 128.9, 128.8, 125.7, 125.1, 123.2, 115.8, 115.6, 113.2, 98.5, 70.6, 64.6, 64.6, 39.2, 33.3, 32.1, 30.9, 30.6, 29.7, 29.4, 29.1, 24.0, 23.2, 22.8, 14.3, 14.2, 11.1 ppm.

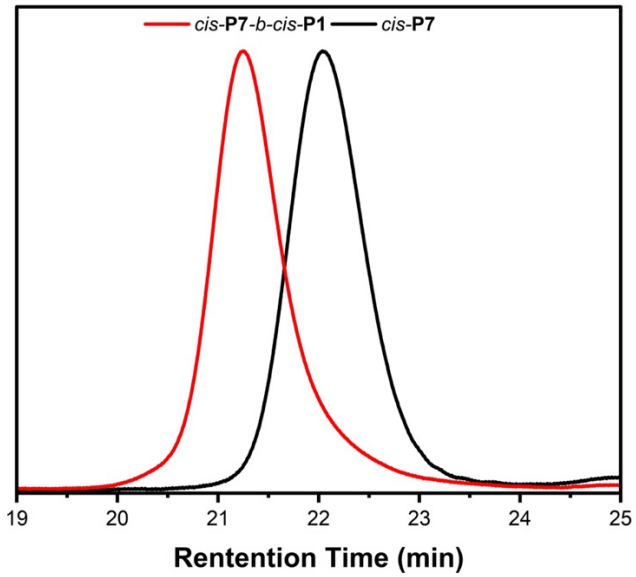

Figure S1. Normalized SEC traces showing chain extension. SEC traces obtained in THF stabilized with BHT using a polystyrene standard.

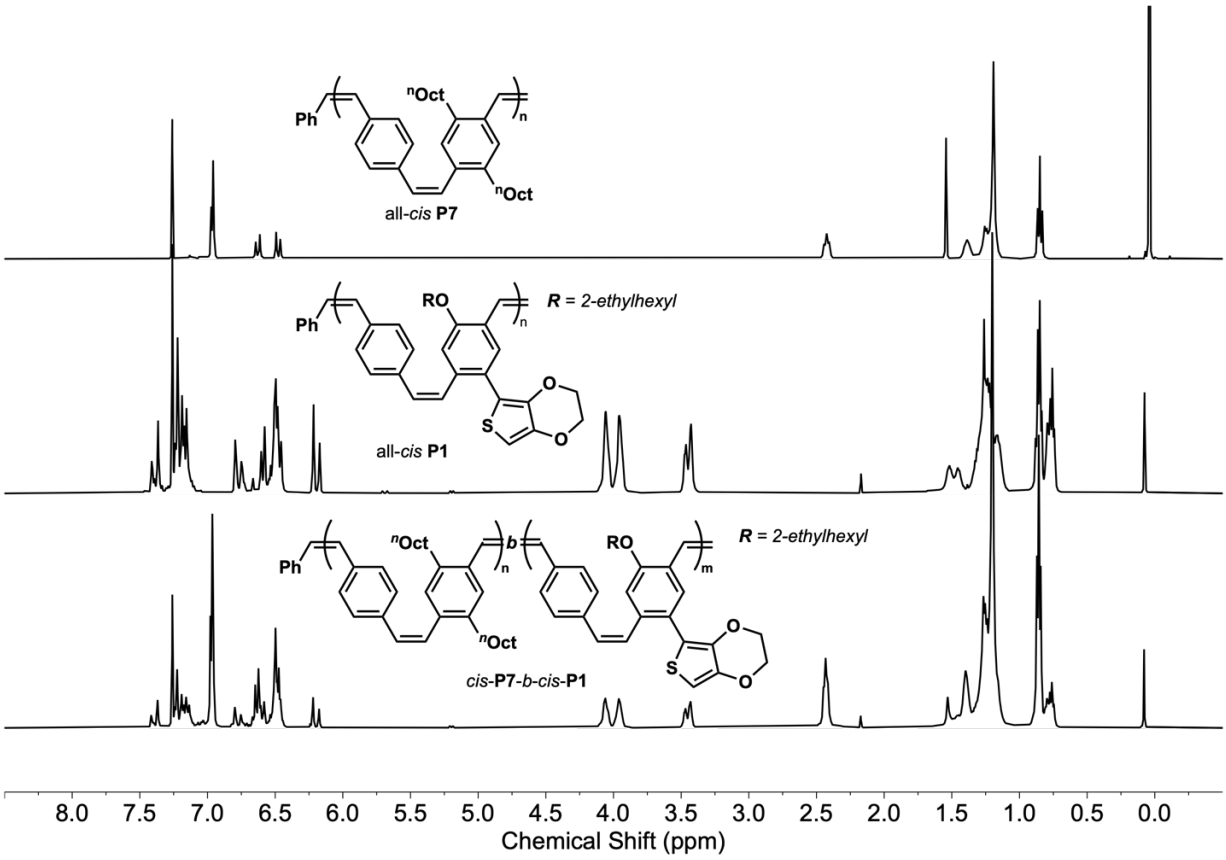

Figure S2. Overlayed ^{1}H NMR spectra of homopolymers all-*cis* **P7** (top) and all-*cis* **P1** (middle), and copolymer *cis*-**P7**-*b*-*cis*-**P1** after isolation (bottom) in $CDCl_3$.

*Random Copolymer Synthesis of cis-**P7**-r-cis-**P1***

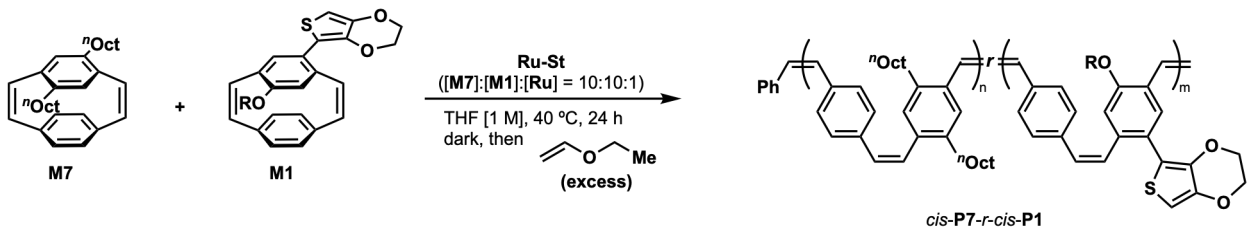

Inside a nitrogen-filled glovebox, **Ru-St** (2 mg, 0.0023 mmol) was weighed into a vial. **Ru-St** was dissolved in THF (0.05 mL). Then the catalyst solution was transferred to the vial containg the measured **M7** (10 mg, 0.023 mmol) and **M1** (11 mg, 0.023 mmol). The reaction was stirred at 40 °C for 24 h. 85% of **M7** and 86% of **M1** was consumed. Once cooled to room temperature, the reaction was quenched inside the glovebox using excess ethyl vinyl ether (0.1 mL) and stirred for an additional 30 min at room temperature. The mixture was then taken outside the glovebox and two cycles of precipation with addition of methanol, centrifugation (9500 rpm for 10 min), and decantation afforded the corresponding isolated polymer *cis*-**P7**-*r*-*cis*-**P1**. The polymer was wrapped in aluminum foil, concentrated under reduced pressure, and stored under a nitrogen atmosphere at –20 °C to prevent any undesired photoisomerization.

Full Polymer: M_n^{theo} = 9.0 kg/mol, M_n^{exp} = 8.8 kg/mol, $Đ$ = 1.11,

^{1}H NMR (500 MHz, $CDCl_3$) δ 7.43–7.33 (m, 1 H), 7.25–7.08 (m, 5 H), 7.05–6.93 (m, 5 H), 6.83–6.72 (m, 1 H), 6.70–6.56 (m, 3 H), 6.54–6.40 (m, 5 H), 6.27–6.14 (m, 1 H), 4.17–3.87 (m, 4 H), 3.54–3.35 (m, 2 H), 2.54–2.28 (m, 4 H), 1.59–1.48 (m, 3 H), 1.42–1.11 (m, 34 H), 0.93–0.70 (m, 14 H) ppm.

^{13}C NMR (126 MHz, $CDCl_3$) δ 156.1, 141.4, 138.4, 138.0, 137.9, 137.4, 137.2, 136.3, 136.0, 135.9, 135.7, 132.3, 130.4, 130.2, 130.1 129.7, 129.6, 129.1, 128.9, 128.8, 125.7, 125.1, 123.2, 115.8, 115.6, 113.2, 98.5, 70.6, 64.6, 64.6, 39.2, 33.3, 32.1, 30.9, 30.6, 29.7, 29.4, 29.1, 24.0, 23.2, 22.8, 14.3, 14.2, 11.1 ppm.

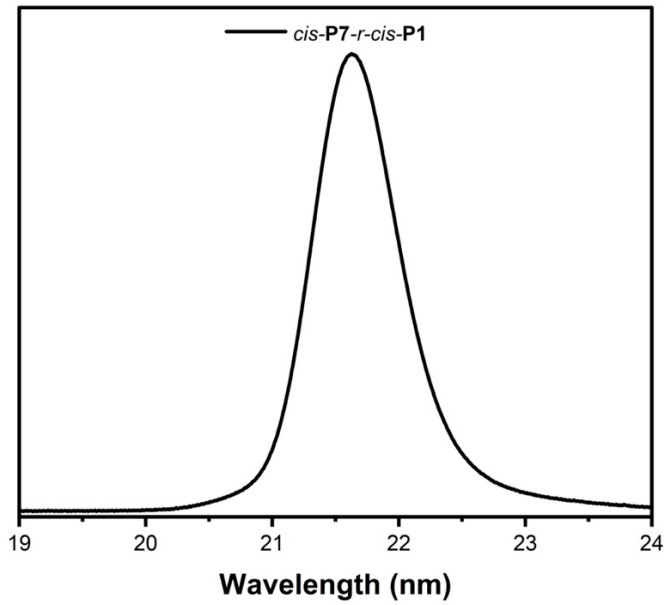

Figure S3. Normalized SEC trace for *cis*-**P7**-*r*-*cis*-**P1** obtained in THF stabilized with BHT using a polystyrene standard.

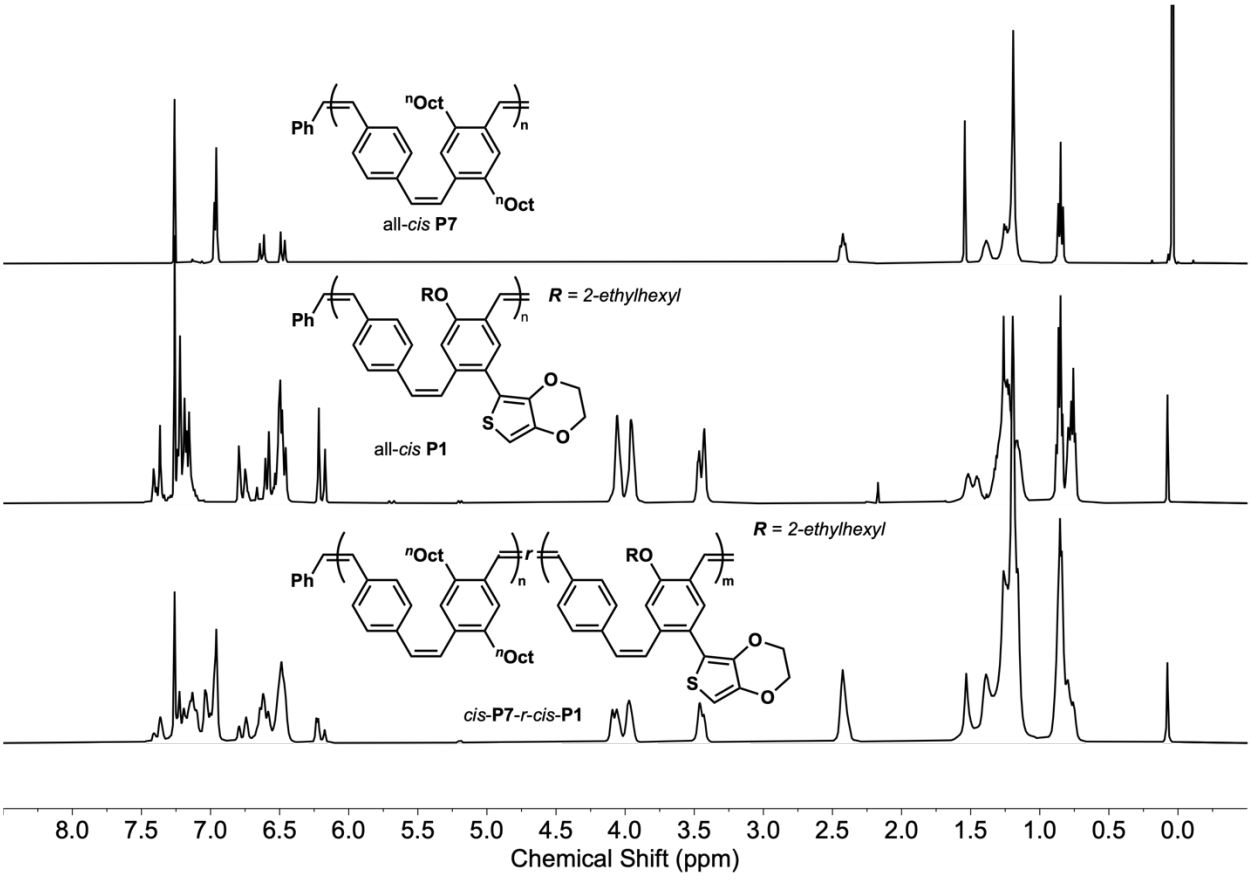

Figure S4. Overlayed ^{1}H NMR spectra of homopolymers all-*cis* **P7** (top) and all-*cis* **P1** (middle), and random copolymer *cis*-**P7**-*r*-*cis*-**P1** after isolation (bottom) in $CDCl_3$.

*Triblock Copolymer Synthesis of cis-**P7**-b-cis-**P8**-b-cis-**P1***

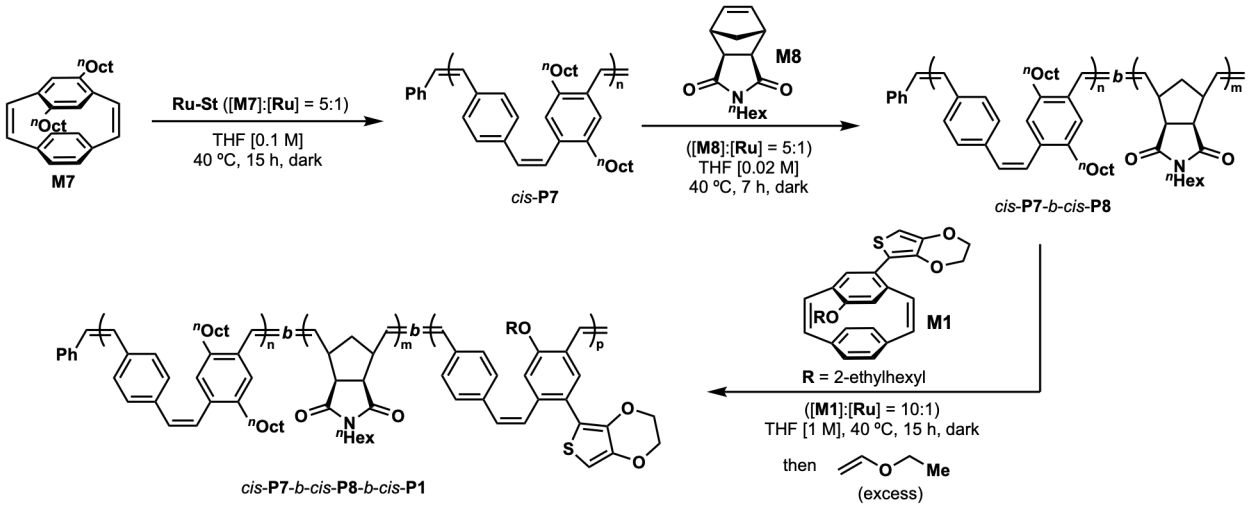

Inside a nitrogen-filled glovebox, a solution of **Ru-St** (5 mg, 0.006 mmol, 1 equiv) in THF (0.3 mL) was added to a 1-dram vial containing monomer **M7** (13 mg, 0.03 mmol, 5 equiv) and a stir bar. The mixture was stirred at 40 °C for 15 h until full conversion of **M7**. 0.1 mL was transferred to another 1-dram vial and quenched with ethyl vinyl ether (50 μL) and allowed to stir for an additional 30 min at room temperature. The remainder of the original mixture was diluted with THF (0.8 mL) then transferred to the vial containing the measured **M8** (5 mg, 0.02 mmol) in THF (1 mL) and a stir bar and was stirred at 40 °C for 7 h until full conversion of **M8**. Half of the mixture (1 mL) was transferred to another 1-dram vial and quenched with ethyl vinyl ether (50 μL) and allowed to stir for an additional 30 min at room temperature. The remainder of the mixture was transferred to a smaller 2 mL vial, sealed with a cap and pierced with a needle. The vial was placed in a Schlenk flask and sealed with electrical tape. The Schlenk flask was removed from the glove box and placed under high vacuum on a Schlenk line for 45 min. After complete removal of the solvent, the Schlenk flask was taken back to the glove box. The remaining residue was diluted with THF (0.04 mL) then transferred to the vial containing the measured **M1** (9 mg, 0.02 mmol) and a stir bar. The reaction was stirred at 40 °C for 48 h and 87% of **M1** was consumed. Once cooled to room temperature, the reaction was quenched inside the glovebox using excess ethyl vinyl ether (0.1 mL) and stirred for an additional 30 min at room temperature. The mixture was then taken outside the glovebox and two cycles of precipitation with addition of methanol, centrifugation (9500 rpm for 10 min), and decantation afforded the corresponding isolated polymer *cis*-**P7**-*b*-*cis*-**P8**-*b*-*cis*-**P1**. The polymer was wrapped in aluminum foil, concentrated under reduced pressure, and stored under a nitrogen atmosphere at –20 °C to prevent any undesired photoisomerization.

First Block: M_n^{theo} = 2.9 kg/mol, M_n^{exp} = 2.3 kg/mol, $Đ$ = 1.11

Diblock Copolymer: M_n^{theo} = 3.4 kg/mol, M_n^{exp} = 4.2 kg/mol, $Đ$ = 1.25

Full Triblock Copolymer: M_n^{theo} = 7.5 kg/mol, M_n^{exp} = 7.3 kg/mol, $Đ$ = 1.18

^{1}H NMR (500 MHz, $CDCl_3$) δ 7.35–7.29 (m, 1 H), 7.17–7.13 (m, 2 H), 7.13–6.94 (m, 4 H), 6.94–6.85 (m, 3 H), 6.76–6.64 (m, 1 H), 6.62–6.48 (m, 2 H), 6.48–6.35 (m, 4 H), 6.18–6.07 (m, 1 H), 5.47–5.34 (m, 1 H), 4.05–3.82 (m, 4 H), 3.43–3.32 (m, 3 H), 3.32–2.81 (m, 2 H), 2.43–2.29 (m, 2 H), 2.29–1.88 (m, 1 H), 1.62–1.40 (m, 3 H), 1.40–1.26 (m, 4 H), 1.26–0.95 (m, 28 H), 0.87–0.74 (m, 10 H), 0.73–0.62 (m, 4 H) ppm.

^{13}C NMR (126 MHz, $CDCl_3$) δ 178.3, 156.1, 141.4, 138.4, 138.0, 137.9, 137.3, 137.2, 136.2, 136.0, 135.9, 135.7, 133.3, 132.2, 130.4, 130.2, 130.1, 129.8, 129.6, 129.1, 128.9, 128.8, 125.7, 125.0, 123.3, 115.8, 115.6, 113.2, 98.5, 70.6, 64.6, 64.4, 52.7, 42.0, 39.2, 39.0, 38.9, 33.3, 32.1, 31.5, 30.9, 30.6, 29.7, 29.4, 29.1, 27.9, 26.7, 26.6, 24.0, 23.2, 22.8, 22.7, 14.3, 14.2, 14.1, 11.1 ppm.

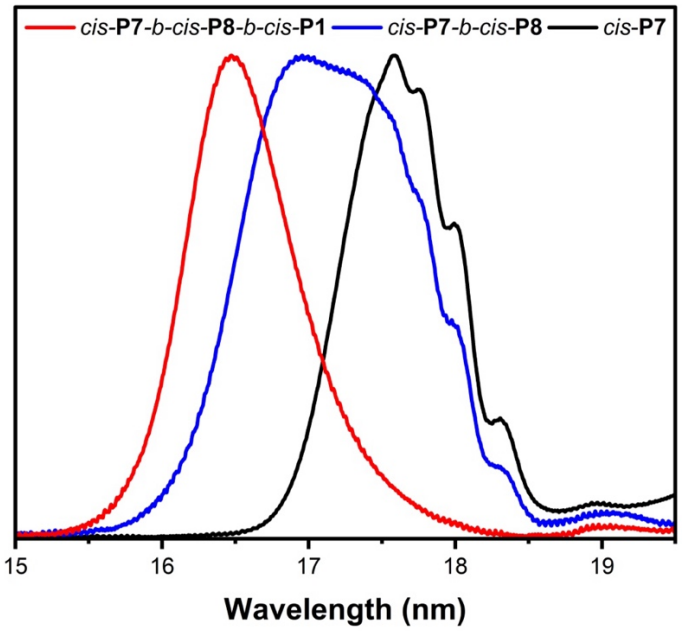

Figure S5. Normalized SEC traces showing chain extension. SEC traces obtained in THF stabilized with BHT using a polystyrene standard.

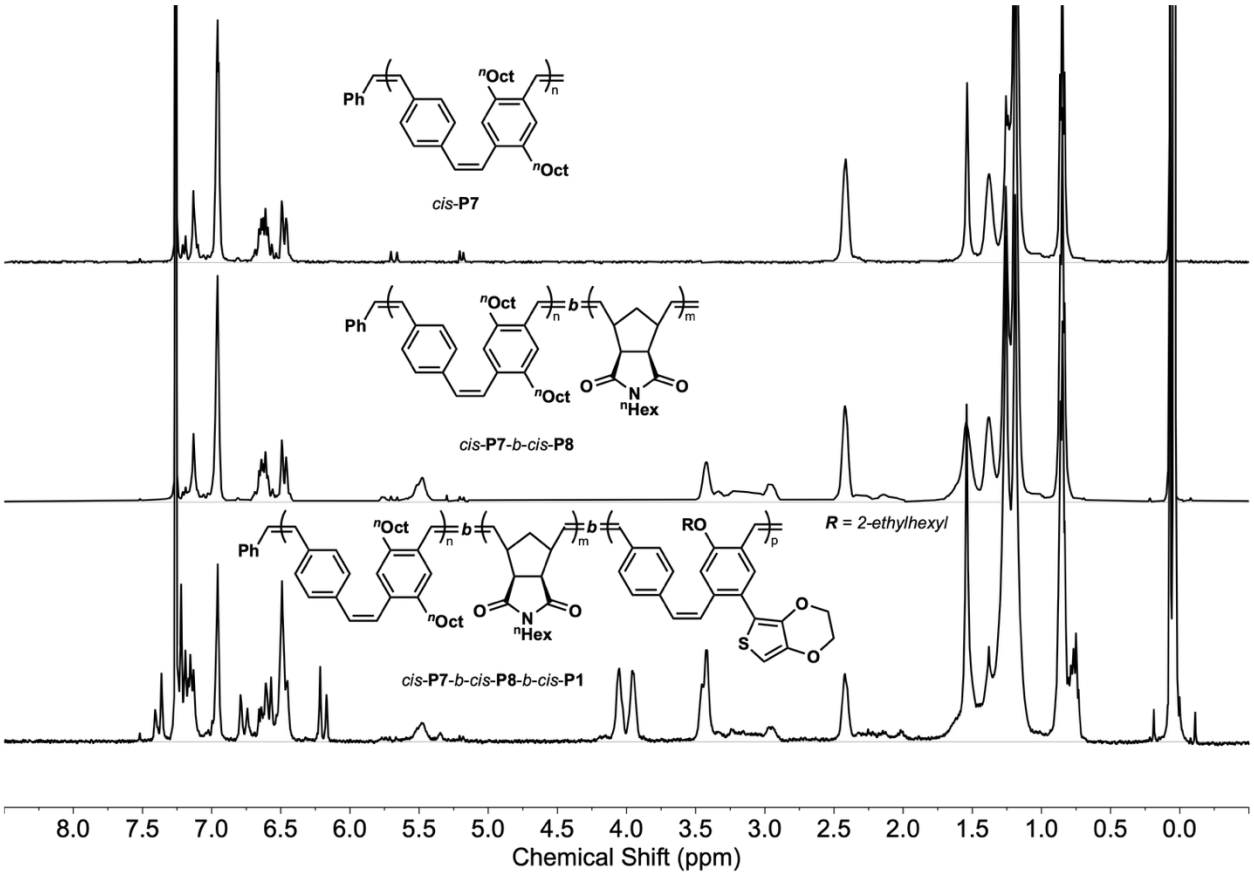

Figure S6. Overlayed ^{1}H NMR spectra of homopolymers all-*cis* **P7** (top) and diblock copolymer *cis*-**P7**-b-*cis*-**P8** (middle), and isolated triblock copolymer *cis*-**P7**-*b*-*cis*-**P8**-*b*-*cis*-**P1** (bottom) in $CDCl_3$.

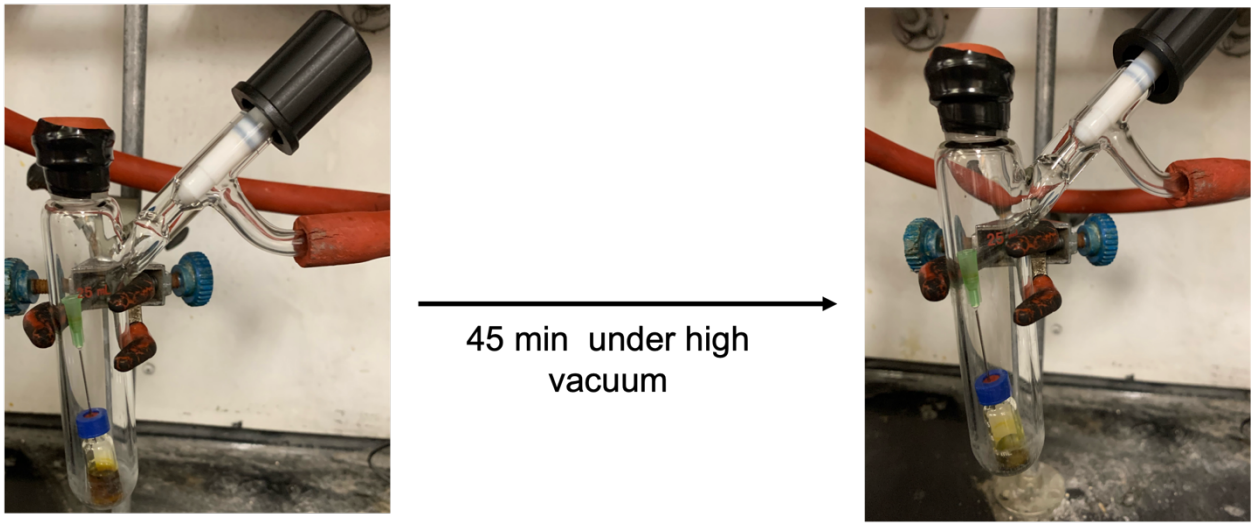

Figure S7. Removal of the solvent under high vacuum outside of the glove box.

Solution-State Photoisomerization:

Photoisomerization of all-cis PPVs to all-trans PPVs: **General Procedure C**

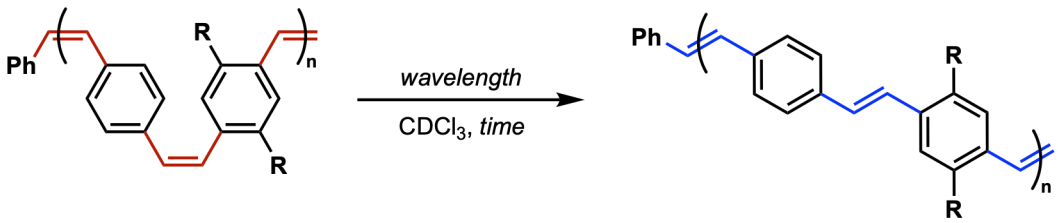

All-*cis* PPV samples at a concentration of 4 mg/mL in $CDCl_3$ were irradiated at room temperature. For UV photoisomerization, two 350 nm UV lamps were placed 5 mm away from the sample and the reaction was monitored over time. For visible light photoisomerization, one Kessil lamp (either 456 nm [55W] or 525 nm [45W]) was placed 5 mm away from the sample and a fan was used to avoid undesired heating of the reaction. Samples were wrapped in aluminum foil between irradiation periods and NMR analyses.

*UV and Visible Light Photoisomerizations of all-cis **P1***

Photoisomerization of all-*cis* **P1** using UV light

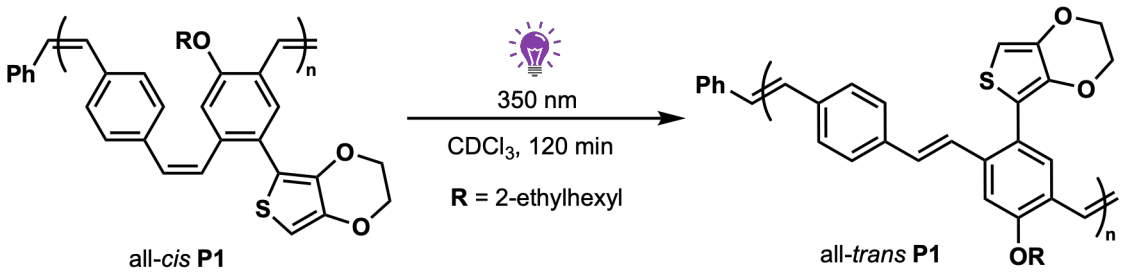

The photoisomerization was conducted following **General Procedure C** using two 350 nm UV lamps. While the poor solubility of all-*trans* **P1** in organic solvents precluded SEC analysis and ^{13}C NMR, almost complete isomerization (98%) was achieved over 2 h as shown by ^{1}H NMR analysis and UV–vis absorption spectroscopy (see UV–Visible Absorption Spectra section below).

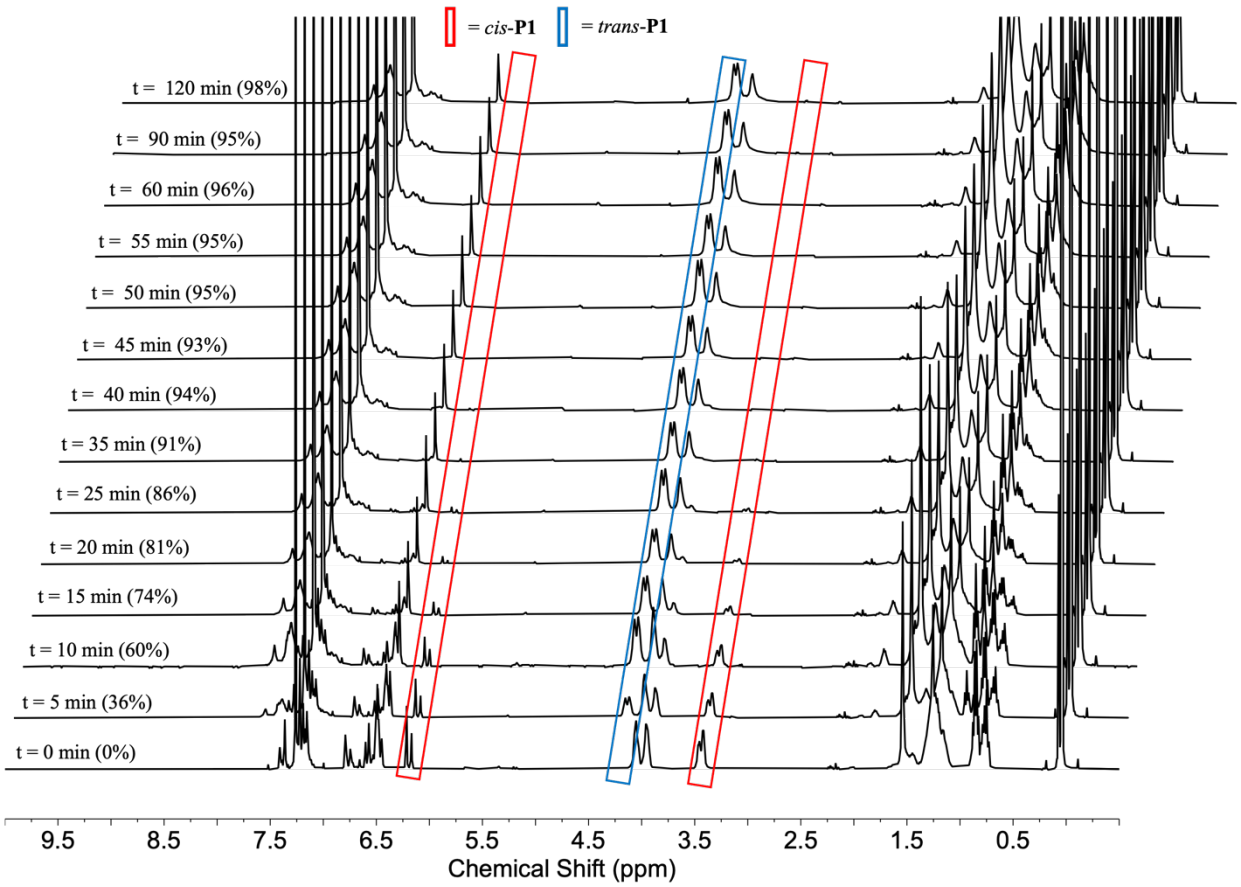

Figure S8. Stacked ^{1}H NMR spectra monitoring the isomerization of all-*cis* **P1** to all-*trans* **P1** under UV light (350 nm) over time in $CDCl_3$. Conversion was determined using hexamethyldisilane as an internal standard by comparing the integration of a characteristc peak of *cis*-**P1** at 6.19 ppm relative to that of the standard (0.08 ppm) over time.

Photoisomerization of all-*cis* **P1** using blue light

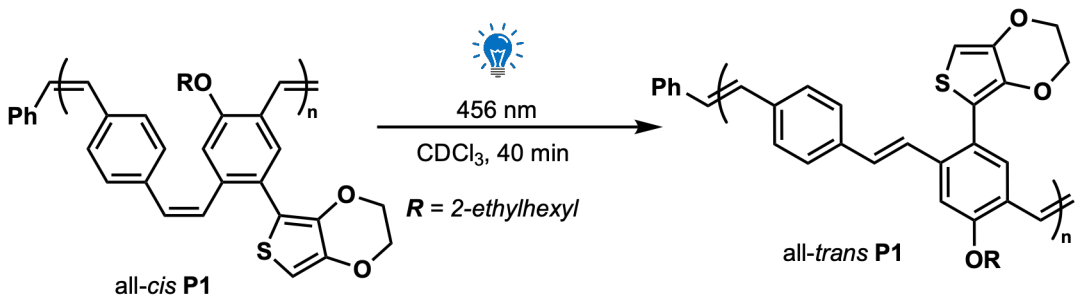

The photoisomerization was conducted following **General Procedure C** using a 456 nm LED. While the poor solubility of all-*trans* **P1** in organic solvents precluded SEC analysis and ^{13}C NMR, complete isomerization (>99%) was achieved over 40 min as shown by ^{1}H NMR analysis and UV–vis absorption spectroscopy (see UV–Visible Absorption Spectra section below).

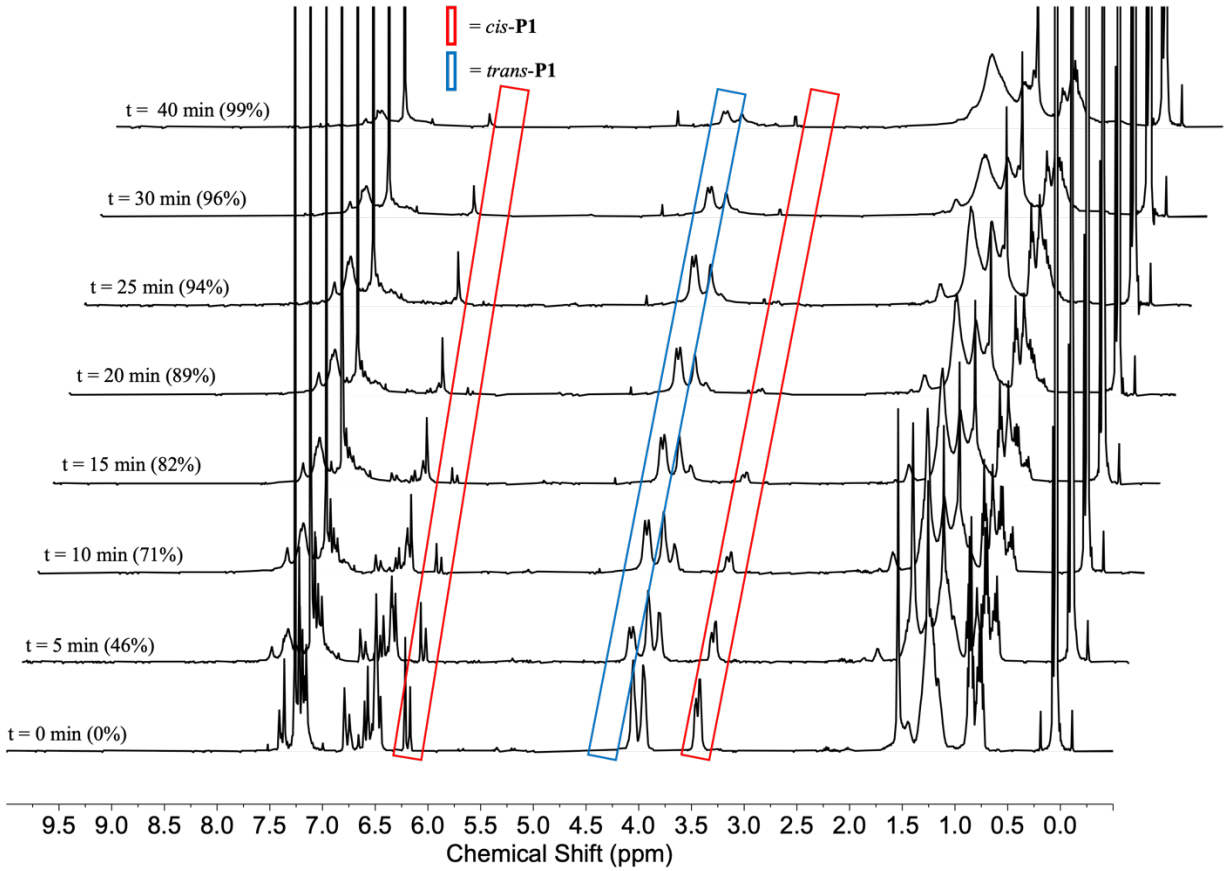

Figure S9. Overlayed ^{1}H NMR spectra of the photoisomerization of all-*cis* **P1** under blue light in $CDCl_3$. Conversion was determined using hexamethyldisilane as an internal standard by comparing the integration of a characteristc peak of *cis*-**P1** at 6.19 ppm relative to a that of the standard (0.08 ppm) over time. The

slight decrease in the *trans*-**P1** signal is attributed to partial insolubility of the polymer as the *trans* content increases.

Photoisomerization of all-*cis* **P1** using green light

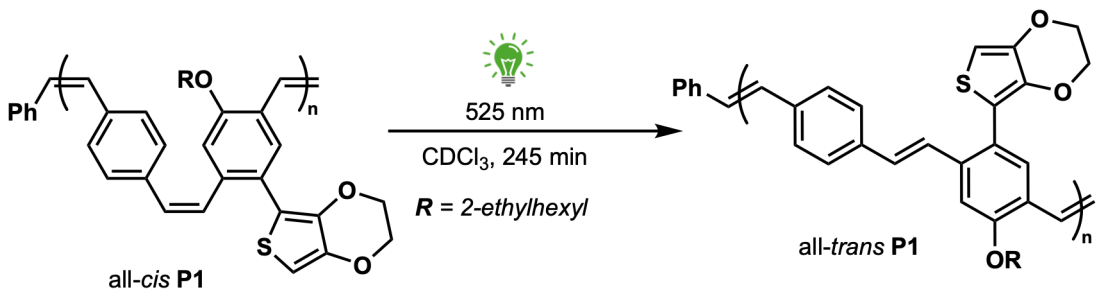

The photoisomerization was conducted following **General Procedure C** using a 525 nm LED. While the poor solubility of all-*trans* **P1** in organic solvents precluded SEC analysis and ^{13}C NMR, almost complete isomerization (98%) was achieved over 245 min as shown by ^{1}H NMR analysis and UV–vis absorption spectroscopy (see UV–Visible Absorption Spectra section below).

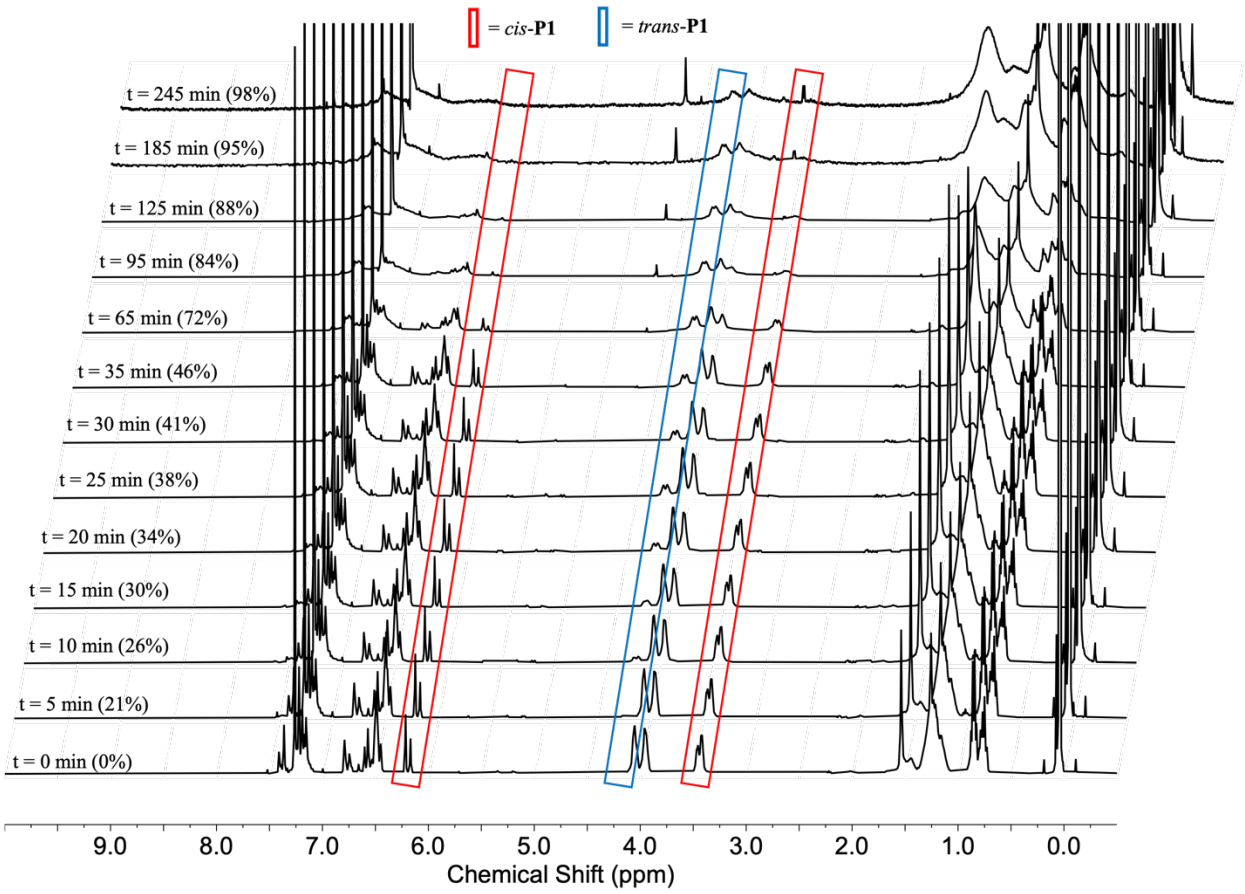

Figure S10. Overlayed ^{1}H NMR spectra of the photoisomerization of all-*cis* **P1** under green light in $CDCl_3$. Conversion determined by comparing difference in integration of a *cis*-**P1** peak (6.19 ppm) relative to a hexamethyldisilane internal standard signal (0.08 ppm) over time. The slight decrease in the *trans*-**P1** signal is attributed to partial insolubility of the polymer as the *trans* content increases.

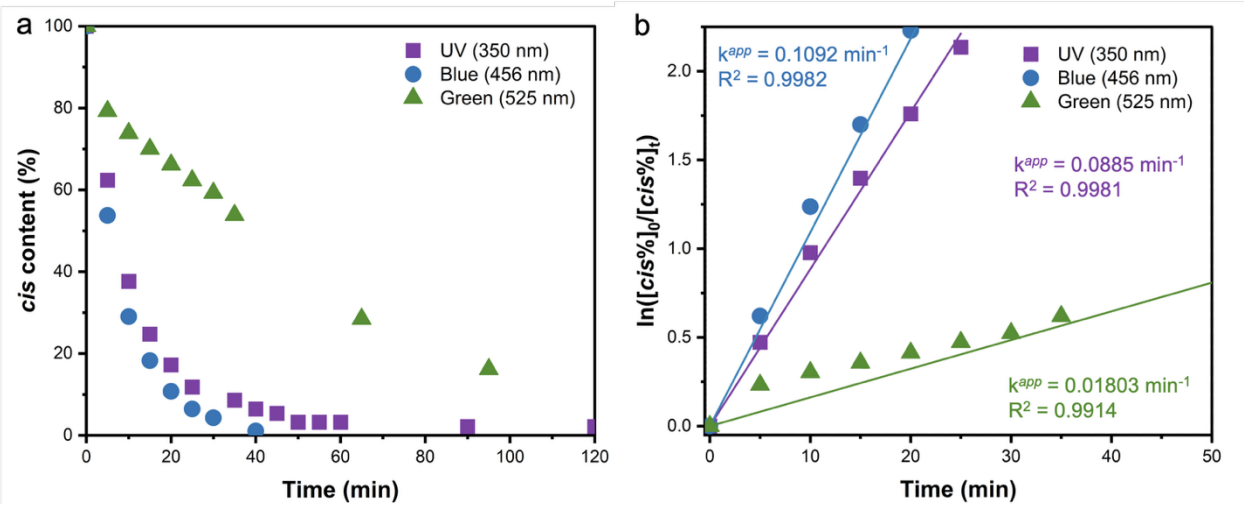

Figure S11. **a**, Monitoring the isomerization (overlayed plots) during the photoisomerization of all-*cis* **P1** using UV, blue, and green light. **b**, Overlayed kinetics plots in the photoisomerization of all-*cis* **P1** using UV, blue, and green light.

*UV and Visible Light Photoisomerizations of all-cis **P7***

Photoisomerization of all-*cis* **P7** using UV light

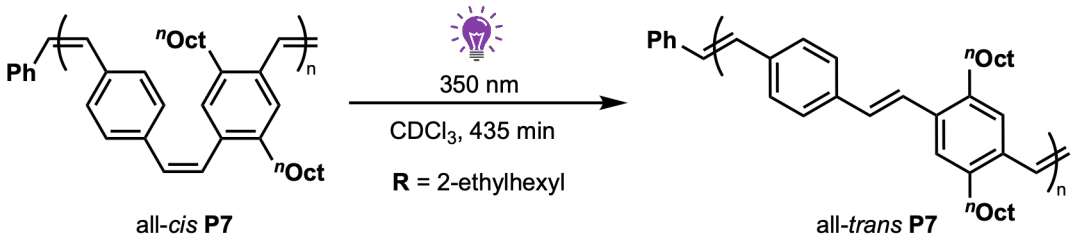

The photoisomerization was conducted following **General Procedure C** using two 350 nm UV lamps. While the poor solubility of all-*trans* **P7** in organic solvents precluded SEC analysis and ^{13}C NMR, complete isomerization (>99%) was achieved over 435 min as shown by ^{1}H NMR analysis and UV–vis absorption spectroscopy (see UV–Visible Absorption Spectra section below).

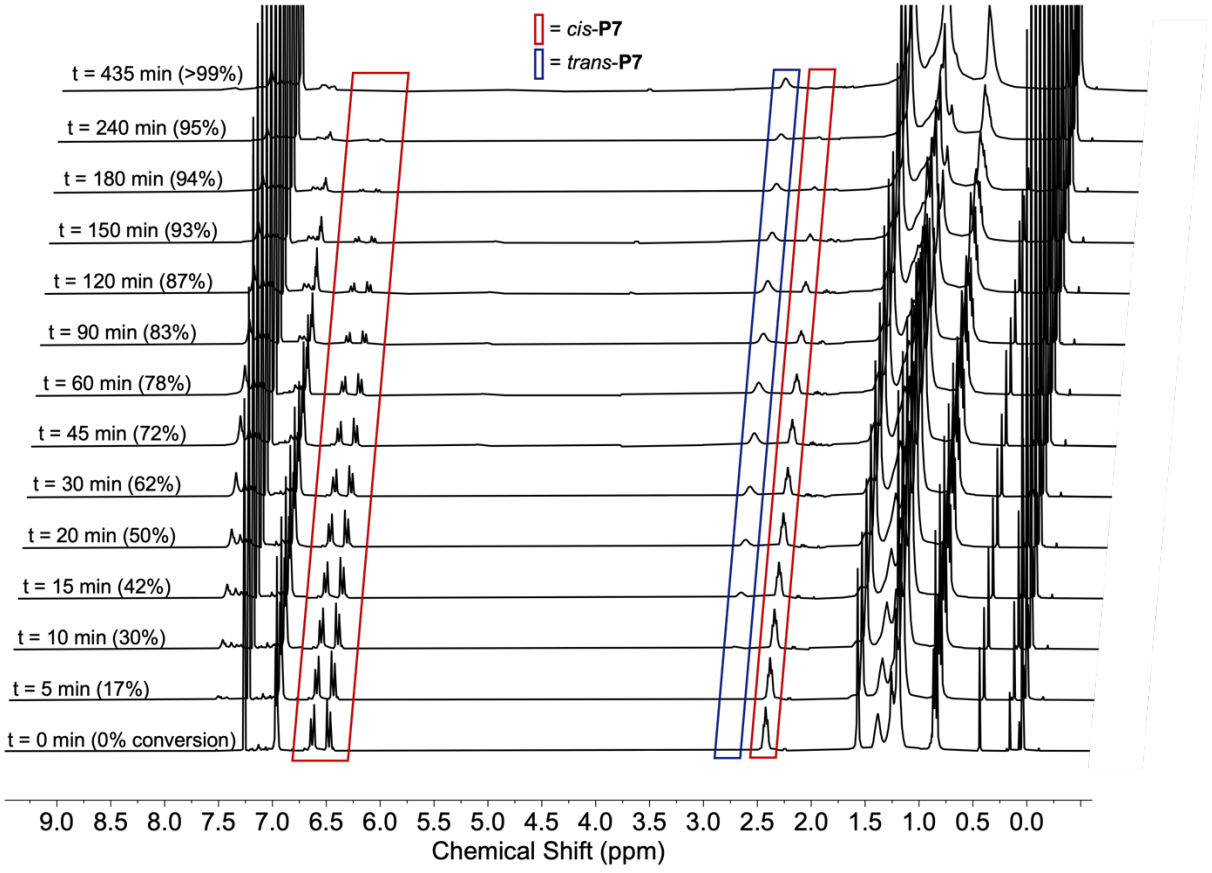

Figure S12. Overlayed ^{1}H NMR spectra of the photoisomerization of all-*cis* **P7** under UV light in $CDCl_3$. Conversion determined by comparing difference in integration of a *cis*-**P7** peak (2.97 ppm) relative to a

hexamethyldisilane internal standard signal (0.08 ppm) over time. The slight decrease in the *trans*-**P7** signal is attributed to partial insolubility of the polymer as the *trans* content increases.

Photoisomerization of all-*cis* **P7** using blue light

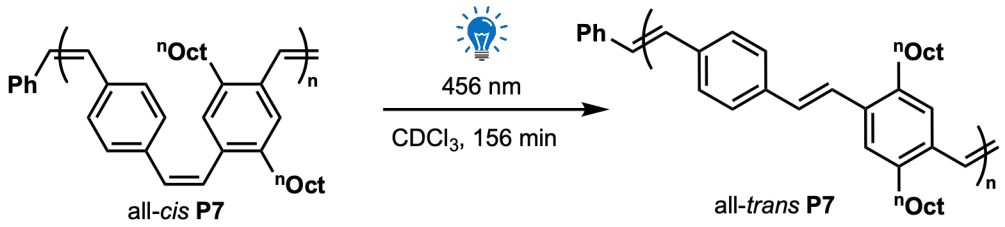

The photoisomerization was conducted following **General Procedure C** using a 456 nm LED. While the poor solubility of all-*trans* **P7** in organic solvents precluded SEC analysis and ^{13}C NMR, almost complete isomerization (97%) was achieved over 156 min as shown by ^{1}H NMR analysis and UV–vis absorption spectroscopy (see UV–Visible Absorption Spectra section below).

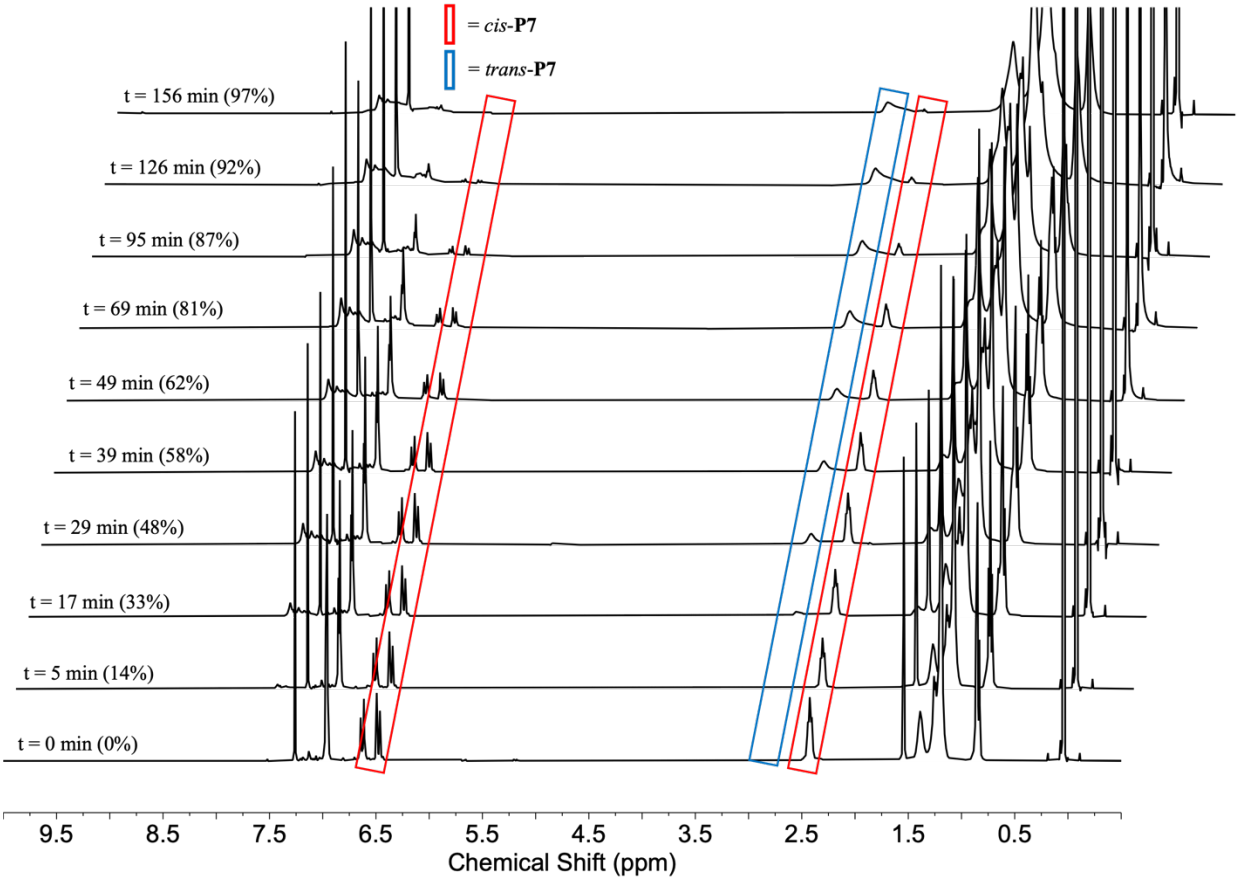

Figure S13. Overlayed ^{1}H NMR spectra of the photoisomerization of all-*cis* **P7** under blue light in $CDCl_3$. Conversion determined by comparing difference in integration of a *cis*-**P7** peak (2.97 ppm) relative to a

hexamethyldisilane internal standard signal (0.08 ppm) over time. The slight decrease in the *trans*-**P7** signal is attributed to partial insolubility of the polymer as the *trans* content increases.

Photoisomerization of all-*cis* **P7** using green light

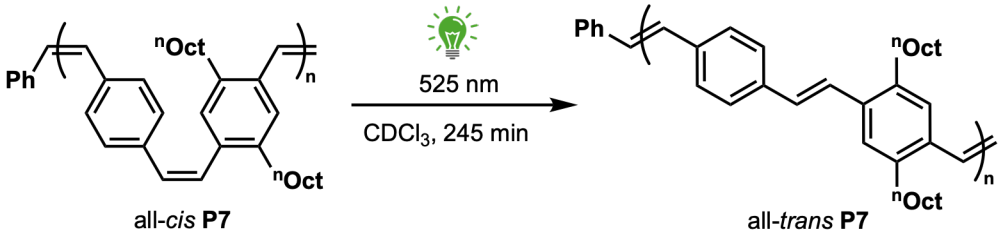

The photoisomerization was attempted following **General Procedure C** using a 525 nm LED. Minimal isomerization (3%) was observed over 4 h of irradiation as shown by ^{1}H NMR analysis.

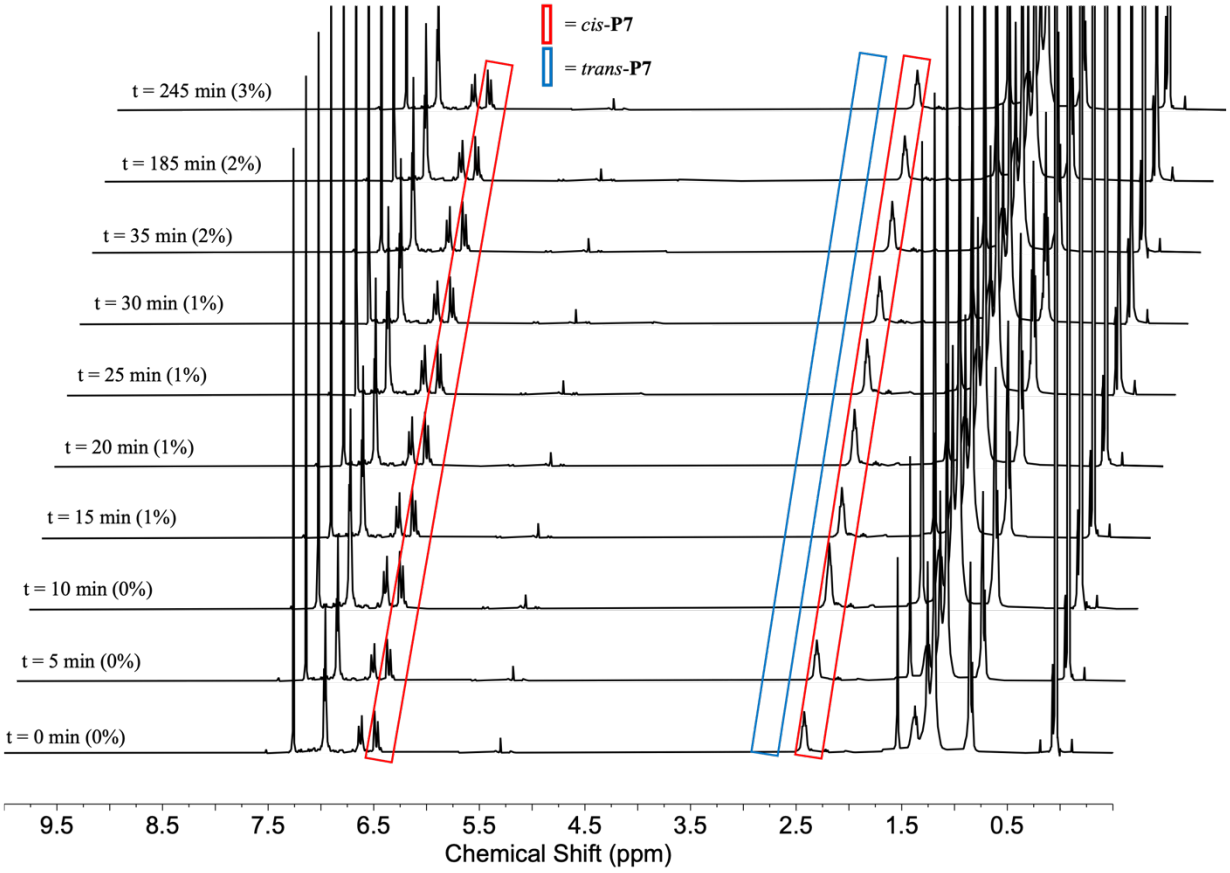

Figure S14. Overlayed ^{1}H NMR spectra of the attempted photoisomerization of *cis*-**P7** under green light in $CDCl_3$. Conversion determined by comparing difference in integration of a *cis*-**P7** peak (2.97 ppm) relative to a hexamethyldisilane internal standard signal (0.08 ppm) over time.

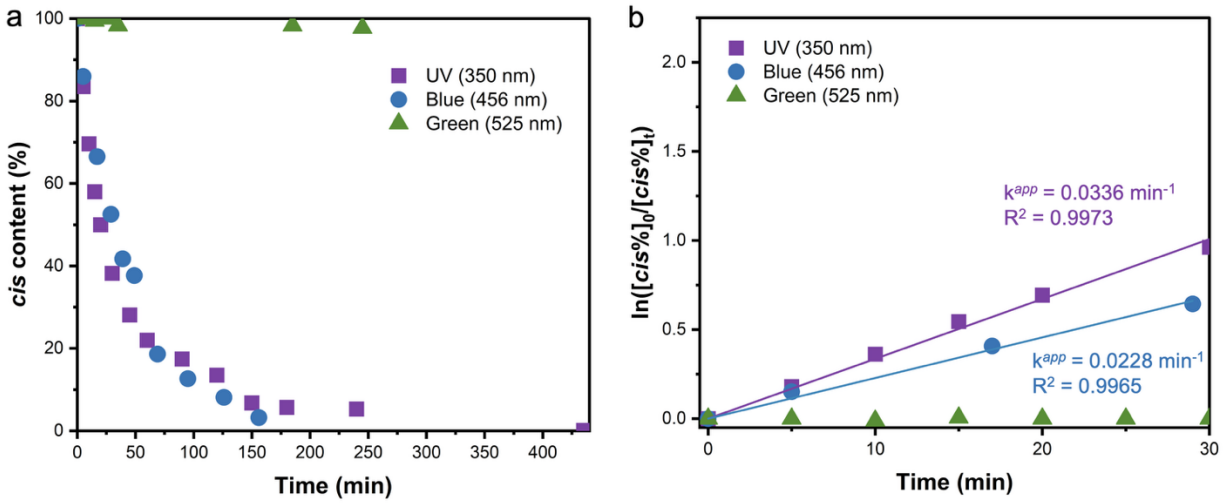

Figure S15. **a**, Monitoring the isomerization (overlayed plots) during the photoisomerization of all-*cis* **P7** using UV, blue, and green light. **b**, Overlayed kinetics plots in the photoisomerization of all-*cis* **P7** using UV, blue, and green light.

UV and Visible Light Photoisomerization of Copolymers

Photoisomerization of *cis*-**P7**-*b*-*cis*-**P1** using UV light

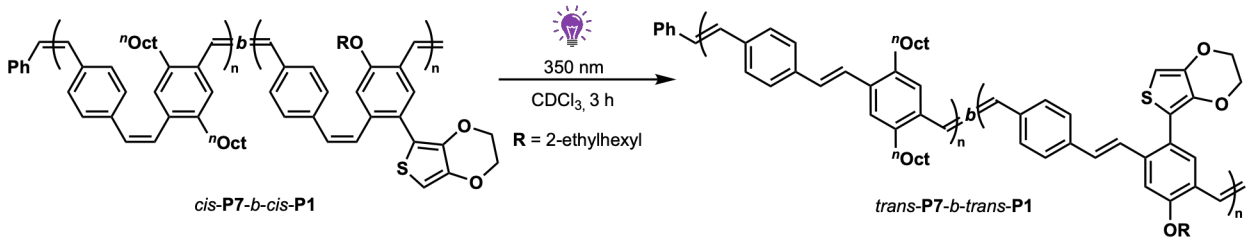

The photoisomerization was conducted following **General Procedure C** using two 350 nm UV lamps. While the poor solubility of *trans*-**P7**-*b*-*trans*-**P1** in organic solvents precluded SEC analysis and ^{13}C NMR, complete isomerization (>99%) of both blocks was achieved over 3 h as shown by ^{1}H NMR analysis and UV–vis absorption spectroscopy (see UV–Visible Absorption Spectra section below).

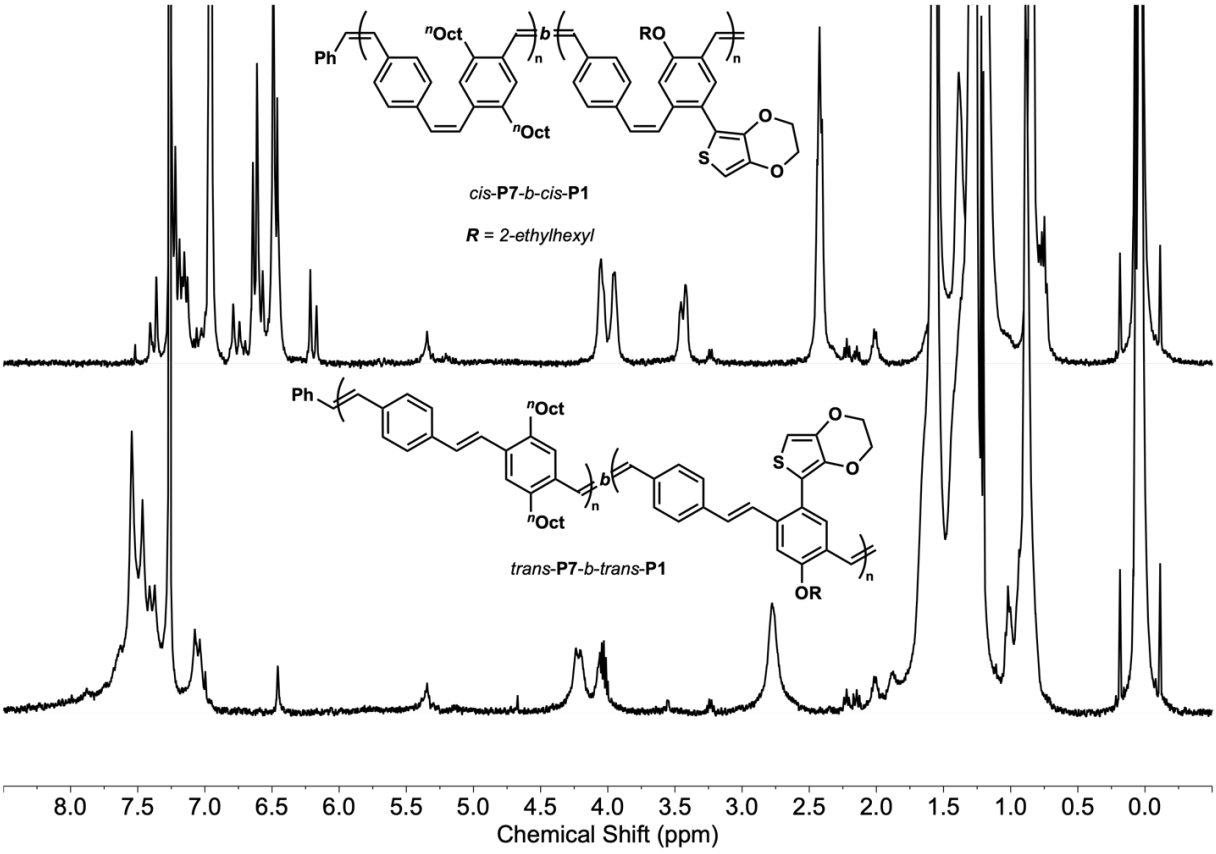

Figure S16. Overlayed ^{1}H NMR spectra comparison of *cis*-**P7**-*b*-*cis*-**P1** (top) and *trans*-**P7**-*b*-*trans*-**P1** (bottom) in $CDCl_3$.

Photoisomerization of *cis*-**P7**-*b*-*cis*-**P1** using green light

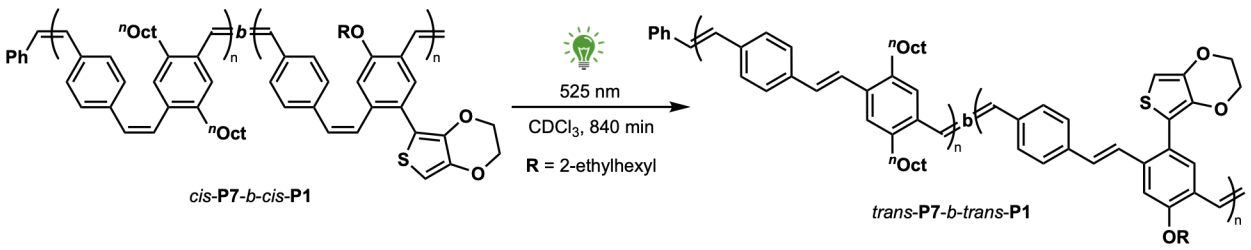

The photoisomerization was conducted following **General Procedure C** using a 525 nm LED. While the poor solubility of *trans*-**P7**-*b*-*trans*-**P1** in organic solvents precluded SEC analysis and ^{13}C NMR, almost complete isomerization (97%) of the **P7** block and complete isomerization (>99%) of the **P1** block was achieved over 14 h as shown by ^{1}H NMR analysis and UV–vis absorption spectroscopy (see UV–Visible Absorption Spectra section below).

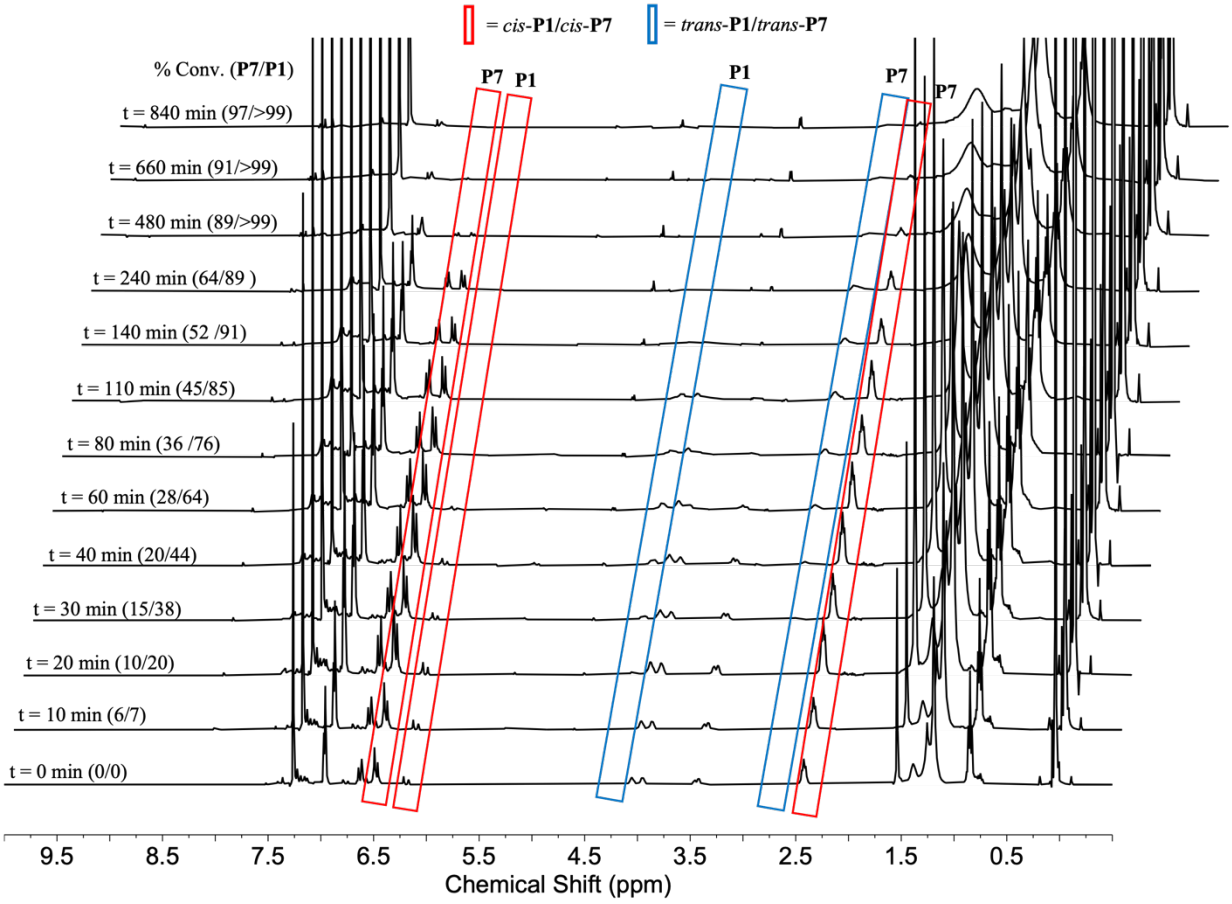

Figure S17. Overlayed ^{1}H NMR spectra of the photoisomerization of *cis*-**P7**-*b*-*cis*-**P1** under green light. Conversion determined through comparing changes in integration of a *cis*-**P1** alkene signal (6.19 ppm), cis-**P7** alkane signal (2.43 ppm) and the hexamethyldisilane internal standard signal (0.06 ppm) over time. The

decrease in the *trans*-**P1** and *trans*-***P7*** signals is attributed to partial insolubility of the polymer as the *trans* content increases.

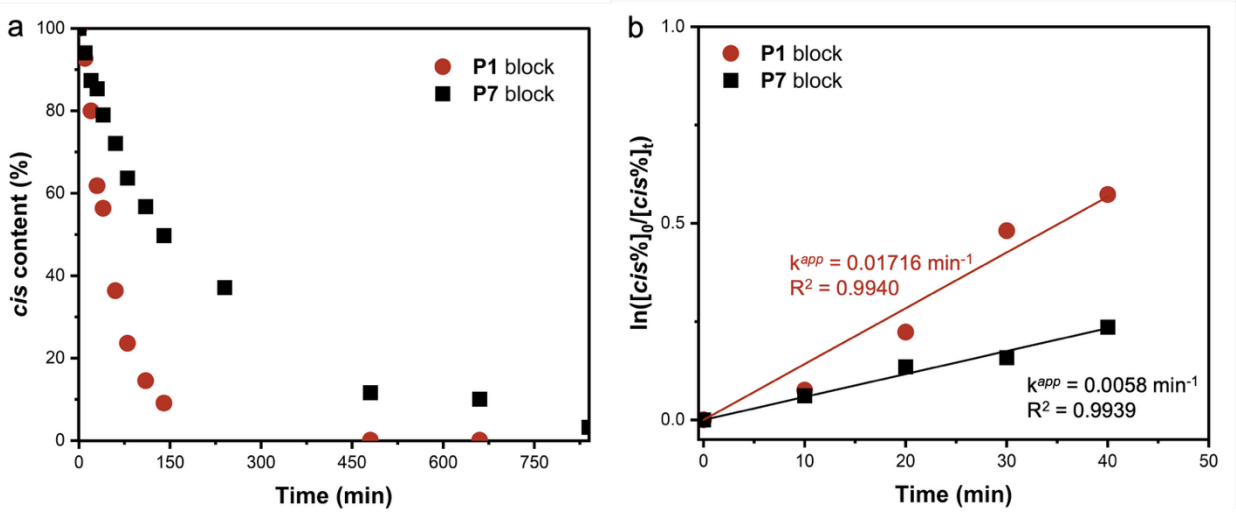

Figure S18. **a**, Monitoring the isomerization of each block (overlayed plots) during the photoisomerization of *cis*-**P7**-*b*-*cis*-**P1** using green light. **b**, Overlayed kinetics plots for each block in the photoisomerization of *cis*-**P7**-*b*-*cis*-**P1** using green light.

Photoisomerization of *cis*-**P7**-*r*-*cis*-**P1** using UV light

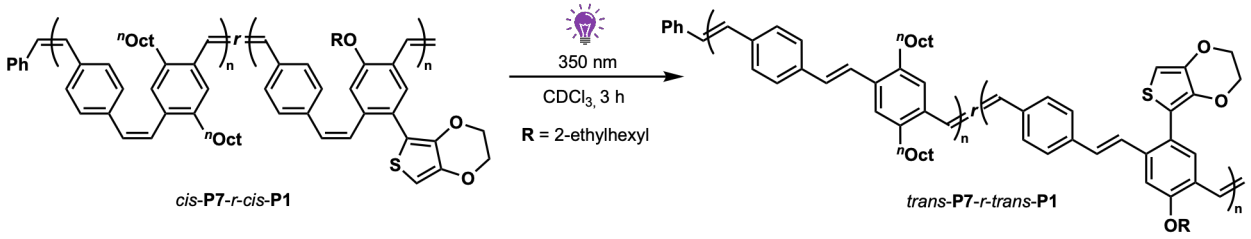

The photoisomerization was conducted following **General Procedure C** using two 350 nm UV lamps. While the poor solubility of *trans*-**P7**-*r*-*trans*-**P1** in organic solvents precluded SEC analysis and ^{13}C NMR, complete isomerization (>99%) of both blocks was achieved over 3 h as shown by ^{1}H NMR analysis and UV–vis absorption spectroscopy (see UV–Visible Absorption Spectra section below).

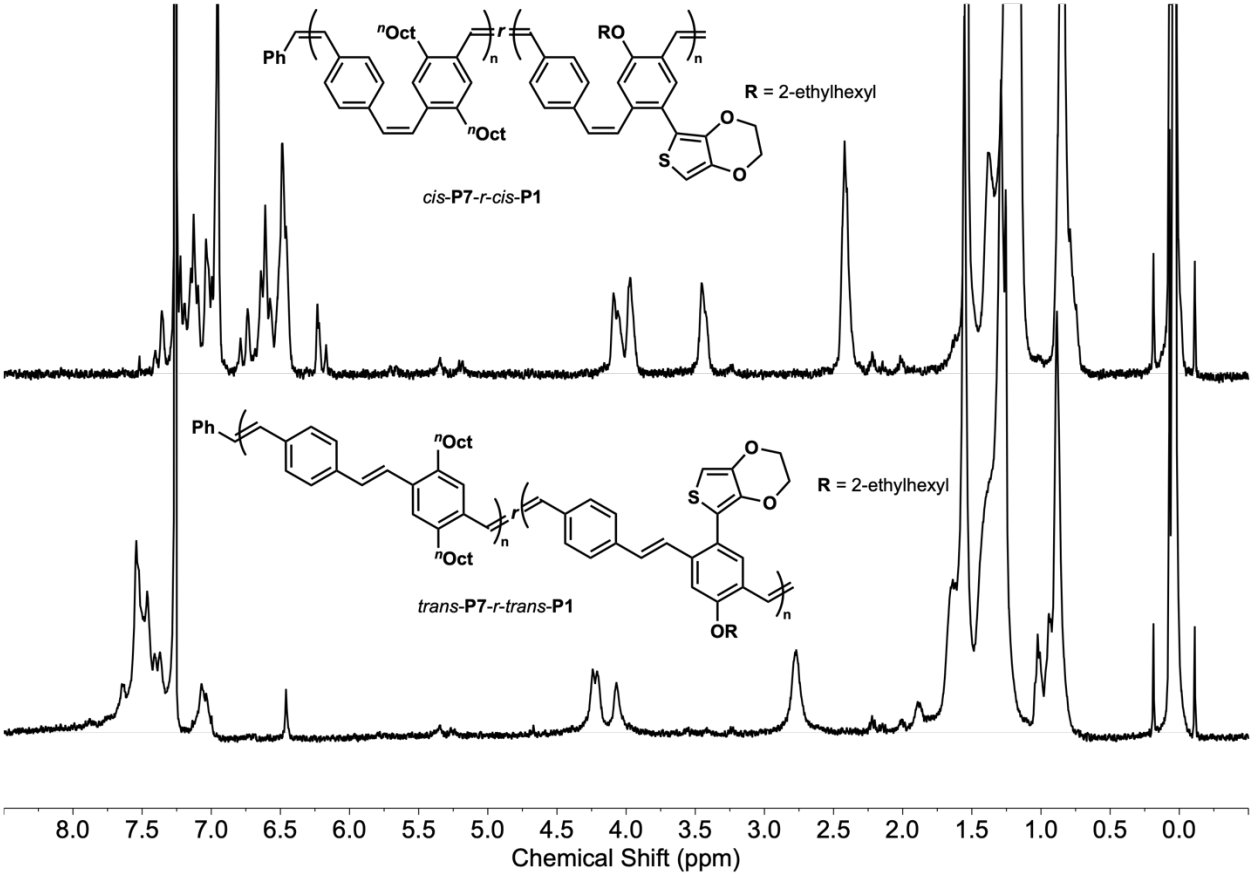

Figure S19. Overlayed ^{1}H NMR spectra comparison of *cis*-**P7**-*r*-*cis*-**P1** (top) and *trans*-**P7**-*r*-*trans*-**P1** (bottom) in $CDCl_3$.

Photoisomerization of *cis*-**P7**-*r*-*cis*-**P1** using green light

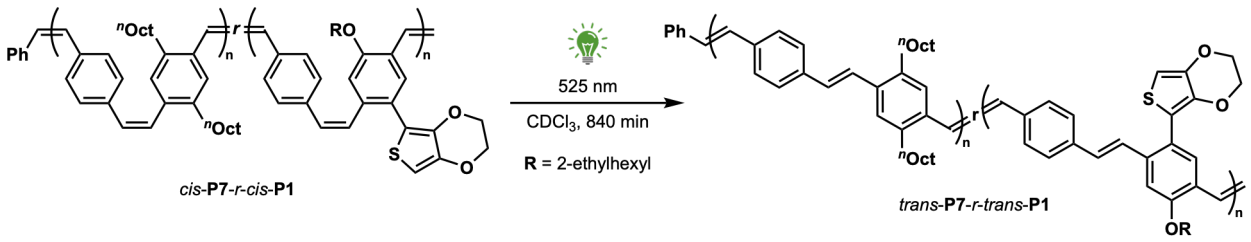

The photoisomerization was conducted following **General Procedure C** using a 525 nm LED. While the poor solubility of *trans*-**P7**-*r*-*trans*-**P1** in organic solvents precluded SEC analysis and ^{13}C NMR, almost complete isomerization (94%) of the **P7** block and (96%) of the **P1** block was achieved over 505 min as shown by ^{1}H NMR analysis and UV–vis absorption spectroscopy (see UV–Visible Absorption Spectra section below).

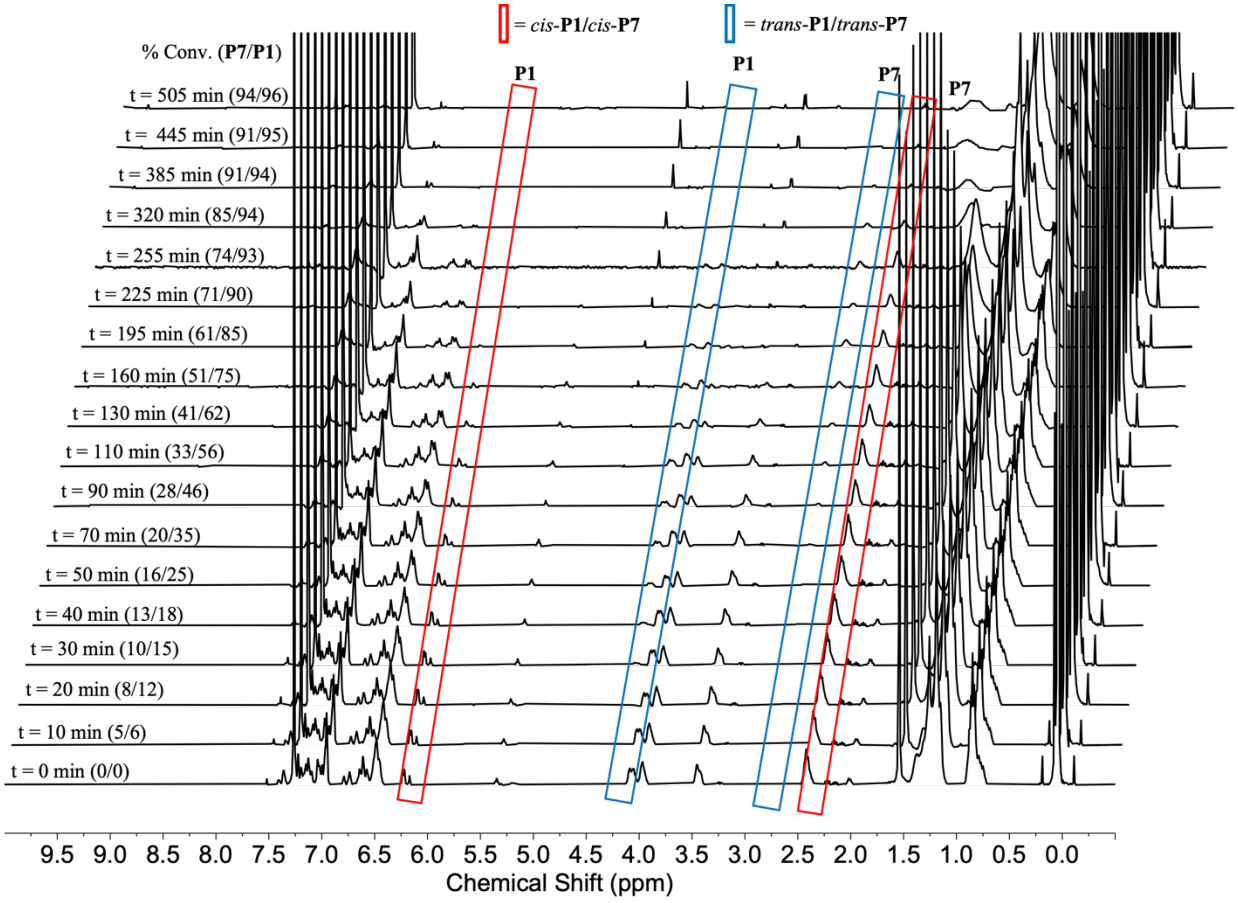

Figure S20. Overlayed ^{1}H NMR spectra of the photoisomerization of *cis*-**P7**-*r*-*cis*-**P1** under green light. Conversion determined through comparing changes in integration of a *cis*-**P1** alkene signal (6.19 ppm), cis-**P7** alkane signal (2.43 ppm) and the hexamethyldisilane internal standard signal (0.06 ppm) over time. The

decrease in the *trans*-**P1** and *trans*-***P7*** signals is attributed to partial insolubility of the polymer as the *trans* content increases.

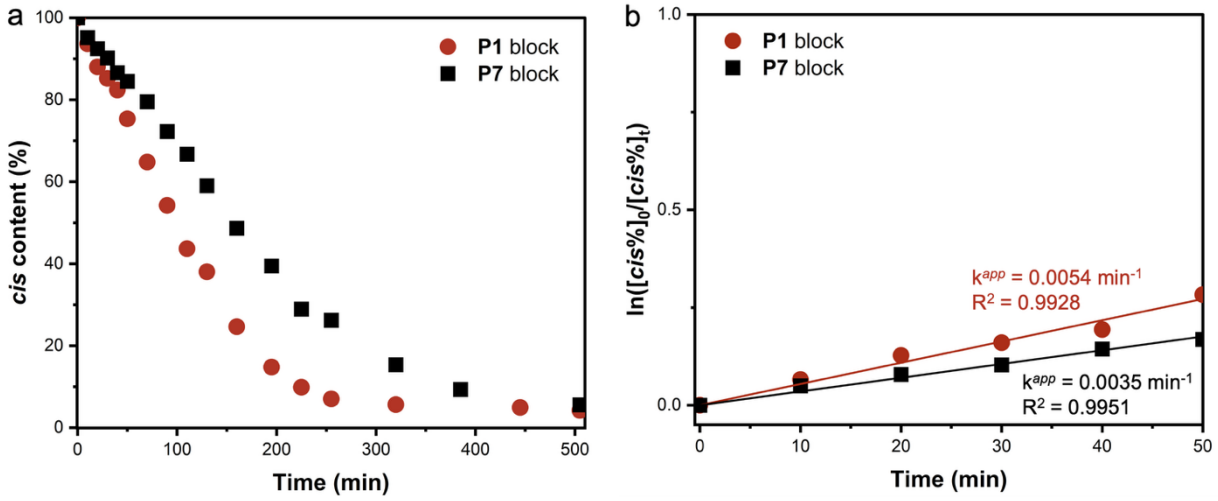

Figure S21. **a**, Monitoring the isomerization of each block (overlayed plots) during the photoisomerization of *cis*-**P7**-*r*-*cis*-**P1** using green light. **b**, Overlayed kinetics plots for each block in the photoisomerization of *cis*-**P7**-*r*-*cis*-**P1** using green light.

Photoisomerization of *cis*-**P7**-*b*-*cis*-**P8**-*b*-*cis*-**P1** using green light

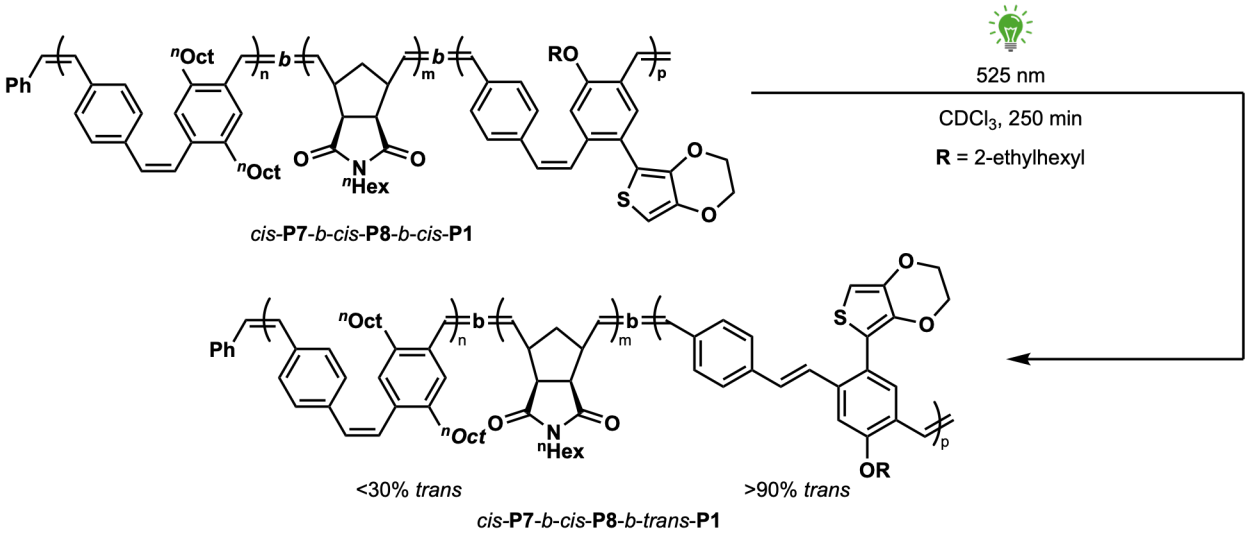

The photoisomerization was conducted following **General Procedure C** using a 525 nm LED. While the poor solubility of *cis*-**P7**-*b*-*cis*-**P8**-*b*-*trans*-**P1** in organic solvents precluded SEC analysis and ^{13}C NMR, almost complete isomerization (91%) of the **P1** block with only partial isomerization (26%) of the **P7** block

was achieved over 230 min as shown by ^{1}H NMR analysis and UV–vis absorption spectroscopy (see UV–Visible Absorption Spectra section below).

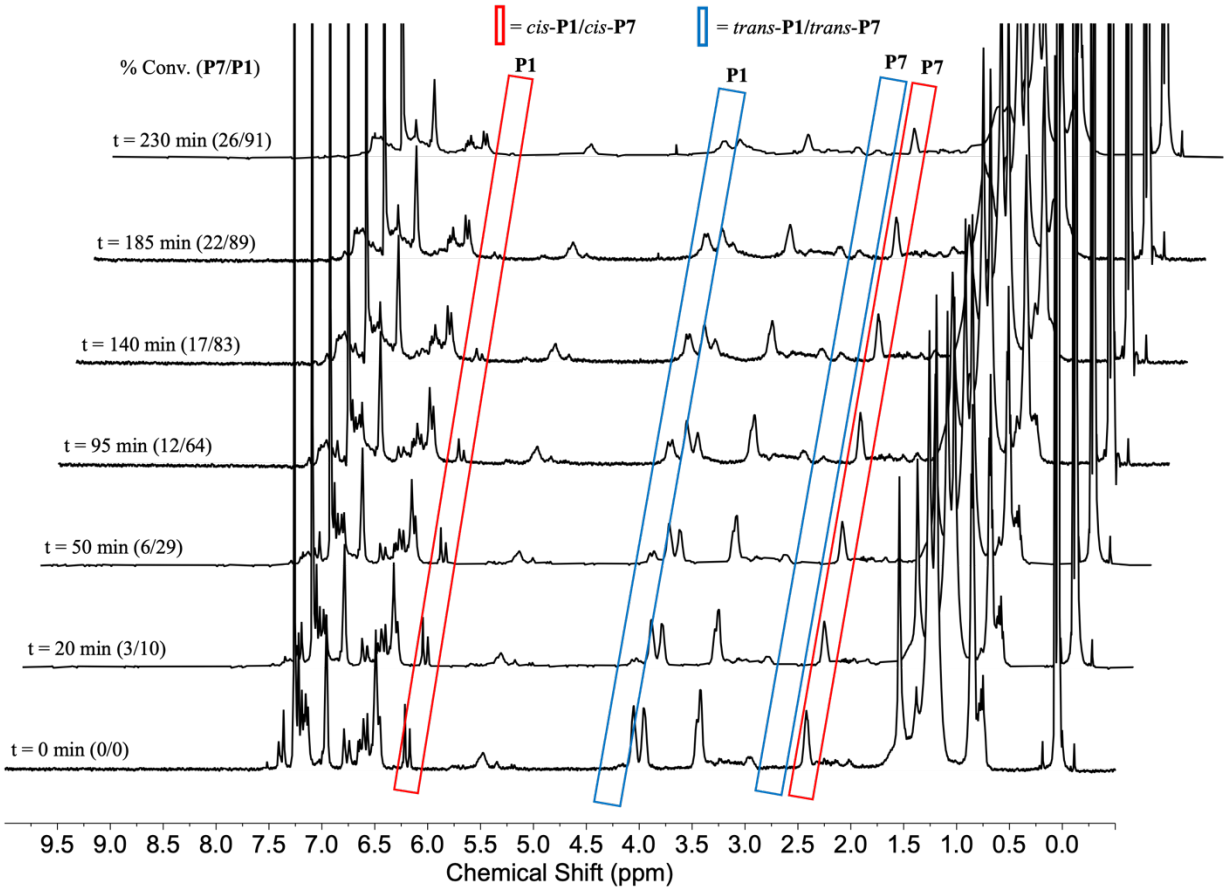

Figure S22. Overlayed ^{1}H NMR spectra of the photoisomerization of *cis*-**P7**-*b*-*cis*-**P8**-*b*-*cis*-**P1** under green light in $CDCl_3$. Conversion determined by comparing difference in integration of a *cis*-**P7** peak (2.47 ppm) and a *cis*-**P1** peak (6.19 ppm) relative to a hexamethyldisilane internal standard signal (0.08 ppm) over time. The decrease in the *trans*-**P1** signals is attributed to partial insolubility of the polymer as the *trans* content increases.

Photoisomerization of *cis*-**P7**-*b*-*cis*-**P8**-*b*-*trans*-**P1** using UV light

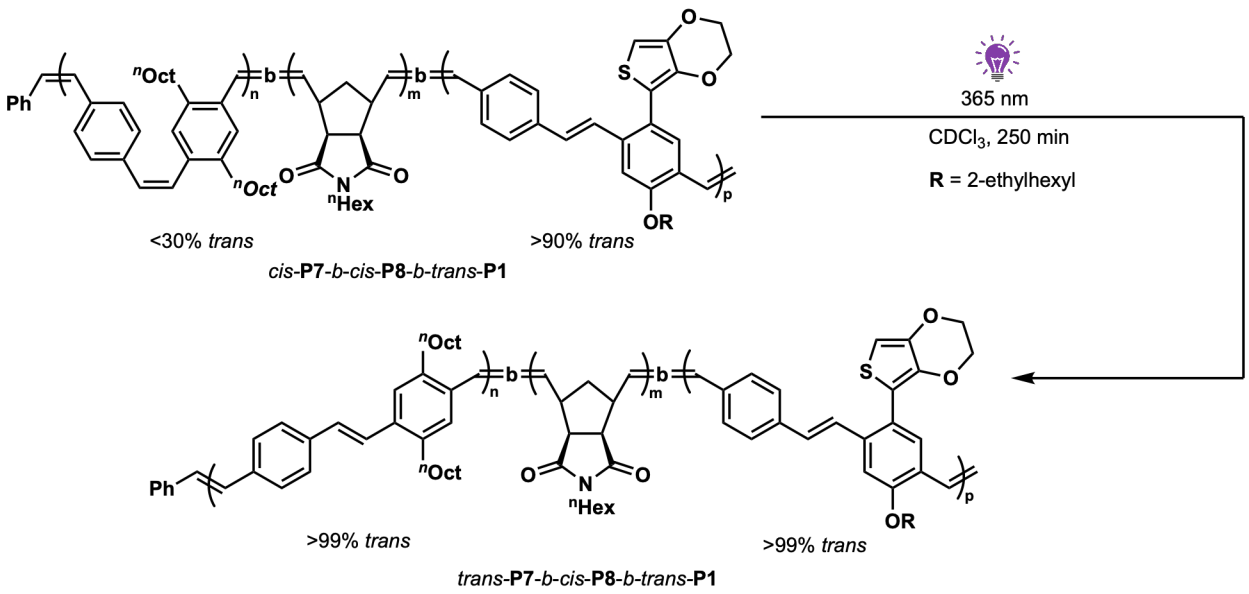

The photoisomerization was conducted following **General Procedure C** using two 350 nm UV lamps. While the poor solubility of *trans*-**P7**-*b*-*cis*-**P8**-*b*-*trans*-**P1** in organic solvents precluded SEC analysis and ^{13}C NMR, almost complete isomerization (97%) of the **P7** block and complete isomerization of the **P1** block was achieved over 4 h (starting at the 230 min time point from **Figure S22**) as shown by ^{1}H NMR analysis and UV–vis absorption spectroscopy (see UV–Visible Absorption Spectra section below).

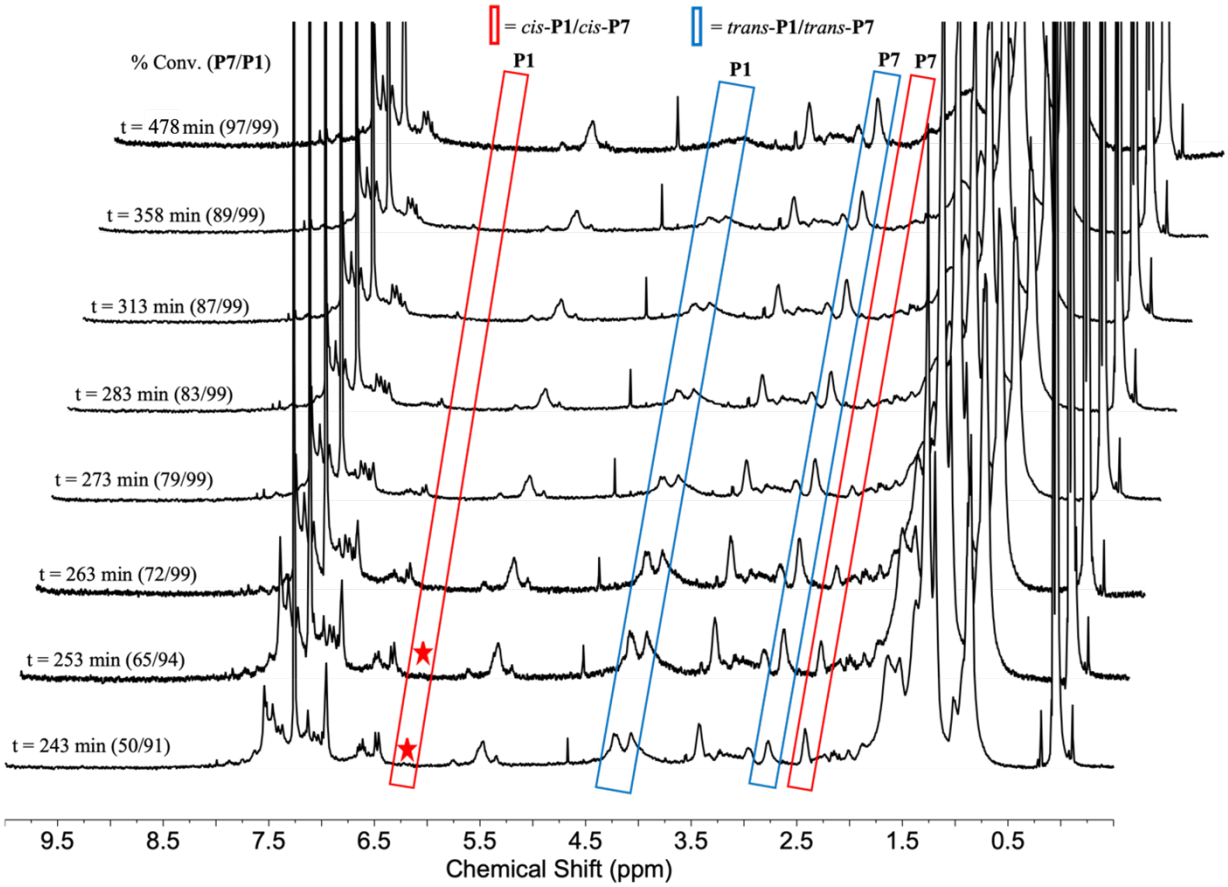

Figure S23. Overlayed ^{1}H NMR spectra of the photoisomerization of *cis*-**P7**-*b*-*cis*-**P8**-*b*-*cis*-**P1** under UV light in $CDCl_3$. Conversion determined by comparing difference in integration of a *cis*-**P7** peak (2.47 ppm) and a *cis*-**P1** peak (6.19 ppm) relative to a hexamethyldisilane internal standard signal (0.08 ppm) over time. The decrease in the *trans*-**P1** signal is attributed to partial insolubility of the polymer as the *trans* content increases.

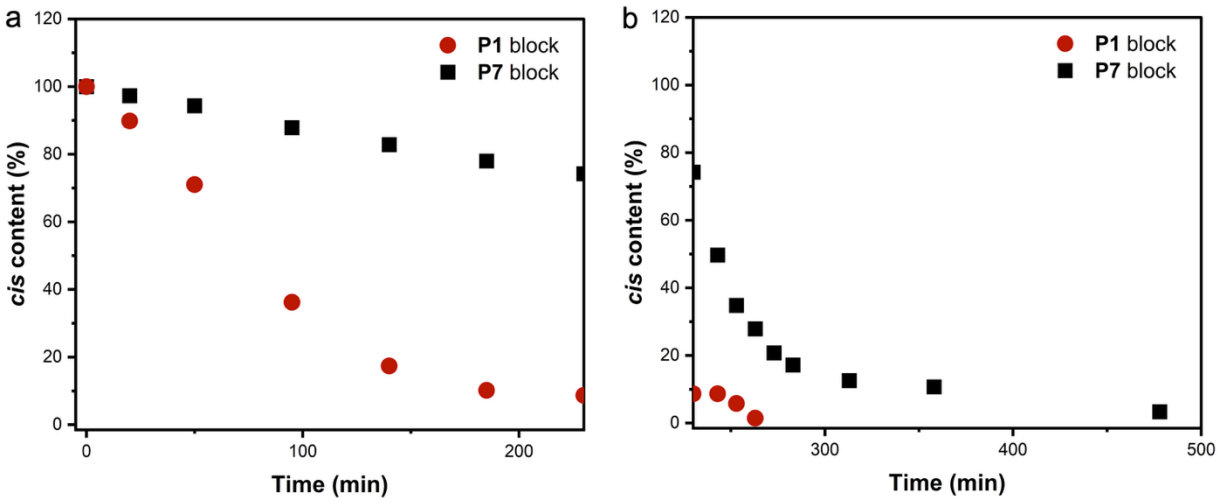

Figure S24. **a**, Overlayed block-resolved *cis* content plots for the photoisomerization of *cis*-**P7**-*b*-*cis*-**P8**-*b*-*cis*-**P1** using green light to access *cis*-**P7**-*b*-*cis*-**P8**-*b*-*trans*-**P1**. **b**, Overlayed block-resolved *cis* content plots for the photoisomerization of *cis*-**P7**-*b*-*cis*-**P8**-*b*-*trans*-**P1** using UV light to access *trans*-**P7**-*b*-*cis*-**P8**-*b*-*trans*-**P1**.

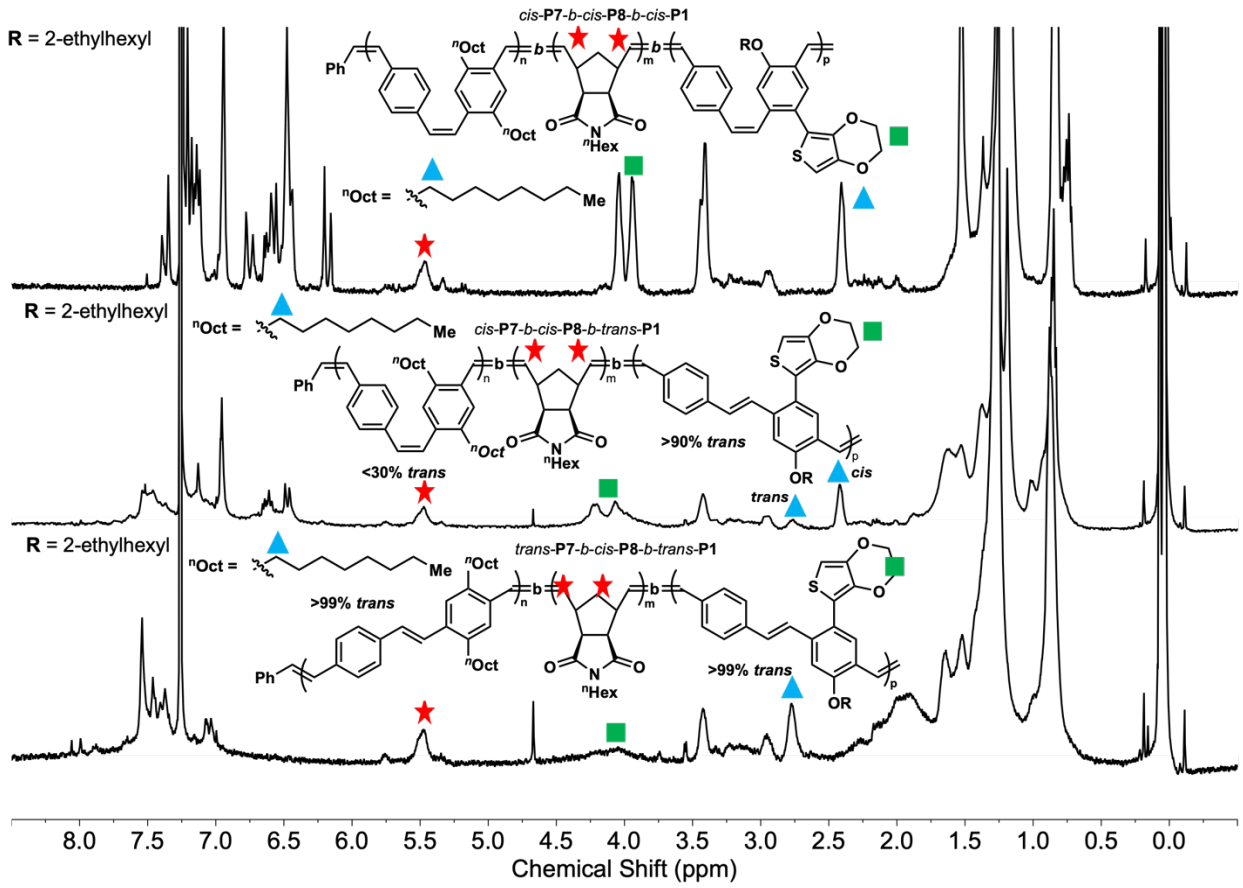

Figure S25. Overlayed ^{1}H NMR spectra of the *cis*-**P7**-*b*-*cis*-**P8**-b-*trans*-**P1** (top), *cis*-**P7**-*b*-*cis*-**P8**-b-*trans*-**P1** (middle) and *trans*-**P7**-*b*-*cis*-**P8**-b-*trans*-**P1** (bottom). Select signals are marked to highlight prominent characteristic signals of each block.

UV–Visible Absorption Spectra

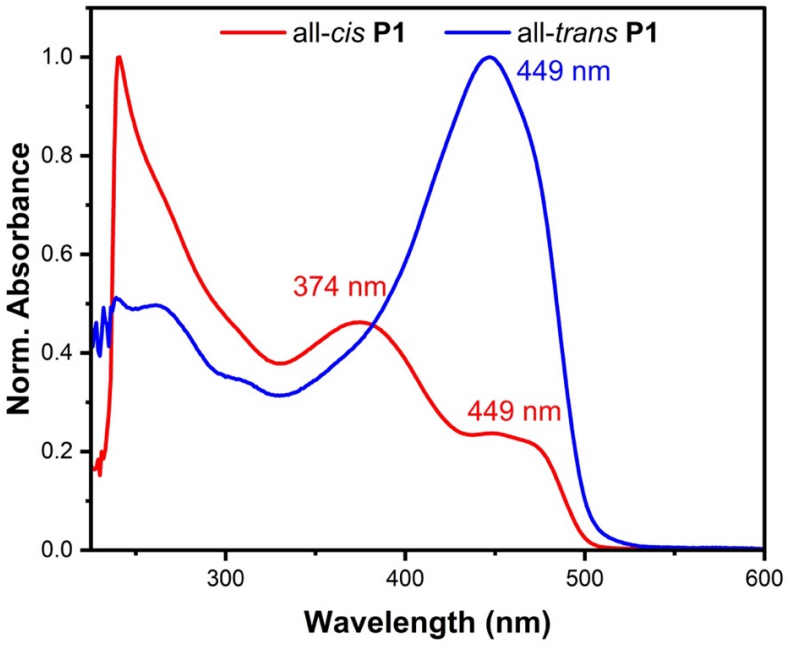

Figure S26. all-*cis* **P1** (M_n^{theo} = 8.6 kg/mol, M_n^{exp} = 9.5 kg/mol, $Đ$ = 1.22) normalized absorbance (C = 5 µg/mL) and all-*trans* **P1** (insolubility prevented SEC analysis in THF) normalized absorbance (C = 5 µg/mL) traces in $CHCl_3$.

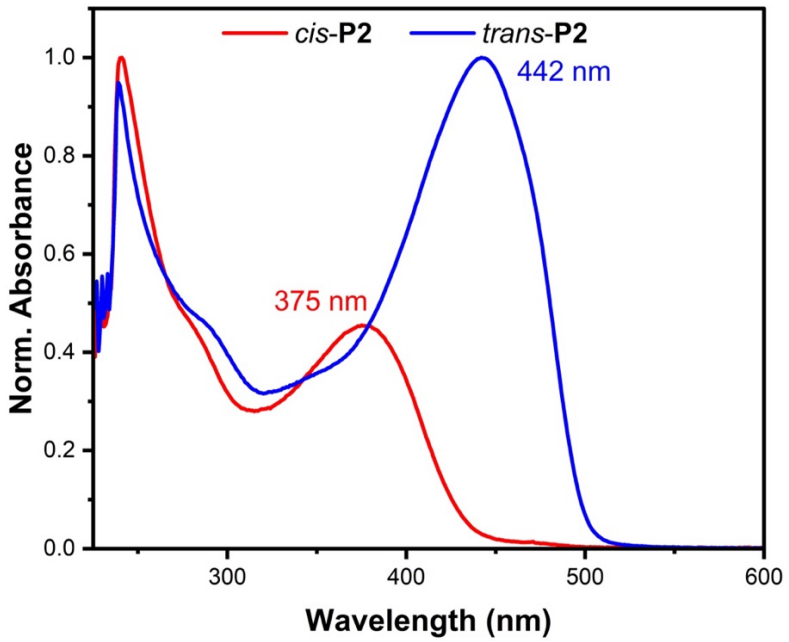

Figure S27. all-*cis* **P2** (M_n^{theo} = 10.8 kg/mol, M_n^{exp} = 9.5 kg/mol, $Đ$ = 1.18) normalized absorbance (C = 5 µg/mL) and all-*trans* **P2** (insolubility prevented SEC analysis in THF) normalized absorbance (C = 5 µg/mL) traces in $CHCl_3$.

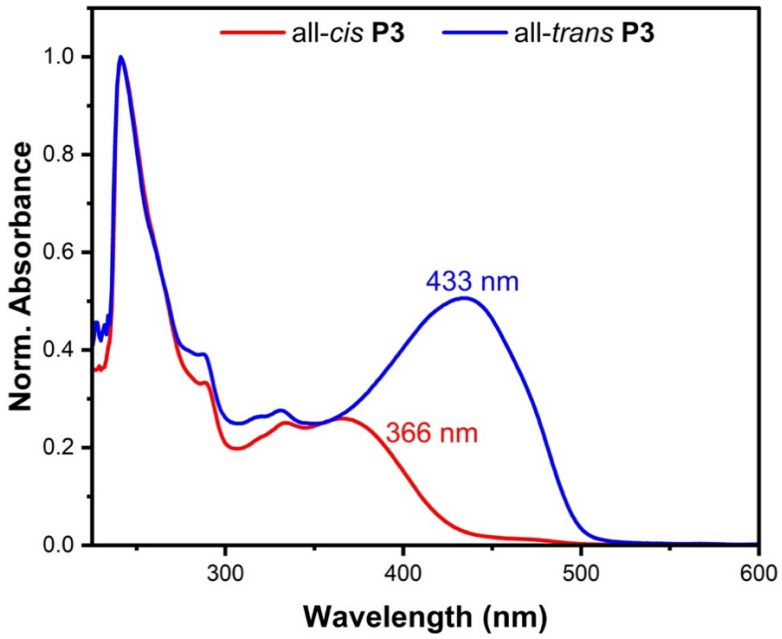

Figure S28. all-*cis* **P3** (M_n^{theo} = 10.3 kg/mol, M_n^{exp} = 11.5 kg/mol, $Đ$ = 1.12) normalized absorbance (C = 5 µg/mL) and all-*trans* **P3** (insolubility prevented SEC analysis in THF) normalized absorbance (C = 5 µg/mL) traces in $CHCl_3$.

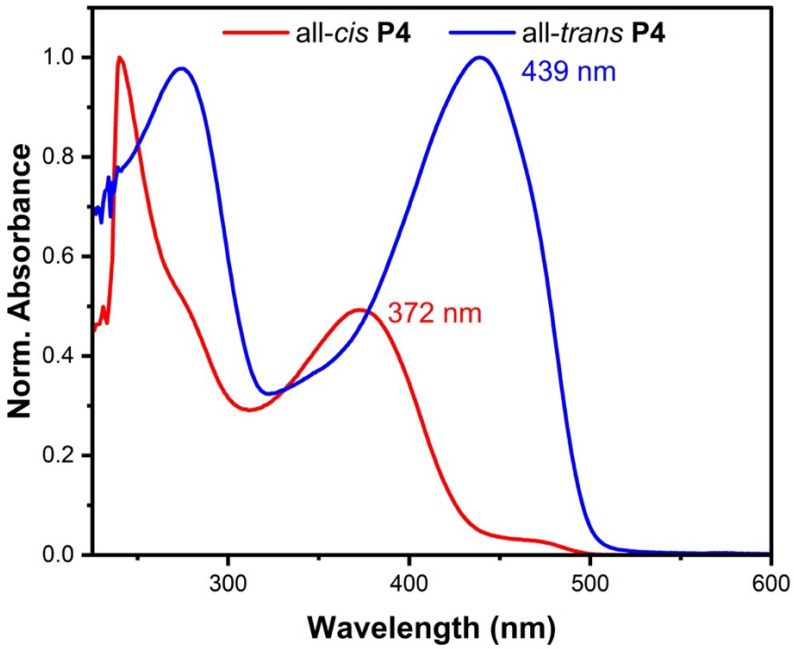

Figure S29. all-*cis* **P4** (M_n^{theo} = 8.5 kg/mol, M_n^{exp} = 10.0 kg/mol, $Đ$ = 1.18) normalized absorbance (C = 5 µg/mL) and all-*trans* **P4** (insolubility prevented SEC analysis in THF) normalized absorbance (C = 5 µg/mL) traces in $CHCl_3$.

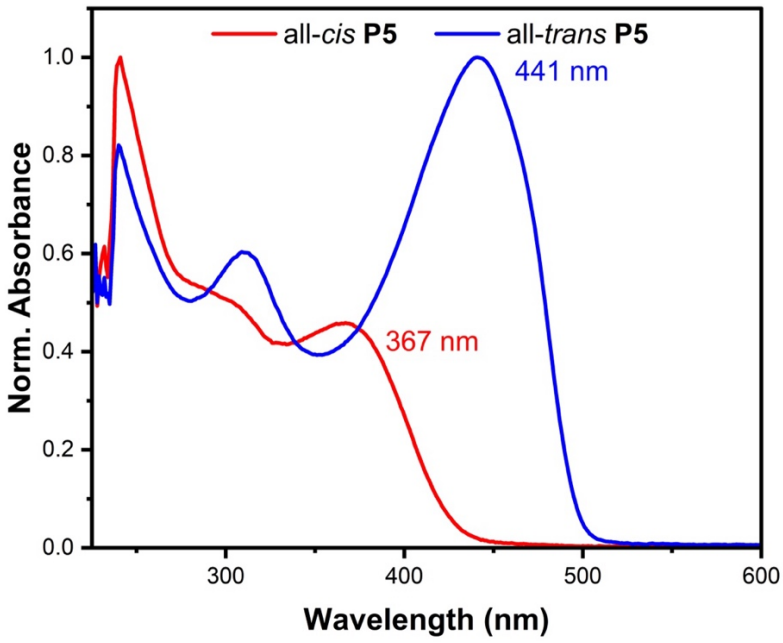

Figure S30. all-*cis* **P5** (M_n^{theo} = 11.3 kg/mol, M_n^{exp} = 6.8 kg/mol, $Đ$ = 1.22) normalized absorbance (C = 5 μg/mL) and all-*trans* **P5** (insolubility prevented SEC analysis in THF) normalized absorbance (C = 5 μg/mL) traces in $CHCl_3$.

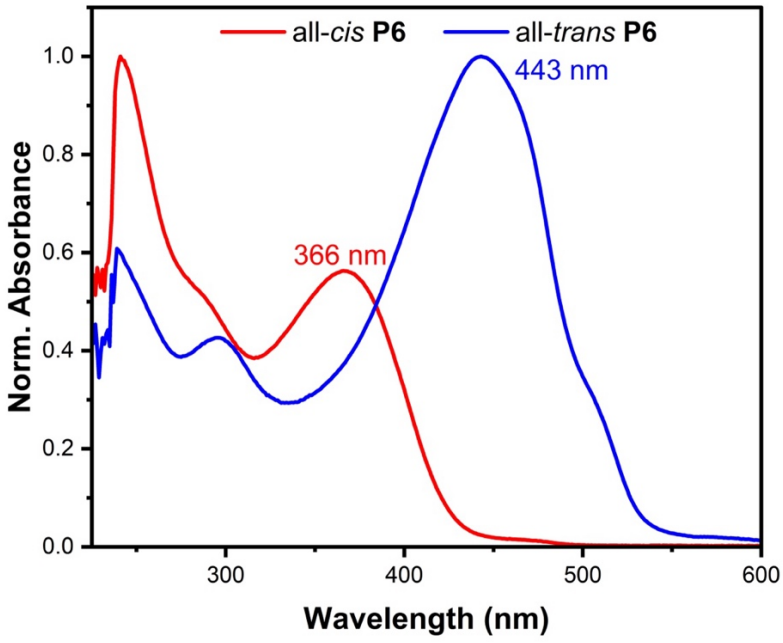

Figure S31. all-*cis* **P6** (M_n^{theo} = 9.6 kg/mol, M_n^{exp} = 9.3 kg/mol, $Đ$ = 1.22) normalized absorbance (C = 5 μg/mL) and all-*trans* **P6** (insolubility prevented SEC analysis in THF) normalized absorbance (C = 5 μg/mL) traces in $CHCl_3$.

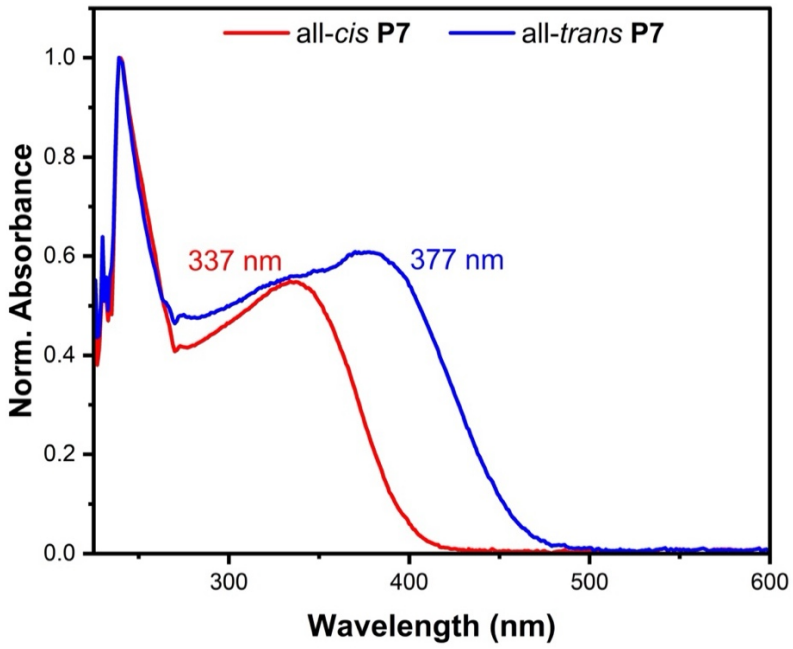

Figure S32. all-*cis* **P7** (M_n^{theo} = 8.7 kg/mol, M_n^{exp} = 8.7 kg/mol, $Đ$ = 1.10) normalized absorbance (C = 5 µg/mL) and all-*trans* **P7** (insolubility prevented SEC analysis in THF) normalized absorbance (C = 5 µg/mL) traces in $CHCl_3$.

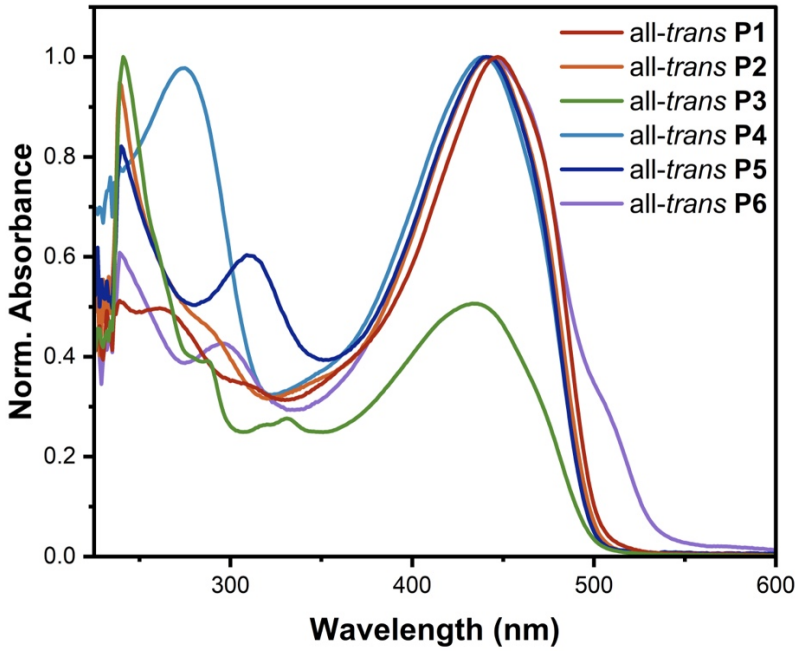

Figure S33. all-*trans* **P1**–**P6** normalized UV-Vis absorption traces in $CHCl_3$ (C = 5 µg/mL).

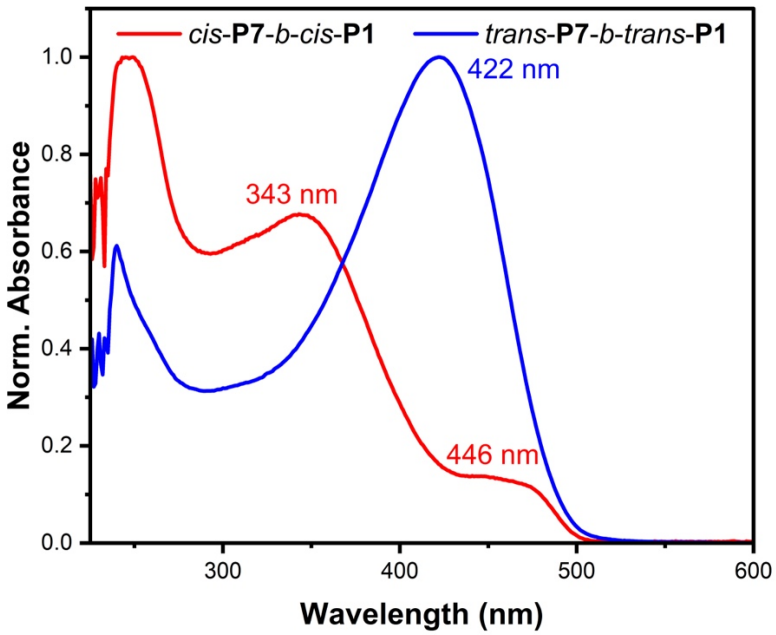

Figure S34. *cis*-**P7**-*b*-*cis*-**P1** (M_n^{theo} = 16.4 kg/mol, M_n^{exp} = 14.7 kg/mol, $Đ$ = 1.46) normalized absorbance (C = 5 μg/mL) and *trans*-**P7**-*b*-*trans*-**P1** (insolubility prevented SEC analysis in THF) normalized absorbance (C = 5 μg/mL) traces in $CHCl_3$.

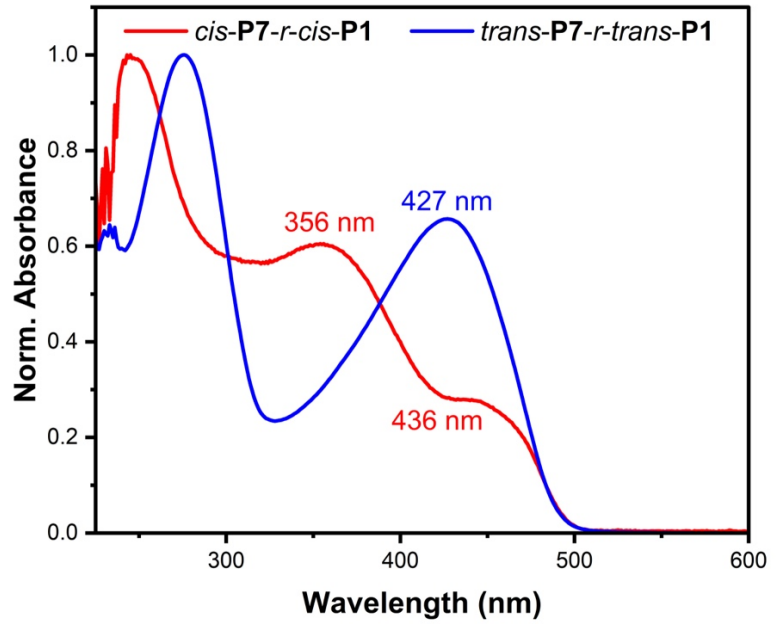

Figure S35. all-*cis*-**P7**-*r*-*cis*-**P1** (M_n^{theo} = 9.0 kg/mol, M_n^{exp} = 8.8 kg/mol, $Đ$ = 1.11) normalized absorbance (C = 5 μg/mL) and all-*trans*-**P7**-*r*-*trans*-**P1** (insolubility prevented SEC analysis in THF) normalized absorbance (C = 5 μg/mL) traces in $CHCl_3$.

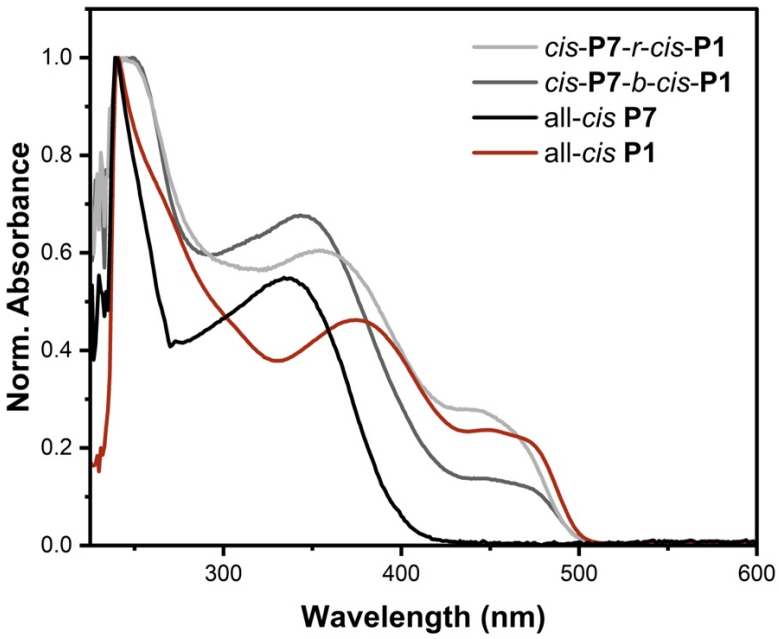

Figure S36. Comparison of normalized absorbance of *cis*-**P7**-*r*-*cis*-**P1** and *cis*-**P7**-*b*-*cis*-**P1** copolymers with all-*cis* **P1** and **P7** (C = 5 μg/mL).

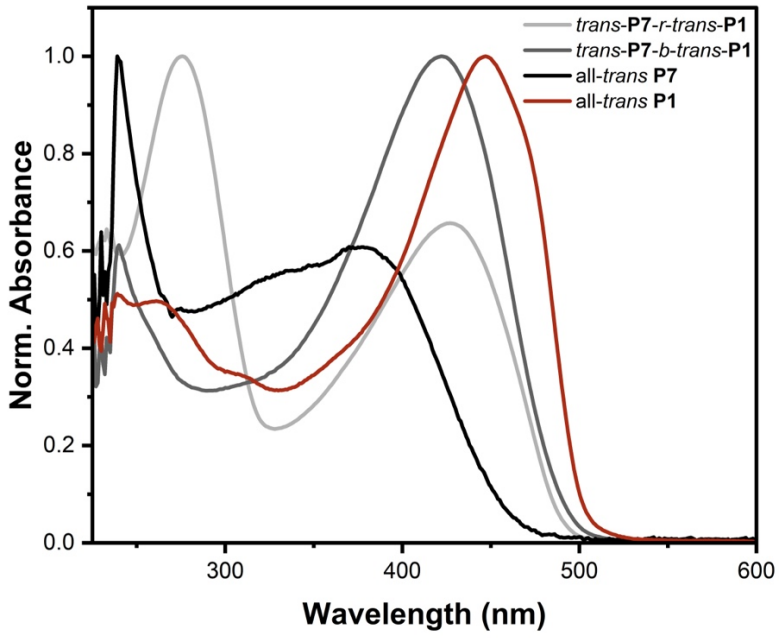

Figure S37. Comparison of normalized absorbance of *trans*-**P7**-*r*-*trans*-**P1** and *trans*-**P7**-*b*-*trans*-**P1** copolymers with all-*trans* **P1** and **P7** (C = 5 μg/mL).

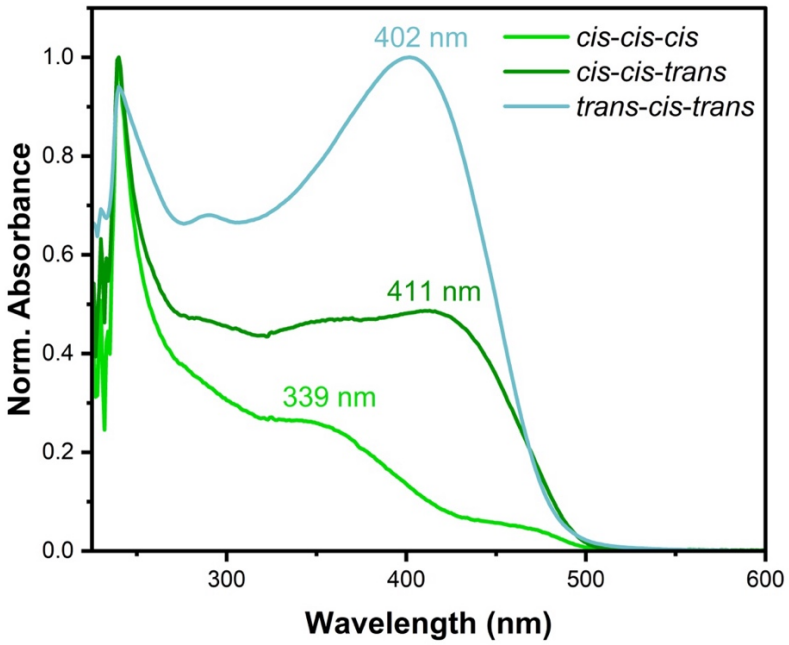

Figure S38. *cis*-**P7**-*b*-*cis*-**P8**-*b*-*cis*-**P1** (abbreviated as *cis*-*cis*-*cis*; M_n^{theo} = 7.5 kg/mol, M_n^{exp} = 7.3 kg/mol, $Đ$ = 1.18) normalized absorbance (C = 5 μg/mL) trace in $CHCl_3$. *cis*-**P7**-*b*-*cis*-**P8**-*b*-*trans*-**P1** (abbreviated as *cis*-*cis*-*trans*) normalized fluorescence emission (C = 5 μg/mL) trace in $CHCl_3$. *trans*-**P7**-*b*-*cis*-**P8**-*b*-*trans*-**P1** (abbreviated as *trans*-*cis*-*trans*) normalized fluorescence emission (C = 5 μg/mL) trace in $CHCl_3$.

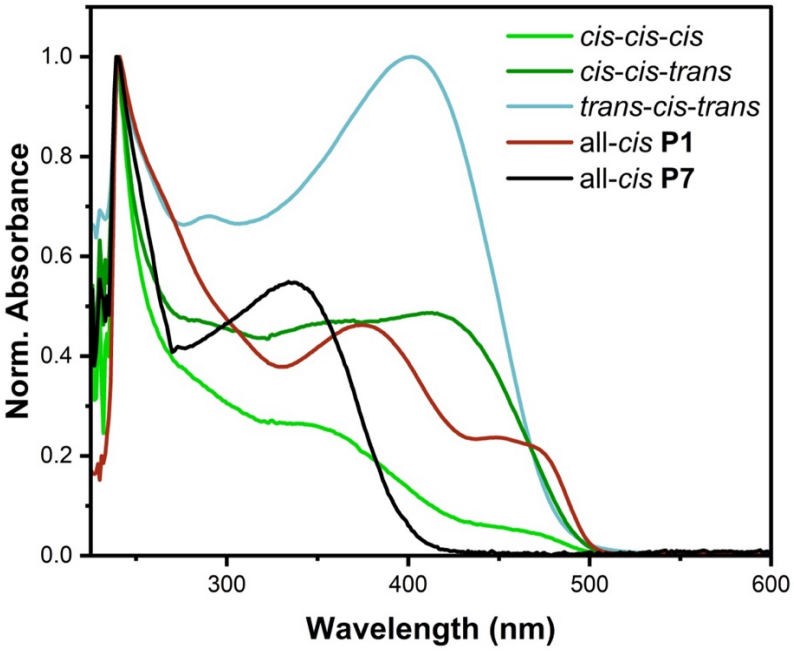

Figure S39. Comparison of normalized absorbance of *cis*-*cis*-*cis*, *cis*-*cis*-*trans*, and *trans*-*cis*-*trans* stereoblock copolymers with all-*cis* **P1** and **P7** (C = 5 μg/mL).

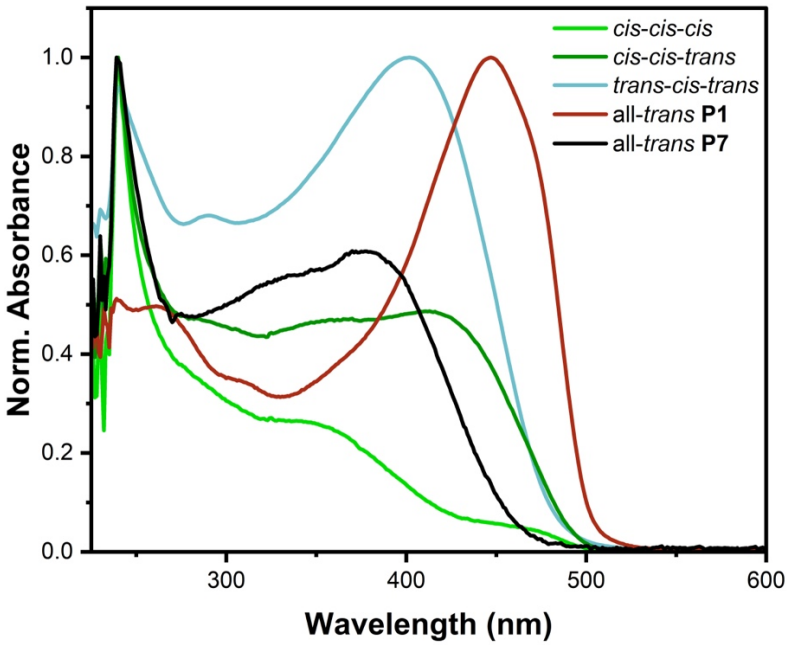

Figure S40. Comparison of normalized absorbance of *cis*-*cis*-*cis*, *cis*-*cis*-*trans*, and *trans*-*cis*-*trans* stereoblock copolymers with all-*trans* **P1** and **P7** (C = 5 μg/mL).

Fluorescence Emission Spectra

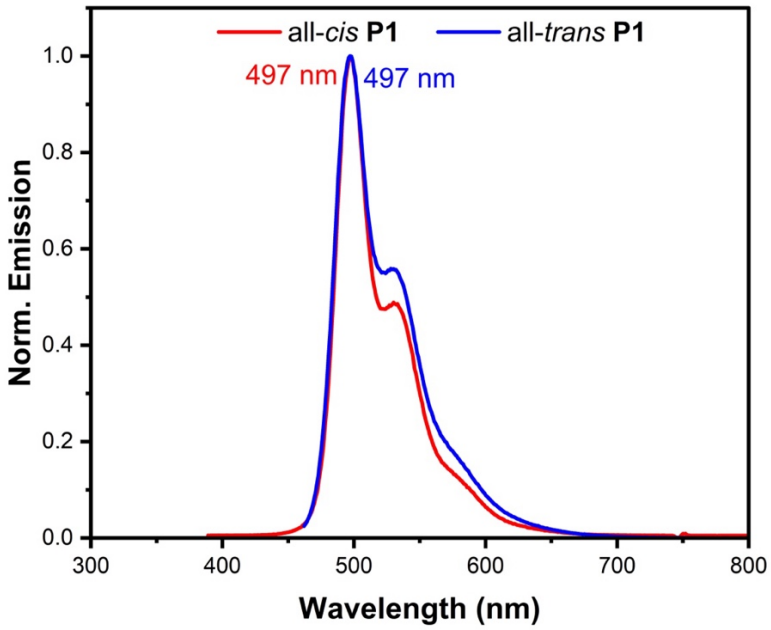

Figure S41. all-*cis* **P1** (M_n^{theo} = 8.6 kg/mol, M_n^{exp} = 9.5 kg/mol, $Đ$ = 1.22) normalized fluorescence emission (λ_{ex} = 374 nm, C = 0.5 µg/mL) trace in $CHCl_3$. all-*trans* **P1** (insolubility prevented SEC analysis in THF) normalized fluorescence emission (λ_{ex} = 449 nm, C = 0.5 µg/mL) trace in $CHCl_3$.

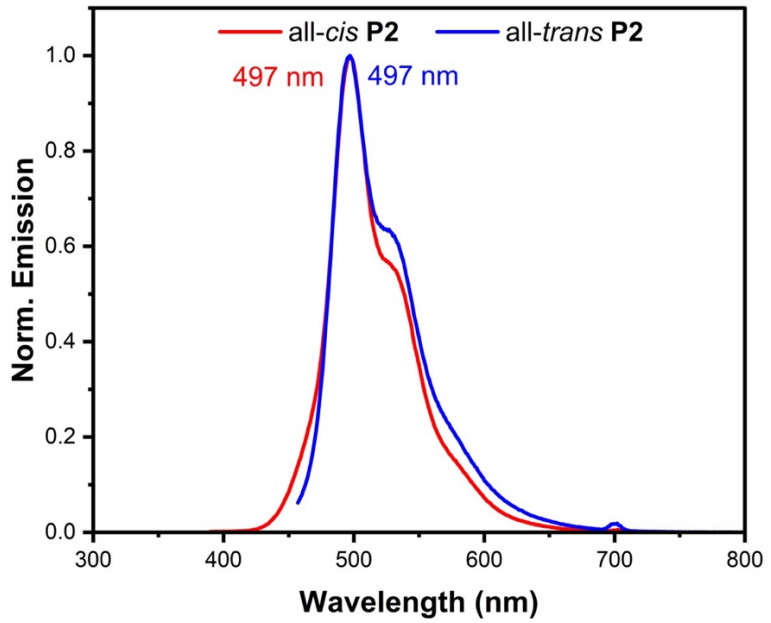

Figure S42. all-*cis* **P2** (M_n^{theo} = 10.8 kg/mol, M_n^{exp} = 9.5 kg/mol, $Đ$ = 1.18) normalized fluorescence emission (λ_{ex} = 375 nm, C = 0.5 µg/mL) trace in $CHCl_3$. all-*trans* **P2** (insolubility prevented SEC analysis in THF) normalized fluorescence emission (λ_{ex} = 442 nm, C = 0.5 µg/mL) trace in $CHCl_3$.

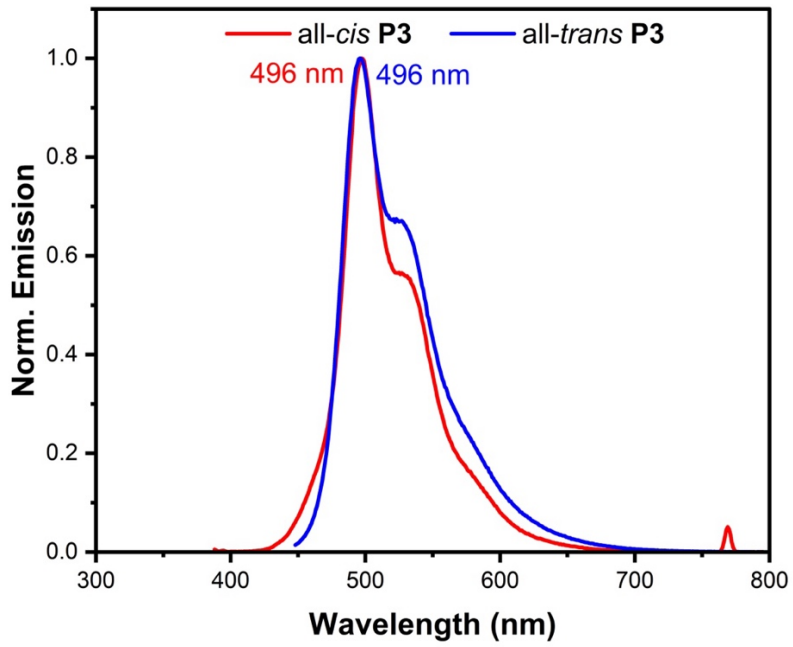

Figure S43. all-*cis* **P3** (M_n^{theo} = 10.3 kg/mol, M_n^{exp} = 11.5 kg/mol, $Đ$ = 1.12) fluorescence emission (λ_{ex} = 366 nm, C = 0.5 μg/mL) trace in $CHCl_3$. all-*trans* **P3** (insolubility prevented SEC analysis in THF) normalized fluorescence emission (λ_{ex} = 433 nm, C = 0.5 μg/mL) trace in $CHCl_3$.

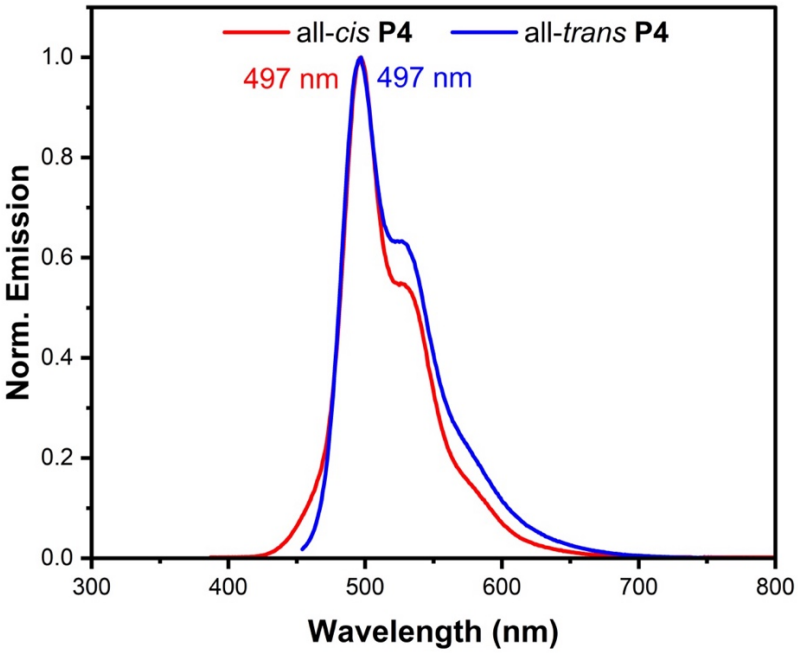

Figure S44. all-*cis* **P4** (M_n^{theo} = 8.5 kg/mol, M_n^{exp} = 10.0 kg/mol, $Đ$ = 1.18) fluorescence emission (λ_{ex} = 372 nm, C = 0.5 μg/mL) trace in $CHCl_3$. all-*trans* **P4** (insolubility prevented SEC analysis in THF) normalized fluorescence emission (λ_{ex} = 439 nm, C = 0.5 μg/mL) trace in $CHCl_3$.

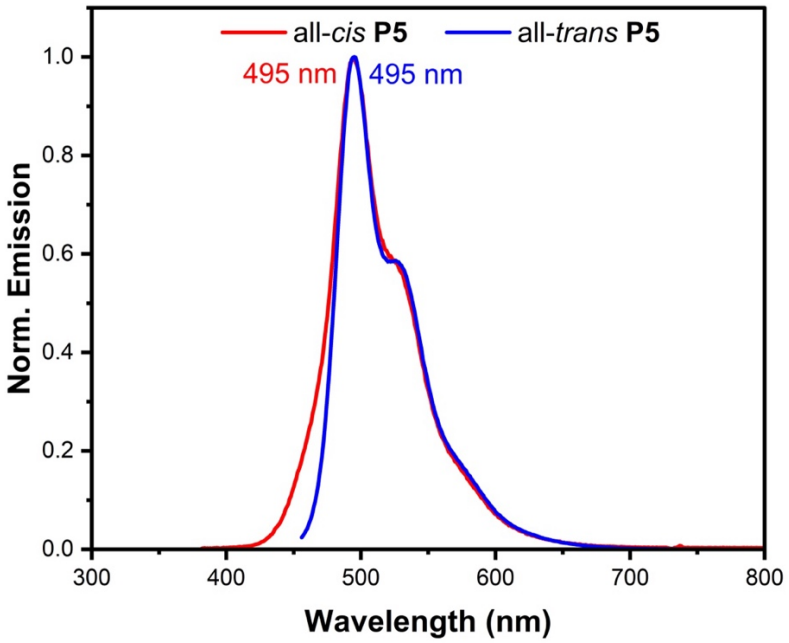

Figure S45. all-*cis* **P5** (M_n^{theo} = 11.3 kg/mol, M_n^{exp} = 6.8 kg/mol, $Đ$ = 1.22) normalized fluorescence emission (λ_{ex} = 367 nm, C = 0.5 µg/mL) trace in $CHCl_3$. all-*trans* **P5** (insolubility prevented SEC analysis in THF) normalized fluorescence emission (λ_{ex} = 441 nm, C = 0.5 µg/mL) trace in $CHCl_3$.

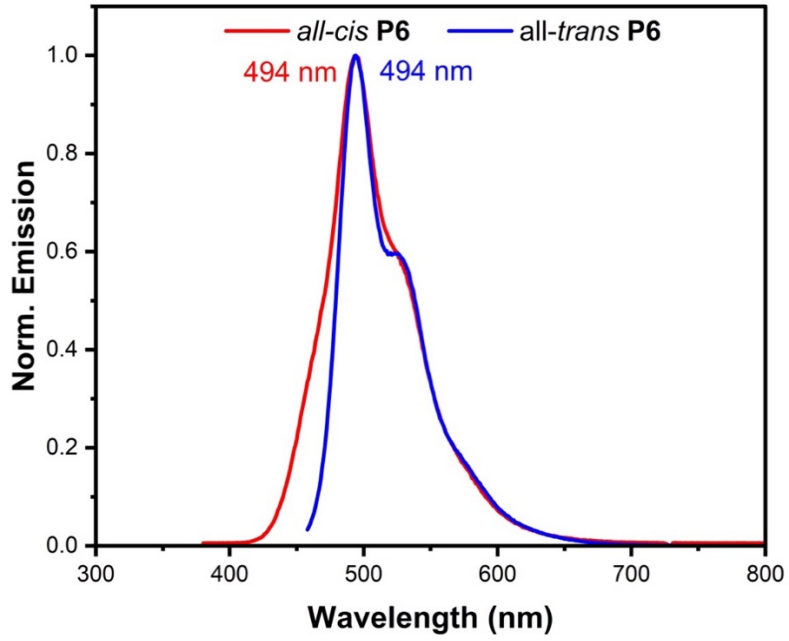

Figure S46. all-*cis* **P6** (M_n^{theo} = 9.6 kg/mol, M_n^{exp} = 9.3 kg/mol, $Đ$ = 1.22) normalized fluorescence emission (λ_{ex} = 366 nm, C = 0.5 µg/mL) trace in $CHCl_3$. all-*trans* **P6** (insolubility prevented SEC analysis in THF) normalized fluorescence emission (λ_{ex} = 443 nm, C = 0.5 µg/mL) trace in $CHCl_3$.

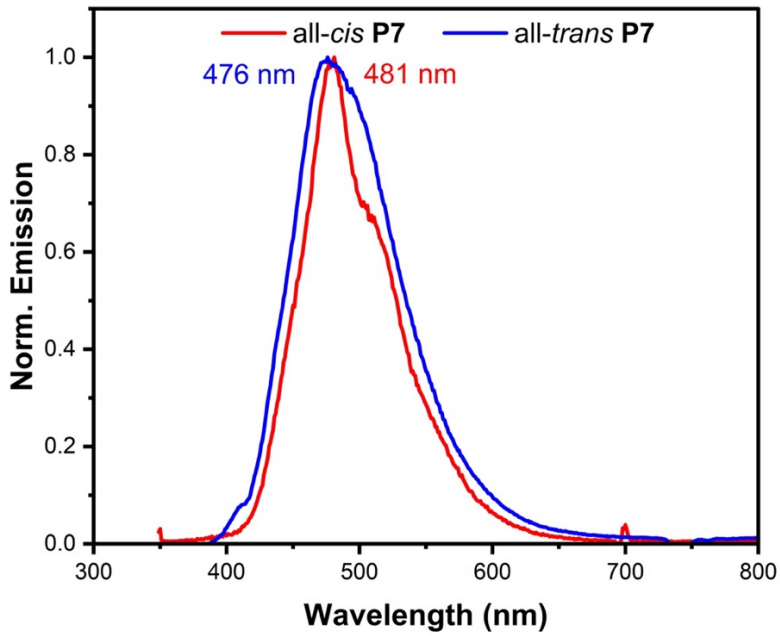

Figure S47. all-*cis* **P7** (M_n^{theo} = 8.7 kg/mol, M_n^{exp} = 8.7 kg/mol, $Đ$ = 1.10) normalized fluorescence emission (λ_{ex} = 337 nm, C = 0.5 µg/mL) trace in $CHCl_3$. all-*trans* **P7** (insolubility prevented SEC analysis in THF) normalized fluorescence emission (λ_{ex} = 377 nm, C = 0.5 µg/mL) trace in $CHCl_3$.

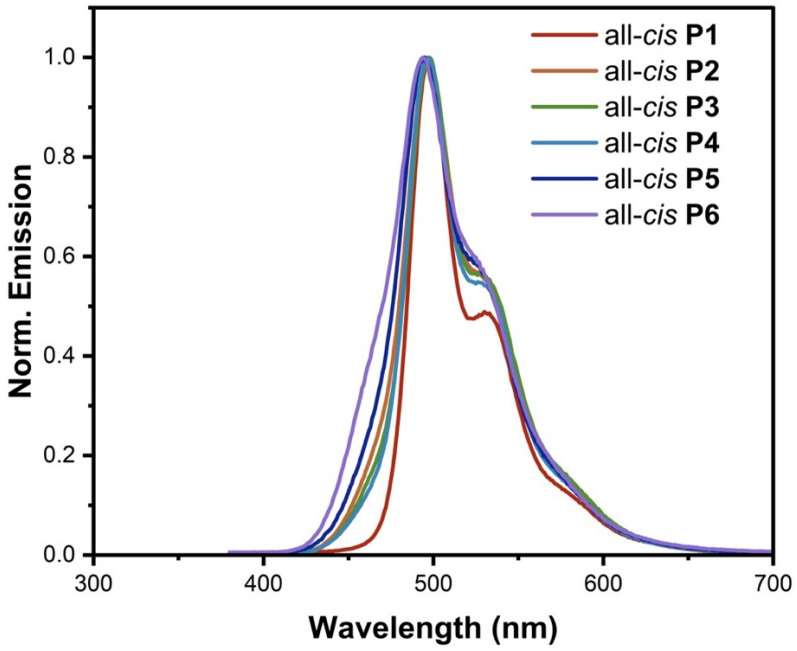

Figure S48. all-*cis* **P1**–**P6** normalized fluorescence emission traces in $CHCl_3$ (C = 0.5 µg/mL).

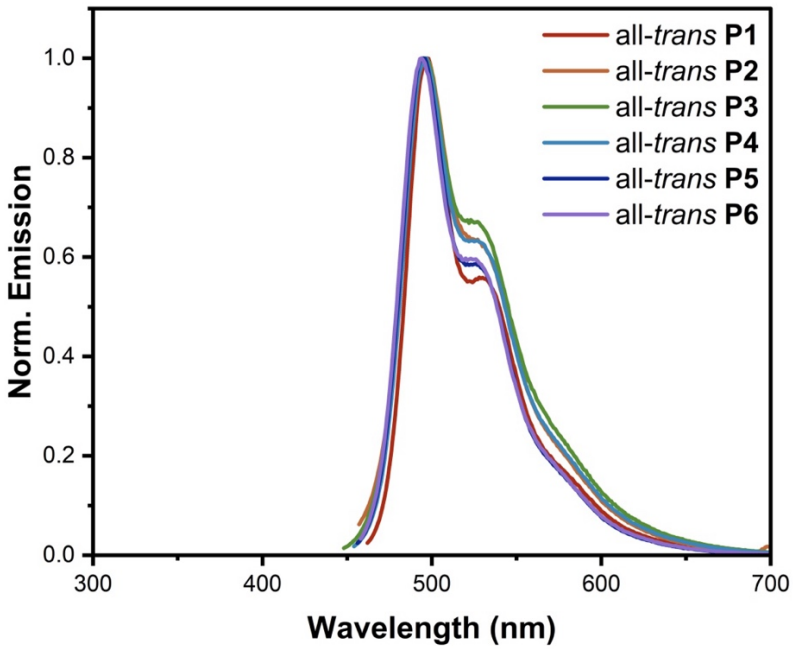

Figure S49. *trans*-**P1**–**P6** normalized fluorescence emission traces in $CHCl_3$ (C = 0.5 μg/mL).

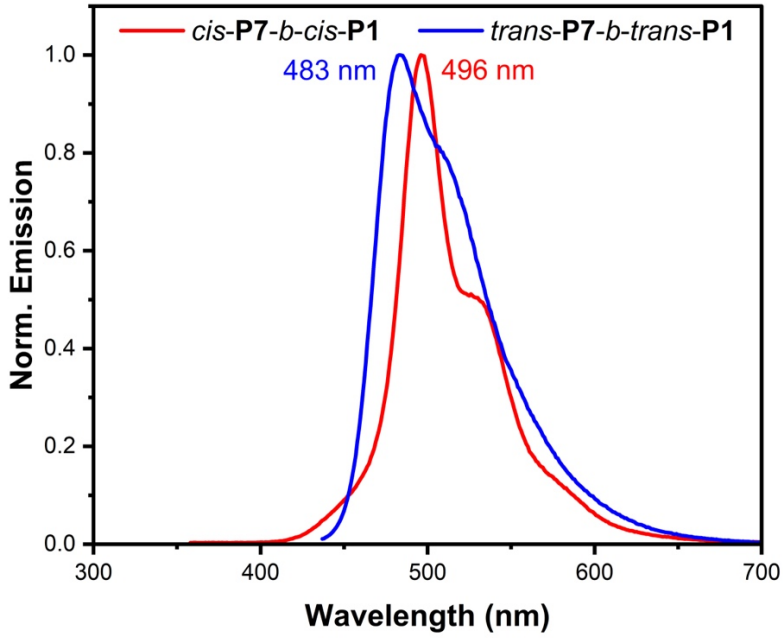

Figure S50. *cis*-**P7**-*b*-*cis*-**P1** (M_n^{theo} = 16.4 kg/mol, M_n^{exp} = 14.7 kg/mol, $Đ$ = 1.46) fluorescence emission (λ_{ex} = 343 nm, C = 0.5 μg/mL) trace in $CHCl_3$. all-*trans*-**P7**-*b*-*trans*-**P1** (insolubility prevented SEC analysis in THF) normalized fluorescence emission (λ_{ex} = 422 nm, C = 0.5 μg/mL) trace in $CHCl_3$.

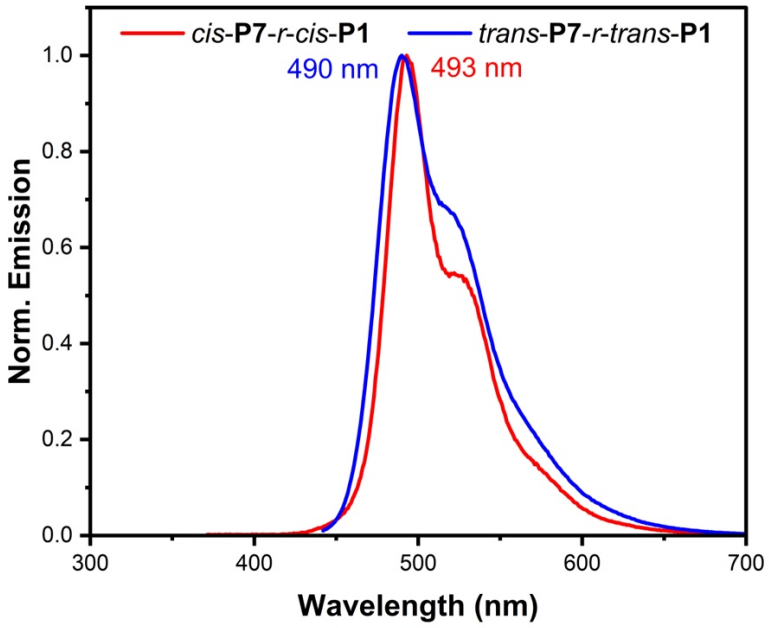

Figure S51. *cis*-**P7**-*r*-*cis*-**P1** (M_n^{theo} = 9.0 kg/mol, M_n^{exp} = 8.8 kg/mol, $Đ$ = 1.11) fluorescence emission (λ_{ex} = 356 nm, C = 0.5 µg/mL) trace in $CHCl_3$. *trans*-**P7**-*r*-*trans*-**P1** (insolubility prevented SEC analysis in THF) normalized fluorescence emission (λ_{ex} = 427 nm, C = 0.5 µg/mL) trace in $CHCl_3$.

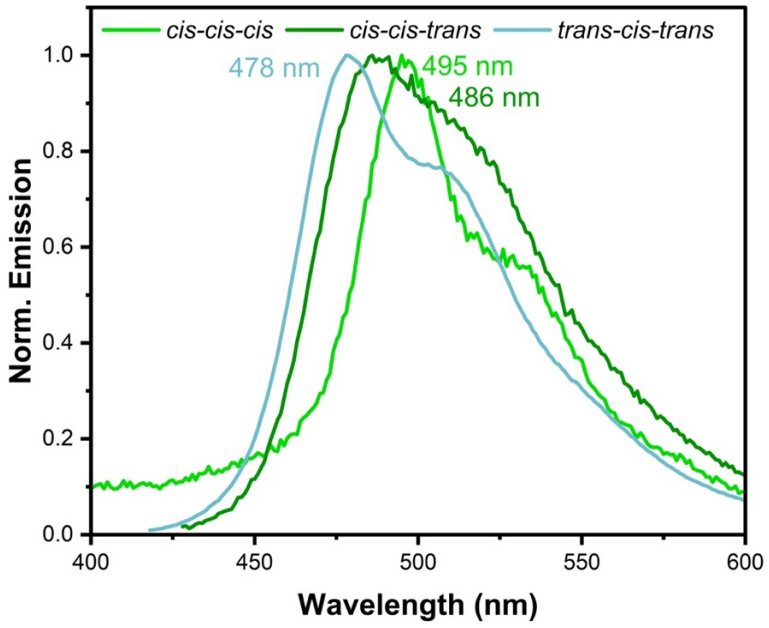

Figure S52. *cis*-**P7**-*b*-*cis*-**P8**-*b*-*cis*-**P1** (M_n^{theo} = 7.5 kg/mol, M_n^{exp} = 7.3 kg/mol, $Đ$ = 1.18) normalized fluorescence emission (λ_{ex} = 495 nm, C = 0.5 µg/mL) trace in $CHCl_3$. *cis*-**P7**-*b*-*cis*-**P8**-*b*-*trans*-**P1** (insolubility prevented SEC analysis in THF) normalized fluorescence emission (λ_{ex} = 486 nm, C = 0.5

μg/mL) trace in $CHCl_3$. *trans*-**P7**-*b*-*cis*-**P8**-*b*-*trans*-**P1** (insolubility prevented SEC analysis in THF) normalized fluorescence emission (λ_{ex} = 478 nm, C = 0.5 μg/mL) trace in $CHCl_3$.

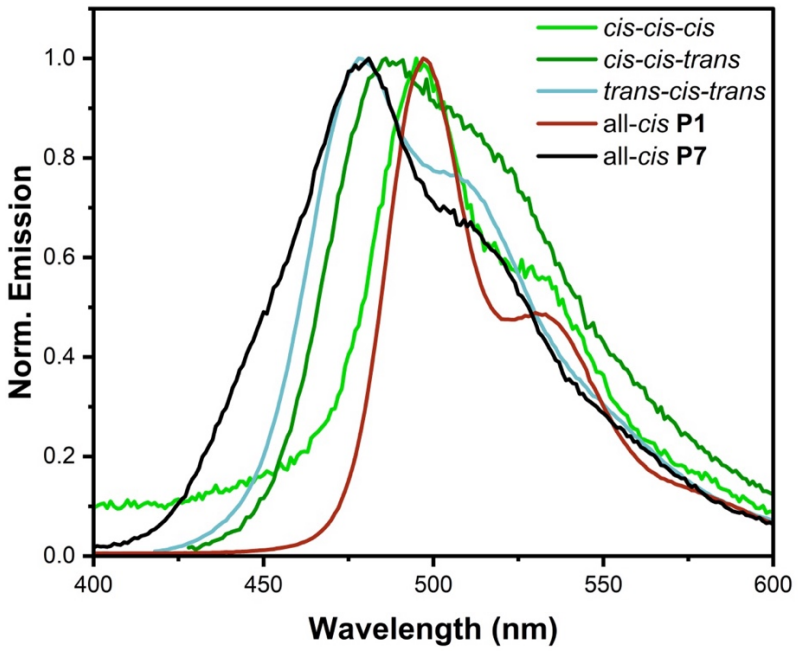

Figure S53. Comparison of fluorescence emission of *cis-cis-cis*, *cis-cis-trans*, and *trans-cis-trans* stereoblock copolymers with all-*cis* **P1** and **P7** (C = 0.5 μg/mL).

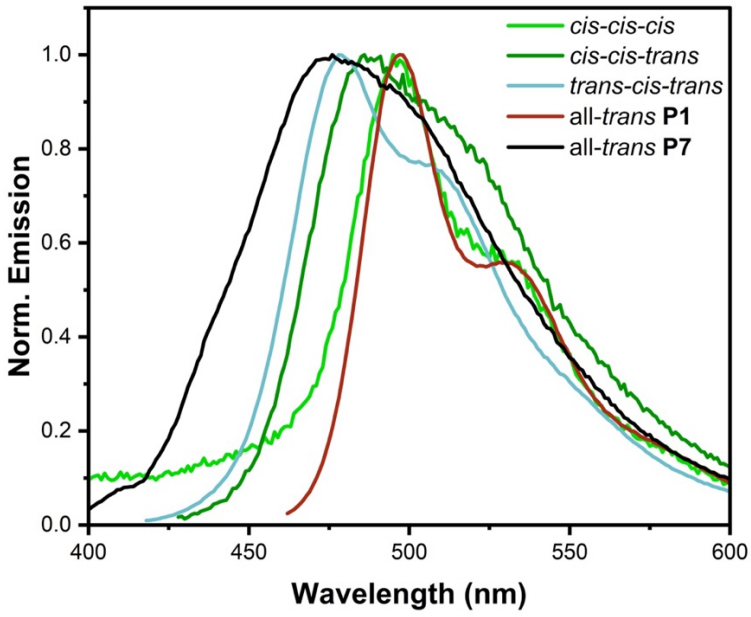

Figure S54. Comparison of fluorescence emission of *cis-cis-cis*, *cis-cis-trans*, and *trans-cis-trans* stereoblock copolymers with all-*trans* **P1** and **P7** (C = 0.5 μg/mL).

Visual Appearance of Polymer Luminescence under Irradiation

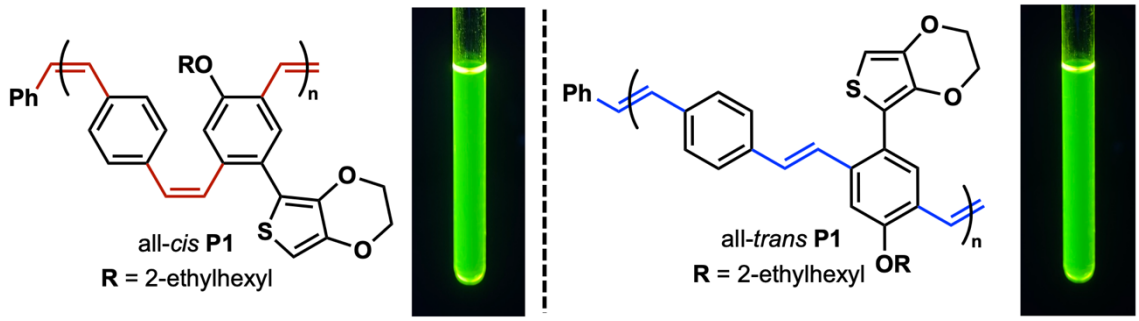

Figure S55. Structures and digital photos of all-*cis*-**P1** and all-*trans* **P1** in $CDCl_3$ (C = 2.0 mg/mL) under 350 nm irradiation.

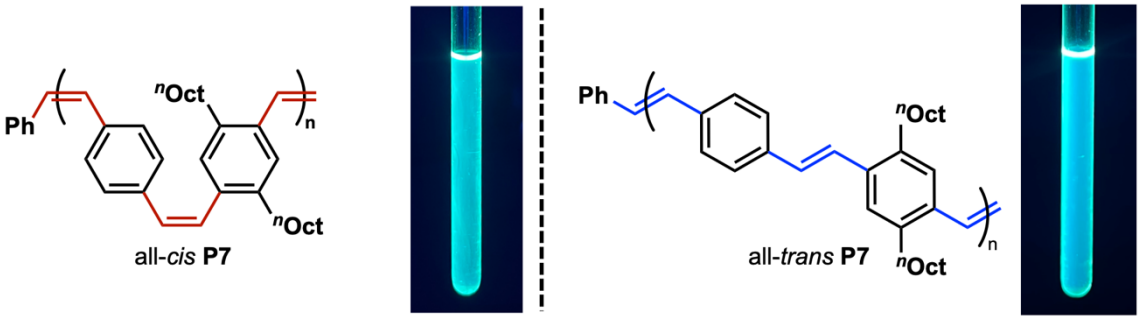

Figure S56. Structures and digital photos of all-*cis*-**P7** and all-*trans* **P7** in $CDCl_3$ (C = 0.5 mg/mL) under 350 nm irradiation.

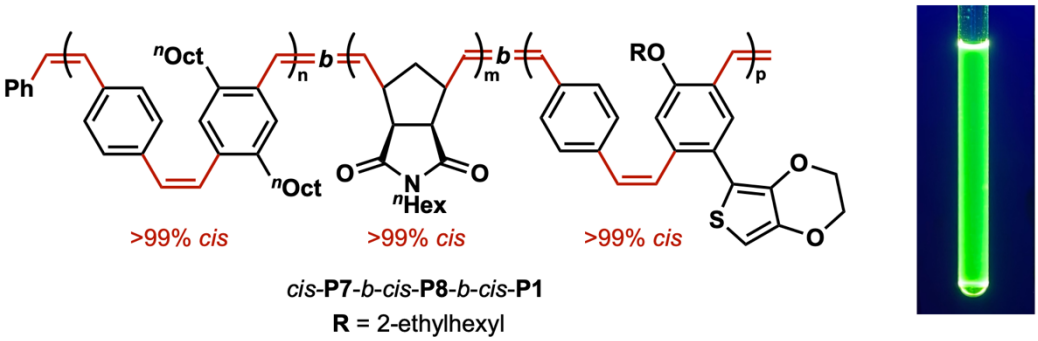

Figure S57. Structure and digital photo of *cis*-**P7**-*b*-*cis*-**P8**-*b*-*cis*-**P1** in $CDCl_3$ (C = 4.0 mg/mL) under 350 nm irradiation.

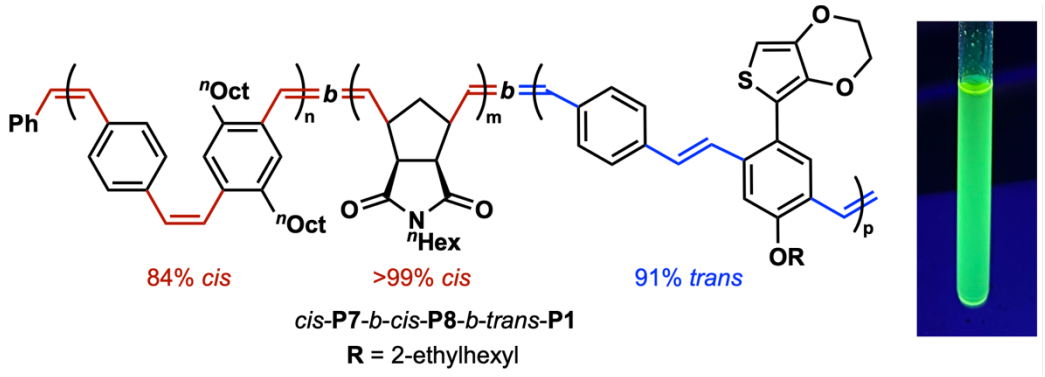

Figure S58. Structure and digital photo of *cis*-**P7**-*b*-*cis*-**P8**-*b*-*trans*-**P1** in $CDCl_3$ (C = 4.0 mg/mL) under 350 nm irradiation.

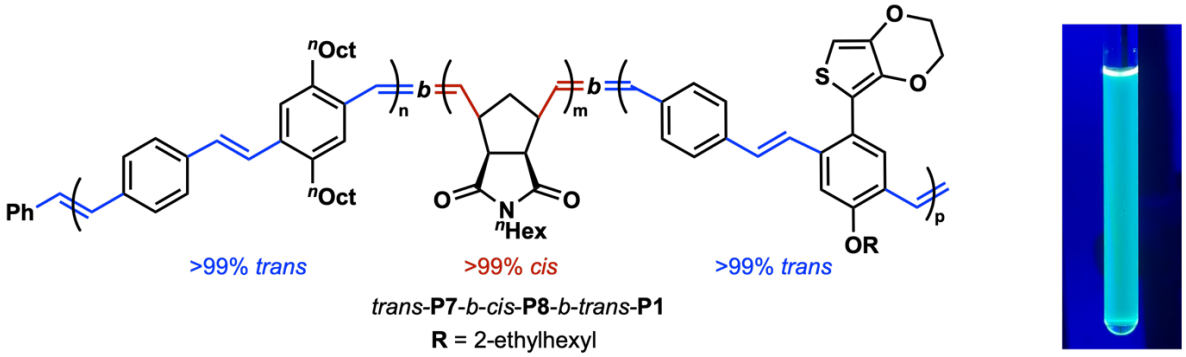

Figure S59. Structure and digital photo of *trans*-**P7**-*b*-*cis*-**P8**-*b*-*trans*-**P1** in $CDCl_3$ (C = 4.0 mg/mL) under 350 nm irradiation.

Digital-Light Projection (DLP) Details

Thin Film Preparation Procedure

Cover glass (VistaVision No1, VWR) and soda-lime glass (1”x1” square and 1.1 mm thick, MSE supplies) were sonicated for 5 minutes in solvents, in the order of acetone, isopropyl alcohol, and distilled water. The desired polymer was dissolved in $CHCl_3$ (5 mg/mL). The cover glass was attached to soda-lime glass substrate and 50 μL of polymer solution was dropped on cover glass. The film was spin-coated for 60 seconds at 600 rpm for the triblock copolymers and at 300 rpm for homopolymer using spin coater (WS-400BZ-6NPP/LITE, Laurell).

DLP on Thin Film Procedure

The inert gas chamber was 3-D printed by stereolithography printer (Form 4, Formlabs) using photo-resin (Clear Resin V5, Formlabs). The spin-coated cover glass was mounted on chamber with the polymer film facing inward and sealed with carbon tape. The entrance window of objective lens (alpha Plan-Apochromat 63X/1.46, Zeiss) was cleaned with optic cleaning tissue (MC-5, Thorlabs) and nitrogen gas. The immersion oil (Immersol 518 F, Zeiss) was dropped on the objective lens. The as prepared inert gas chamber assembly was mounted on the microscopy slide holder (MAX3SLH, Thorlabs) fixed with spring clips and the argon gas was purged for 15 minutes. The lateral and axial position of mounted device were adjusted by a tilt stage (#66–545, Edmund Optics) integrated with a 3-axis manual stage (PT3, Thorlabs) that has 1” travel range with 1 μm-resolution-micrometer (DM713, Thorlabs) until the clear image of the 532 nm laser beam was detected using the surface detection system. Then the UV pattern was projected onto the film for 180 seconds.

DLP Pattern Designs and Dimensions

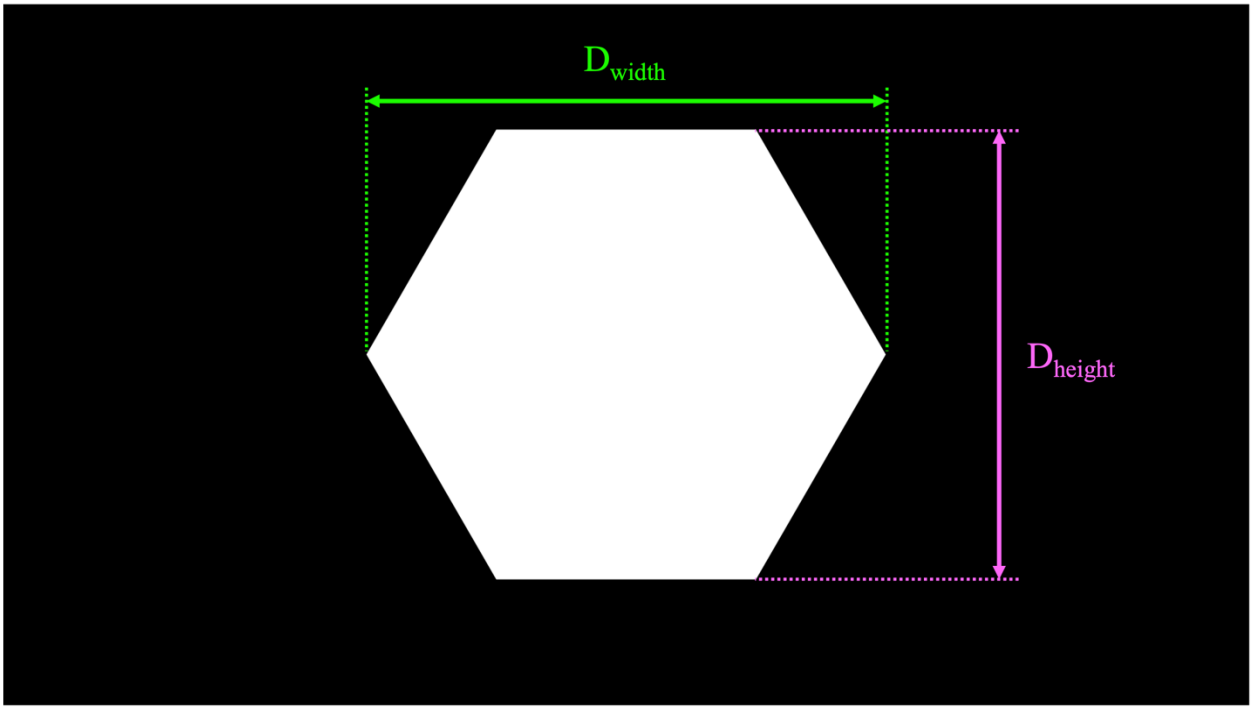

Figure S60. Hexagon pattern, D_{height} = 18 µm, D_{width} = 21 µm

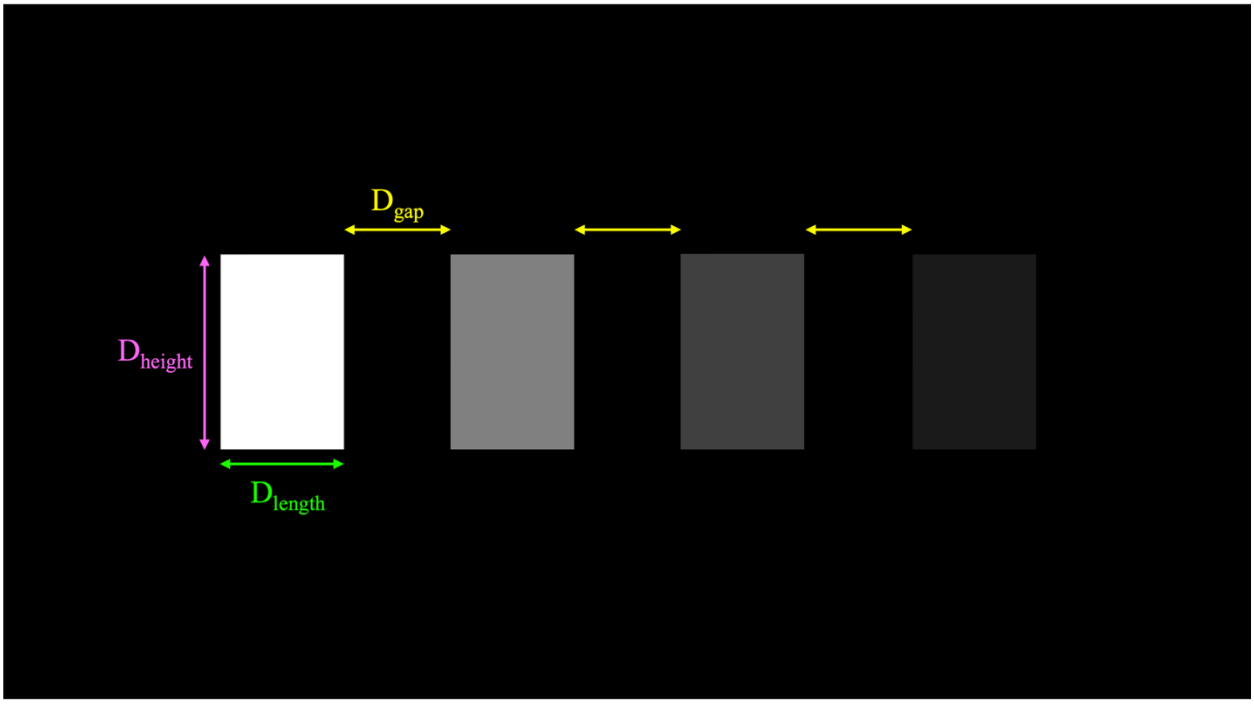

Figure S61. Grayscale bars pattern. Grayscale intensities from left to right are as follows for the four rectangles: 100%, 50%, 25%, and 10%. D_{height} = 8 µm, D_{length} = 5 µm, and D_{gap} = 4.3 µm.

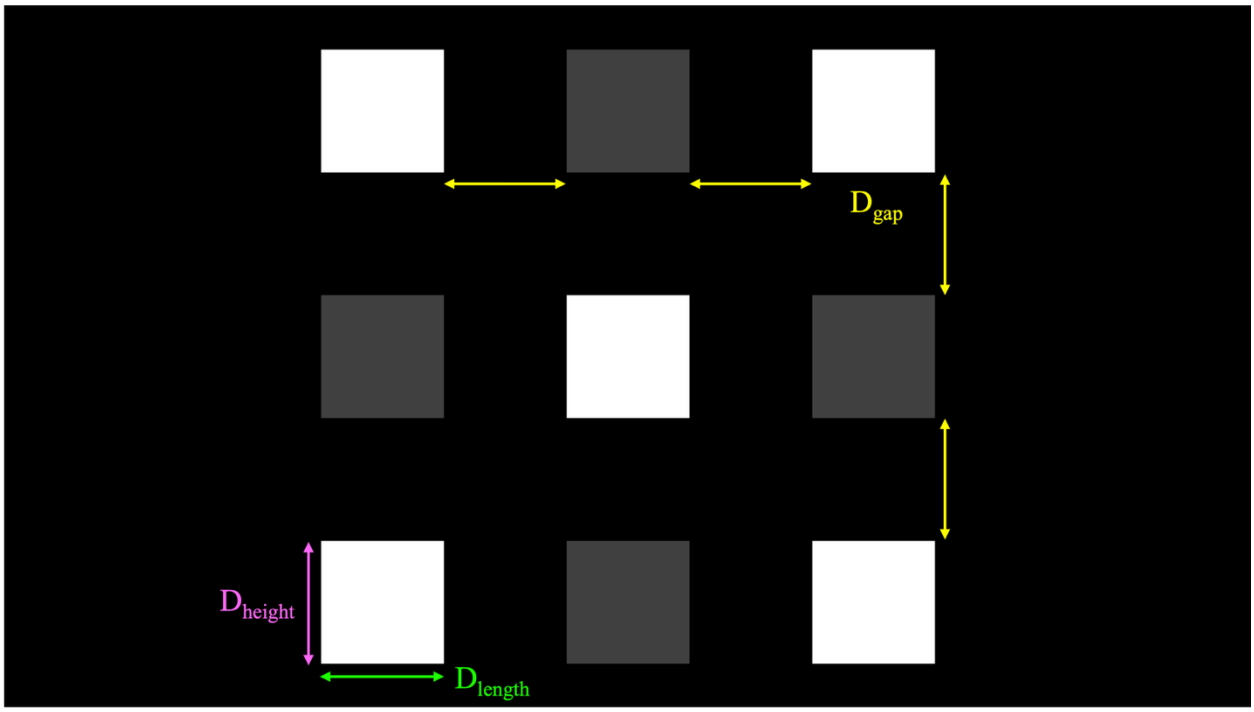

Figure S62. Grayscale 3x3 grid pattern. Grayscale intensities are alternating 100% and 25%. D_{height} = 5 µm, D_{length} = 5 µm, and D_{gap} = 5 µm.

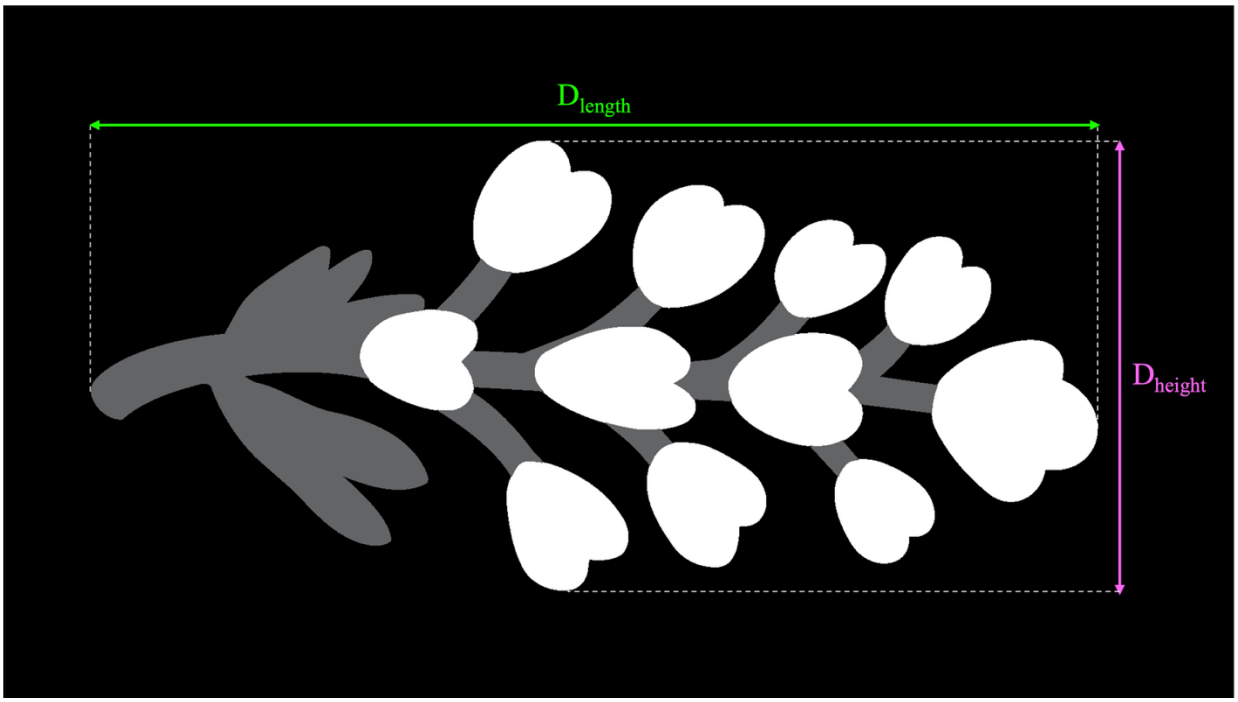

Figure S63. Grayscale bluebonnet pattern. Grayscale intensities are 100% for the petals and 40% for the stem and leaves. D_{height} = 18.5 µm and D_{length} = 41.5 µm.

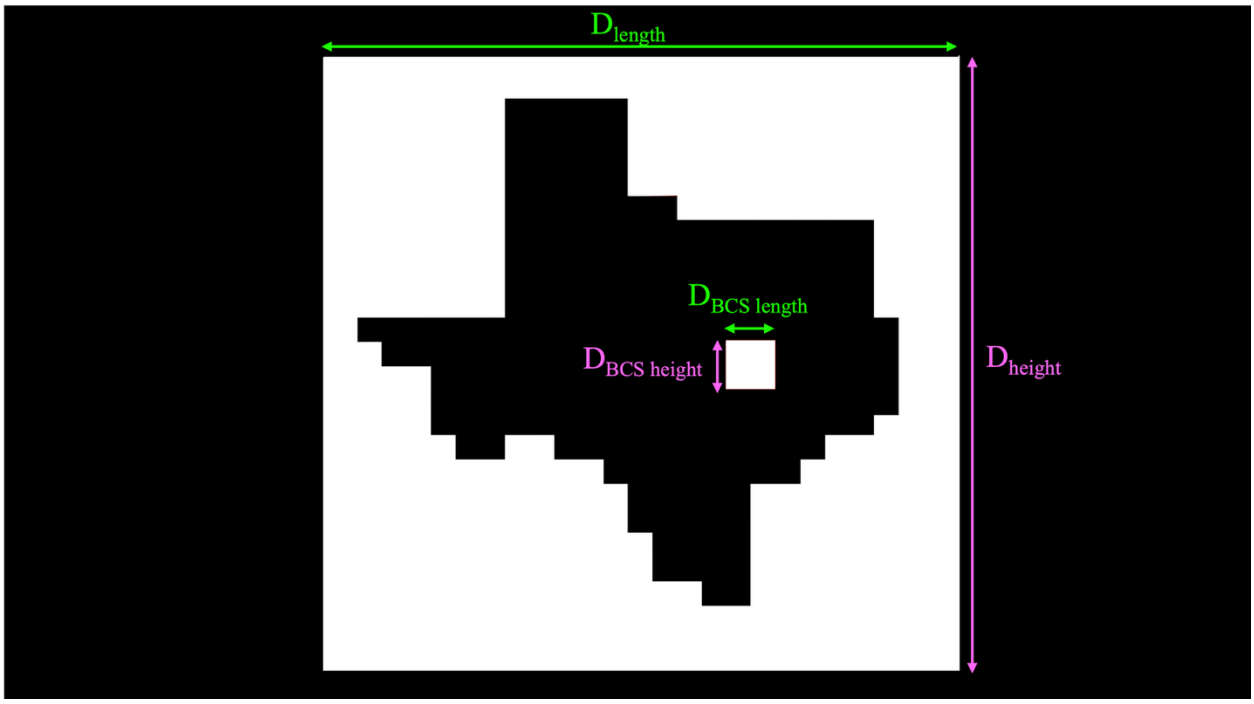

Figure S64. Inverse Texas pattern with Bryan-College Station (BCS) square. Grayscale intensity is all 100%. D_{height} = 26 µm, D_{length} = 25 µm, $D_{BCS\ height}$ = 2 µm, $D_{BCS\ length}$ = 2 µm.

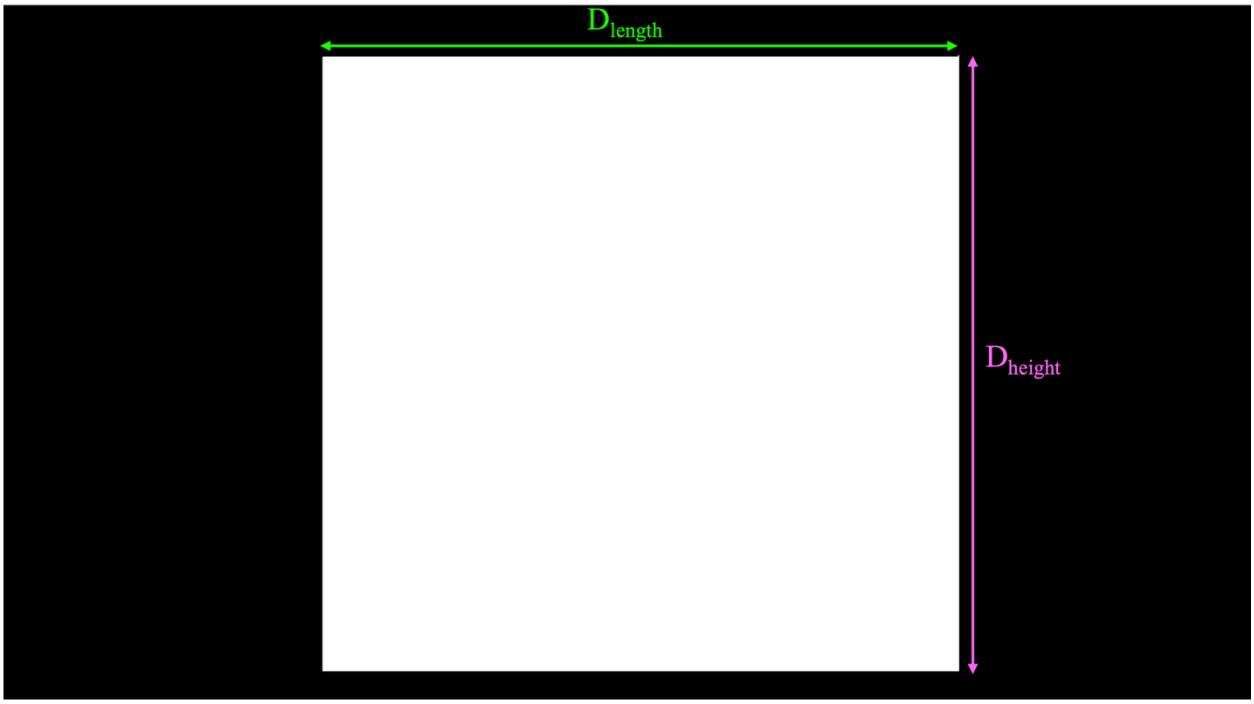

Figure S65. Widefield illumination following inverse Texas pattern. Grayscale intensity is all 100%. D_{height} = 26 µm and D_{length} = 25 µm.

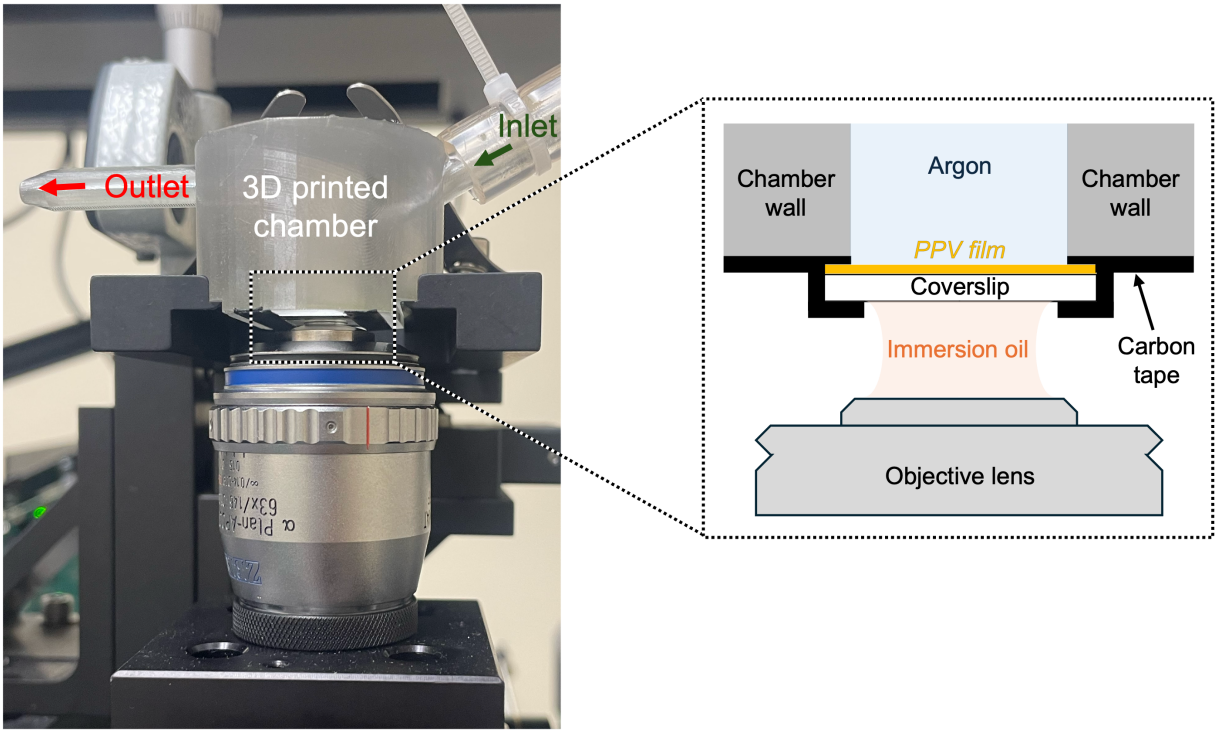

Figure S66. Digital photo and schematic image of cross-sectional view of photopatterning setup.

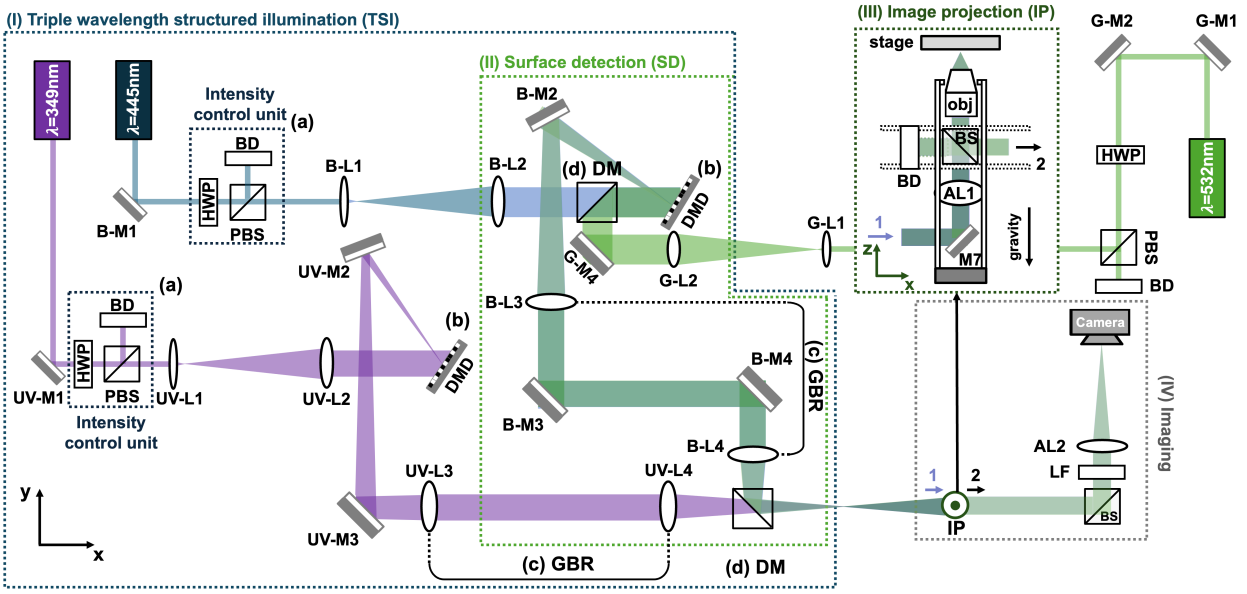

Figure S67. Schematic image of full digital light processing-based triple-wavelength image projection platform composed of four systems (structured illumination system, surface detection system, image projection system, and imaging system). **(a)** Intensity control unit, **(b)** Digital micromirror device (DMD), **(c)** Galilean beam reducer (GBR), **(d)** Dichroic mirror (DM). (HWP: half-wave plate, PBS: polarizing beam splitter, BD: beam dump, M#: dielectric mirror, L#: plano-convex lens, AL#: achromatic lens, BS: plate beamsplitter, obj: objective lens, LF: long-pass filter)

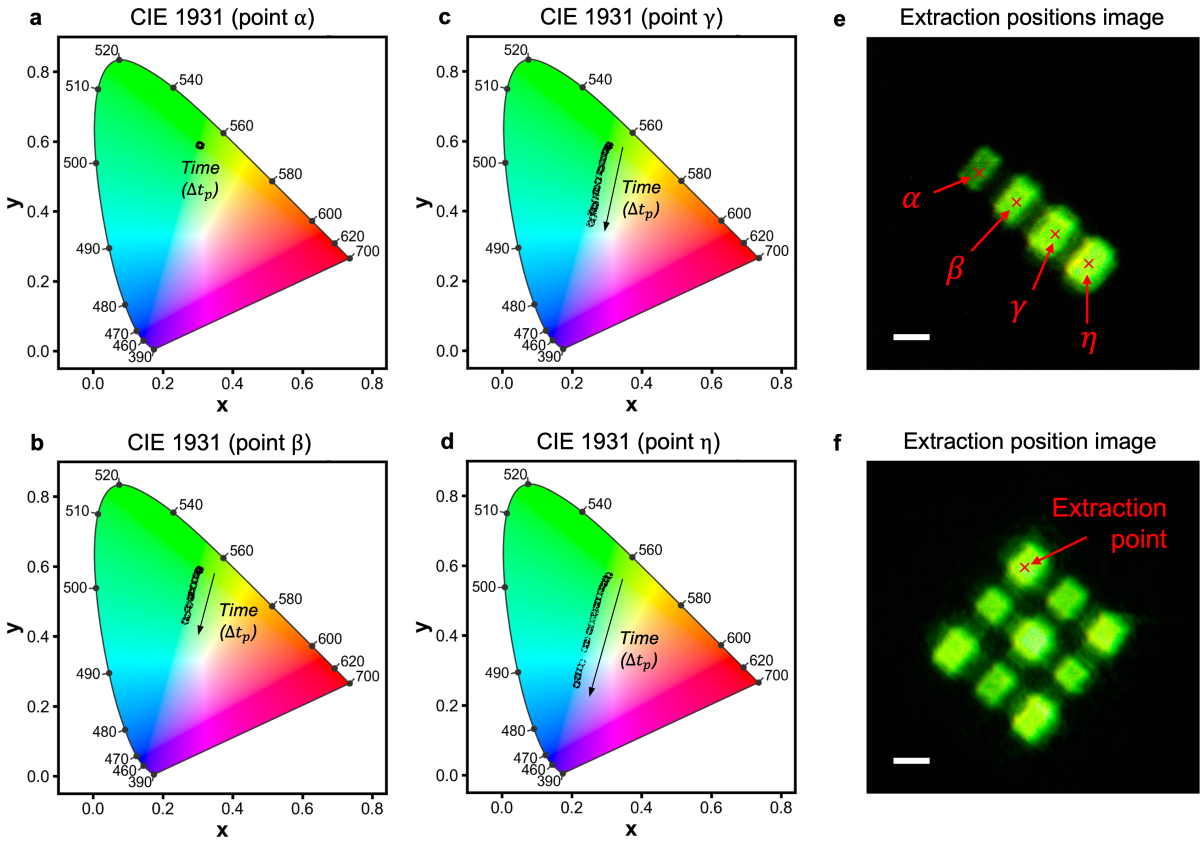

Figure S68. a-d, CIE 1931 chromaticity diagram with extracted color at four points α, β, γ, and η within different grayscale patterns during the same time duration ($\Delta t_p = 130\ [s]$). **e and f**, Fluorescence image showing extraction points for CIE 1931 chromaticity diagram in **a-d** and **Fig. 4d**.

Supporting NMR Data

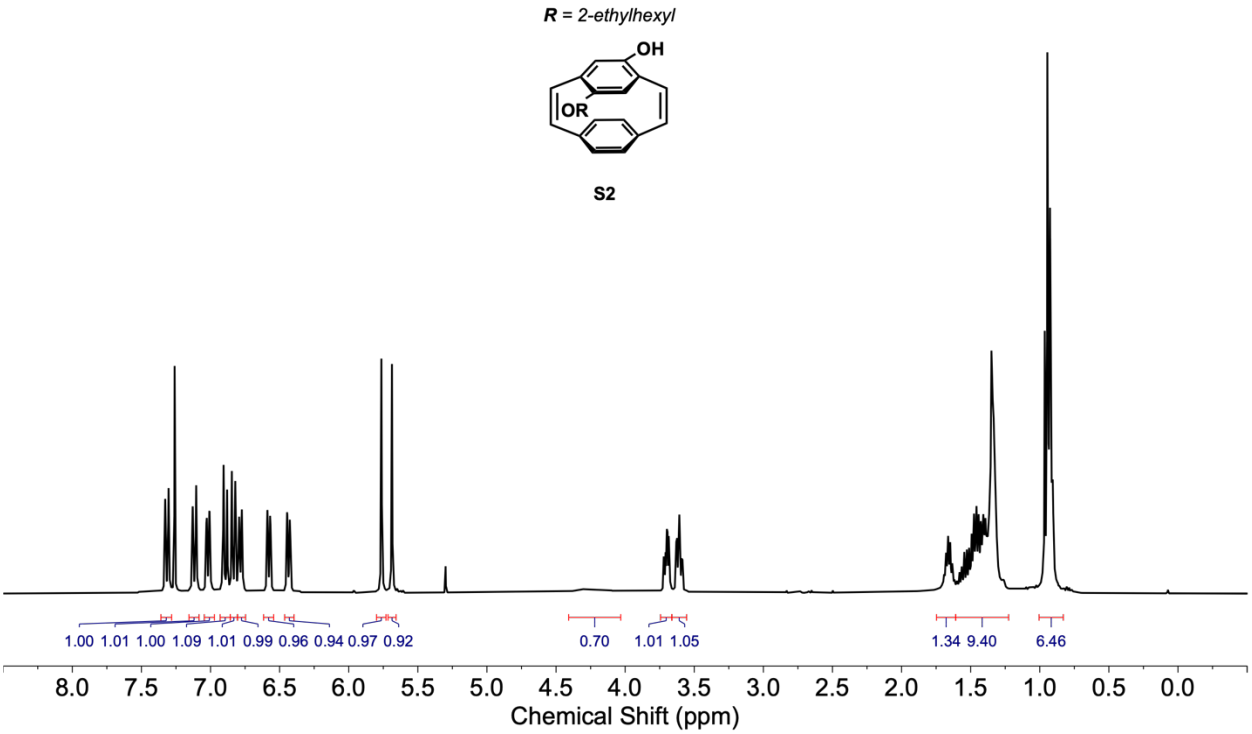

Figure S69. ^{1}H NMR (500 MHz, $CDCl_3$) spectrum of **S2**.

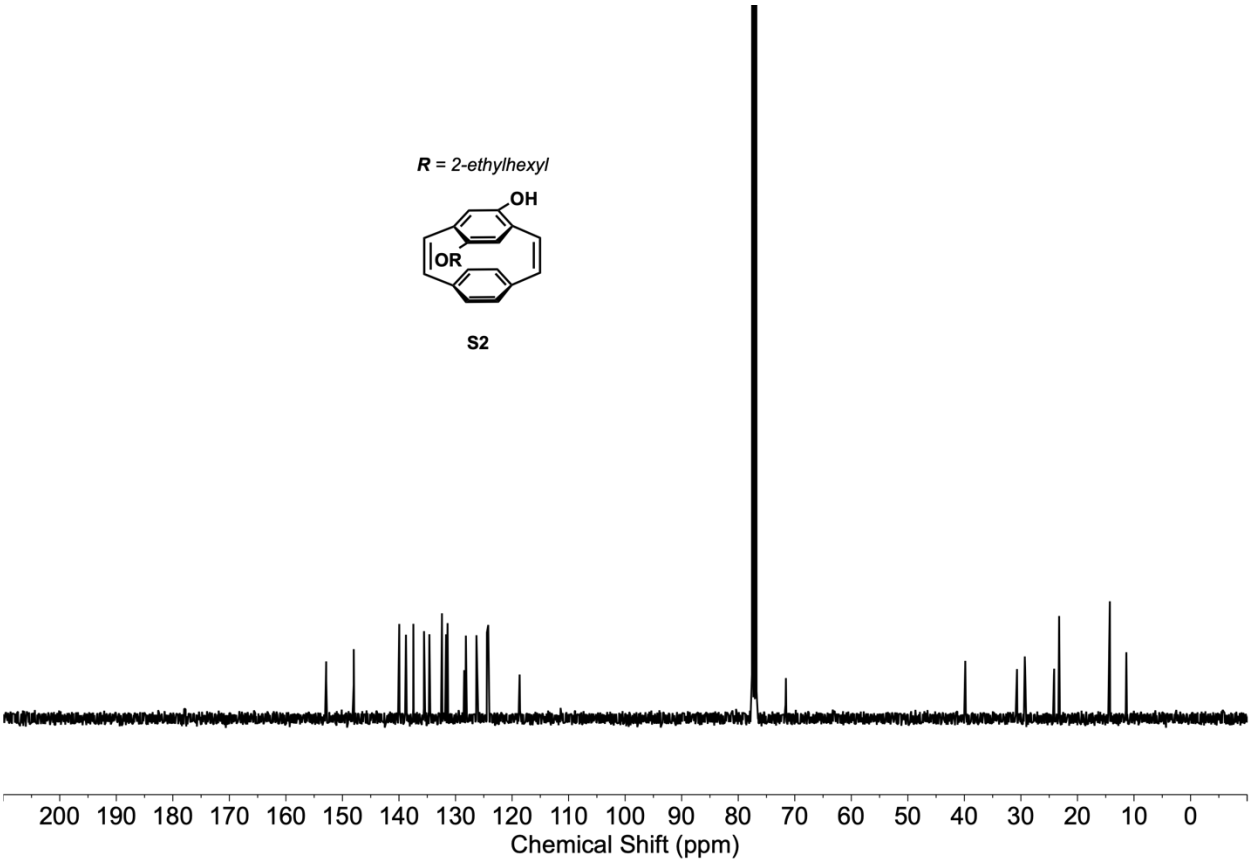

Figure S70. ^{13}C NMR (126 MHz, $CDCl_3$) spectrum of **S2**.

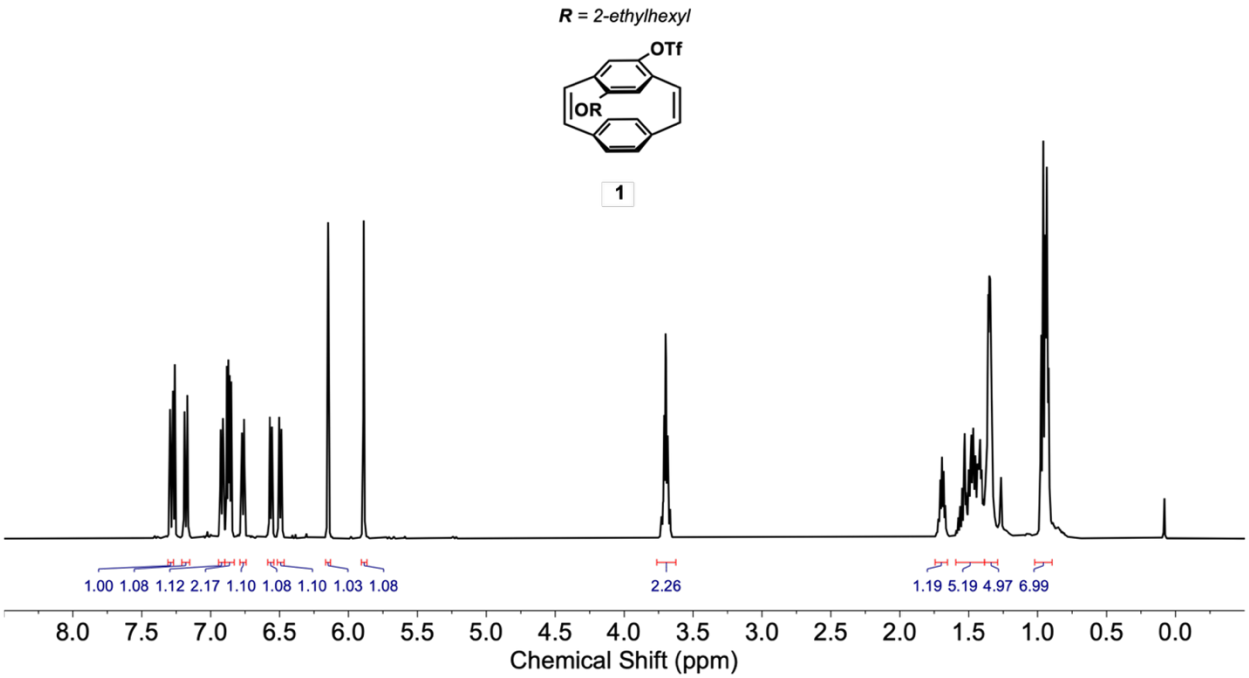

Figure S71. ^{1}H NMR (500 MHz, $CDCl_3$) spectrum of **S1**.

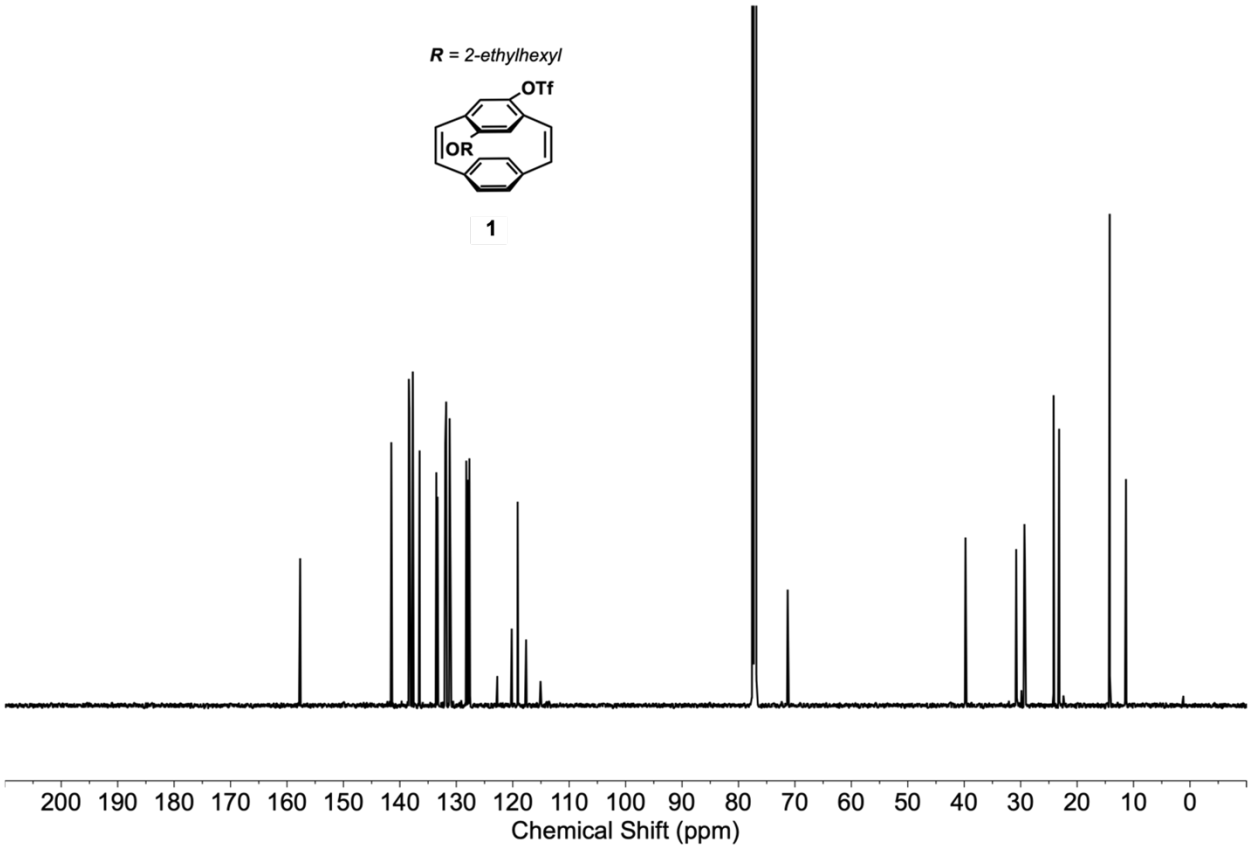

Figure S72. ^{13}C NMR (126 MHz, $CDCl_3$) spectrum of **1**.

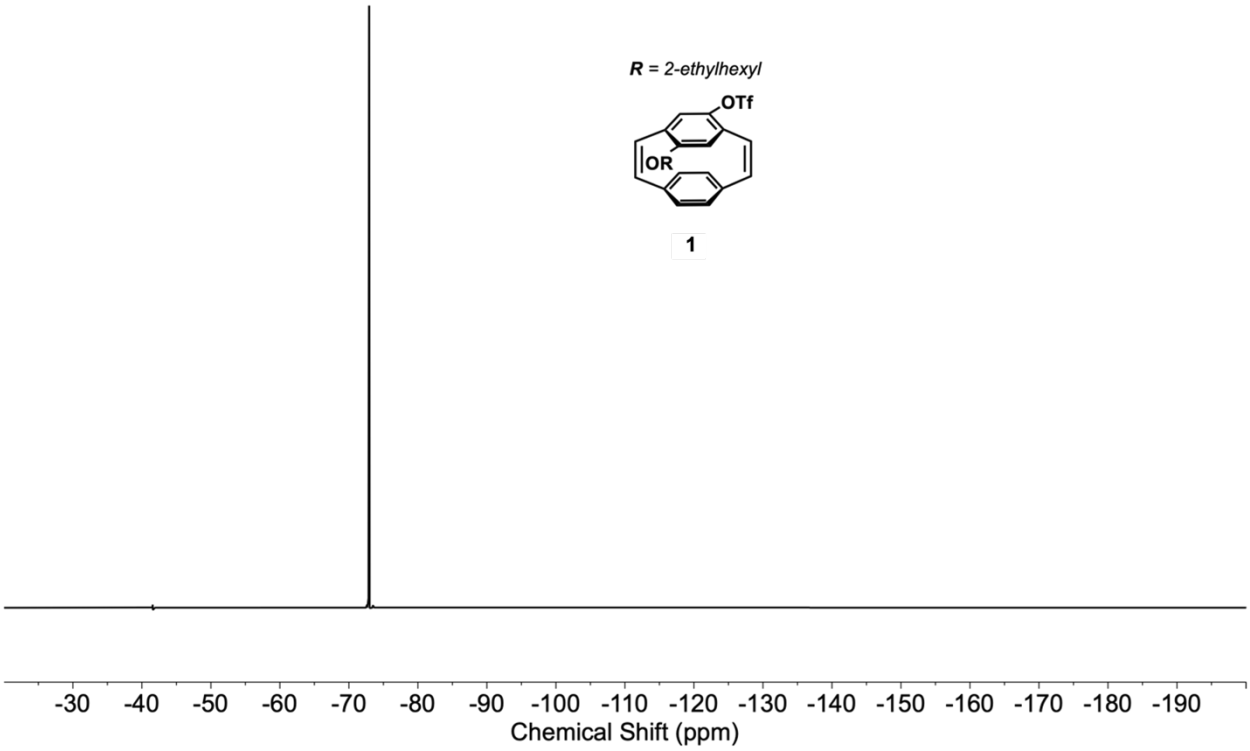

Figure S73. ^{19}F NMR (376 MHz, $CDCl_3$) spectrum of **1**.

Monomer NMR Spectra

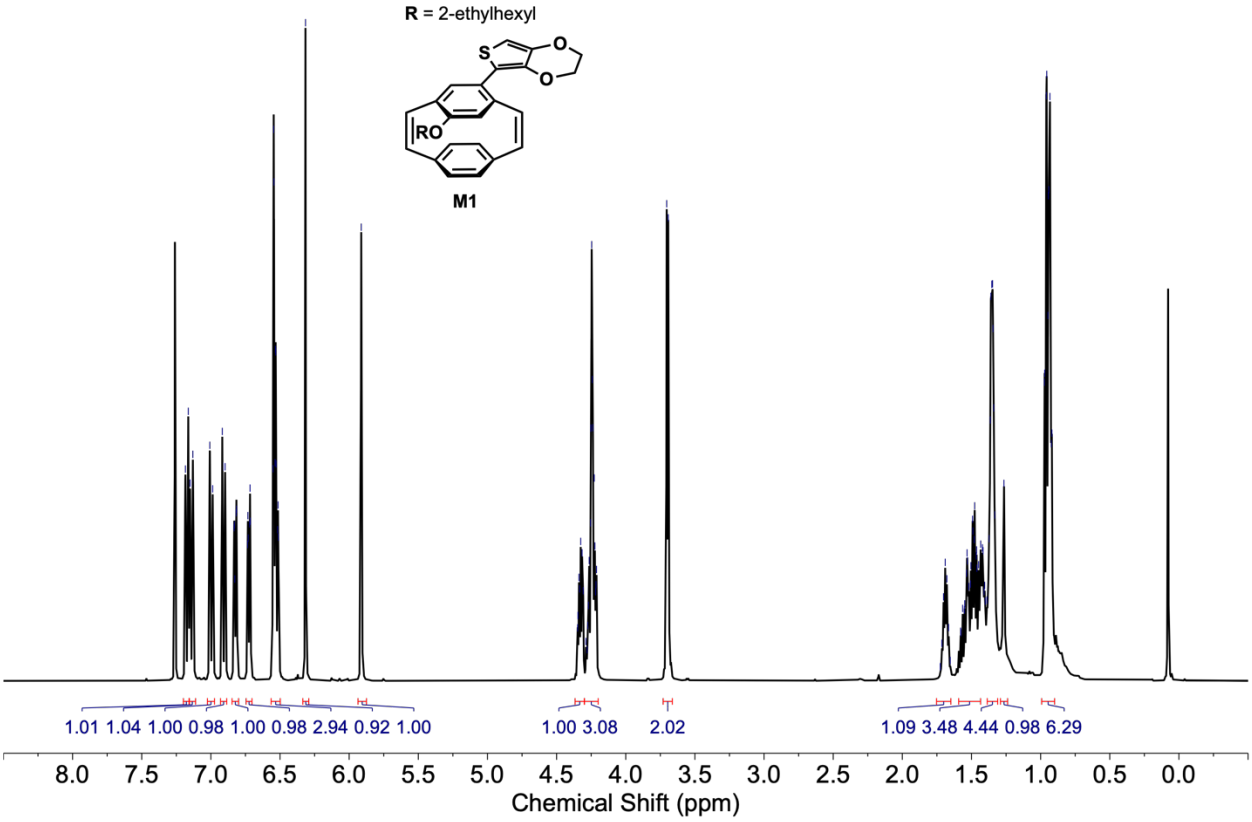

Figure S74. ^{1}H NMR (500 MHz, $CDCl_3$) spectrum of **M1**.

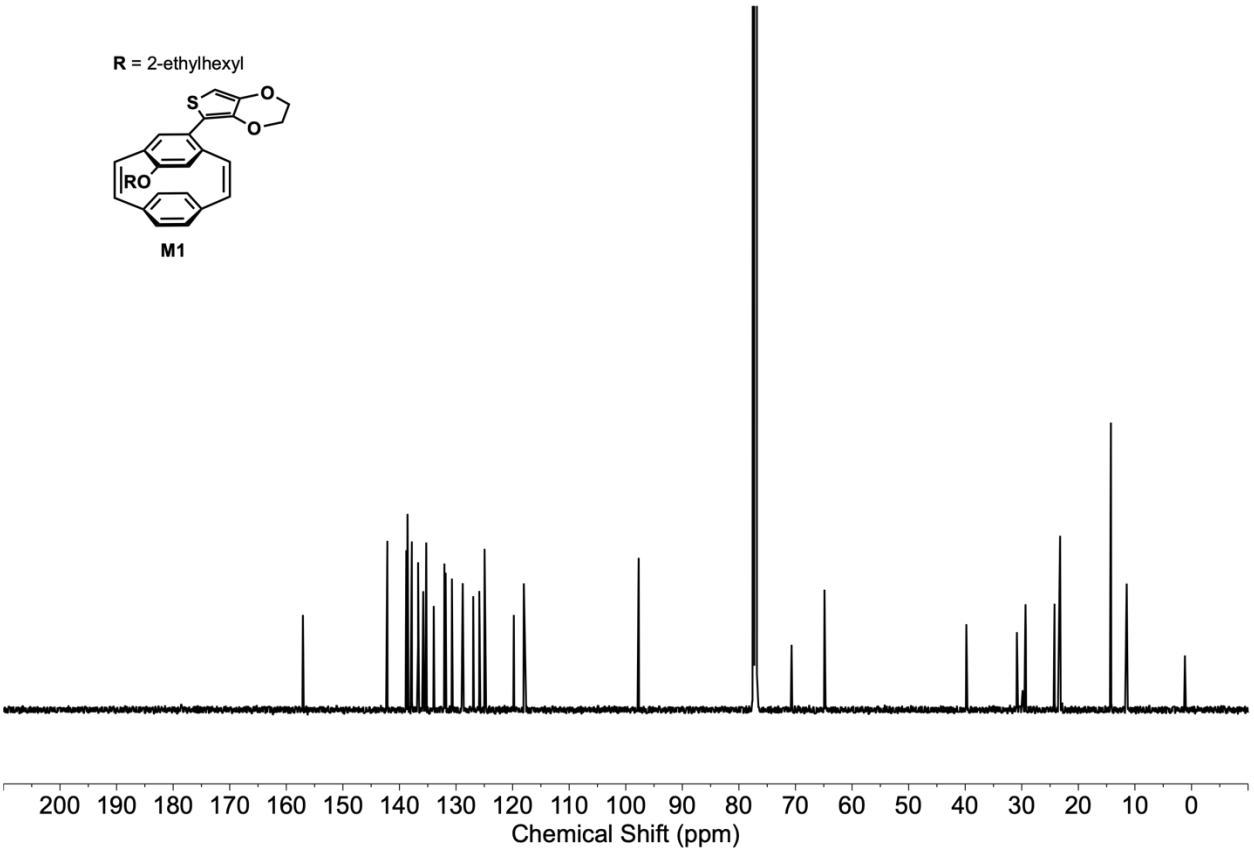

Figure S75. ^{13}C NMR (126 MHz, $CDCl_3$) spectrum of **M1**.

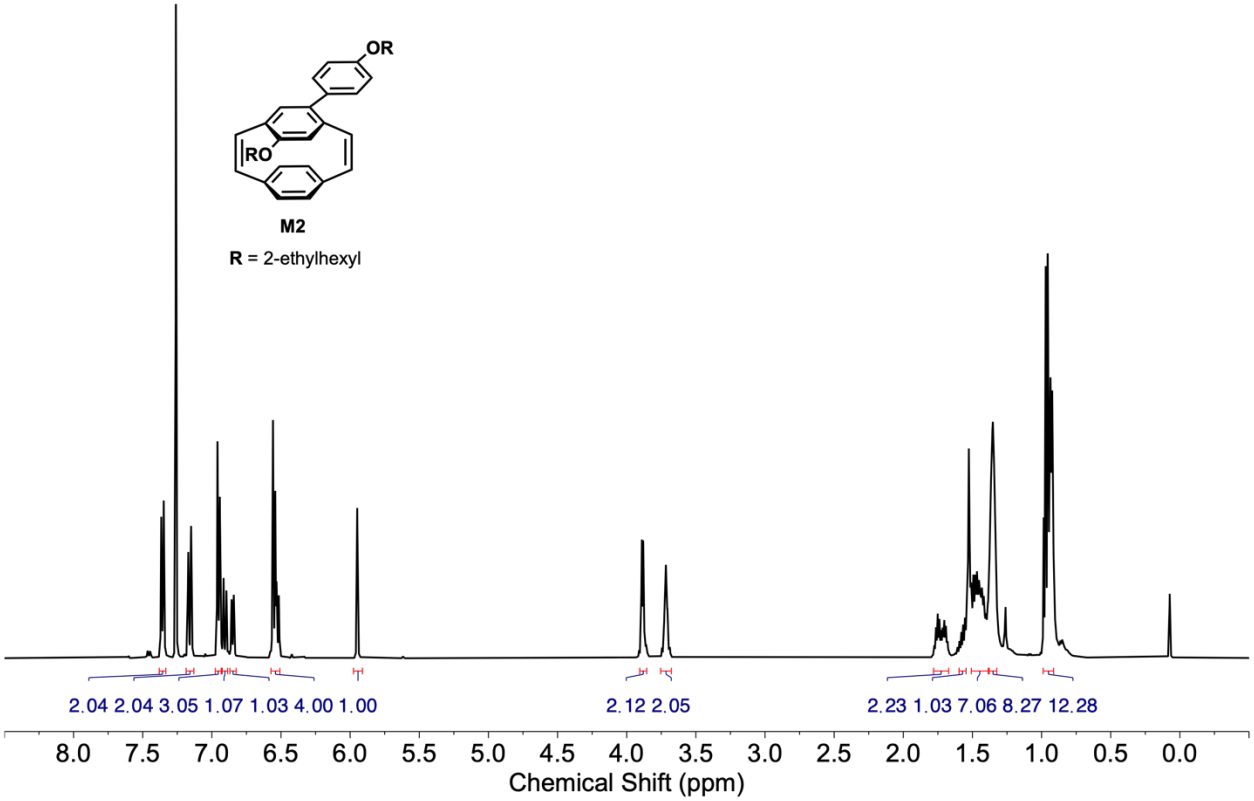

Figure S76. ^{1}H NMR (500 MHz, $CDCl_3$) spectrum of **M2**.

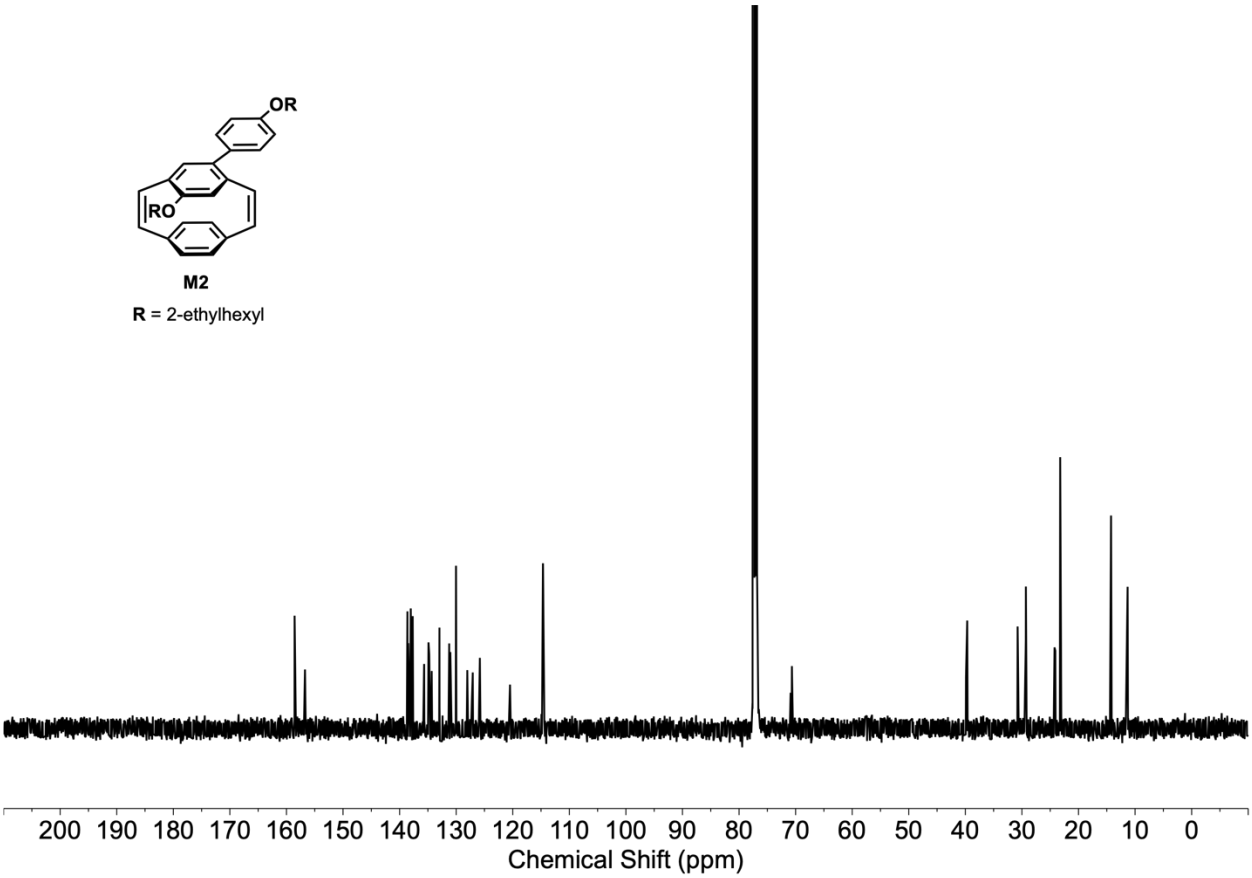

Figure S77. ^{13}C NMR (126 MHz, $CDCl_3$) spectrum of **M2**.

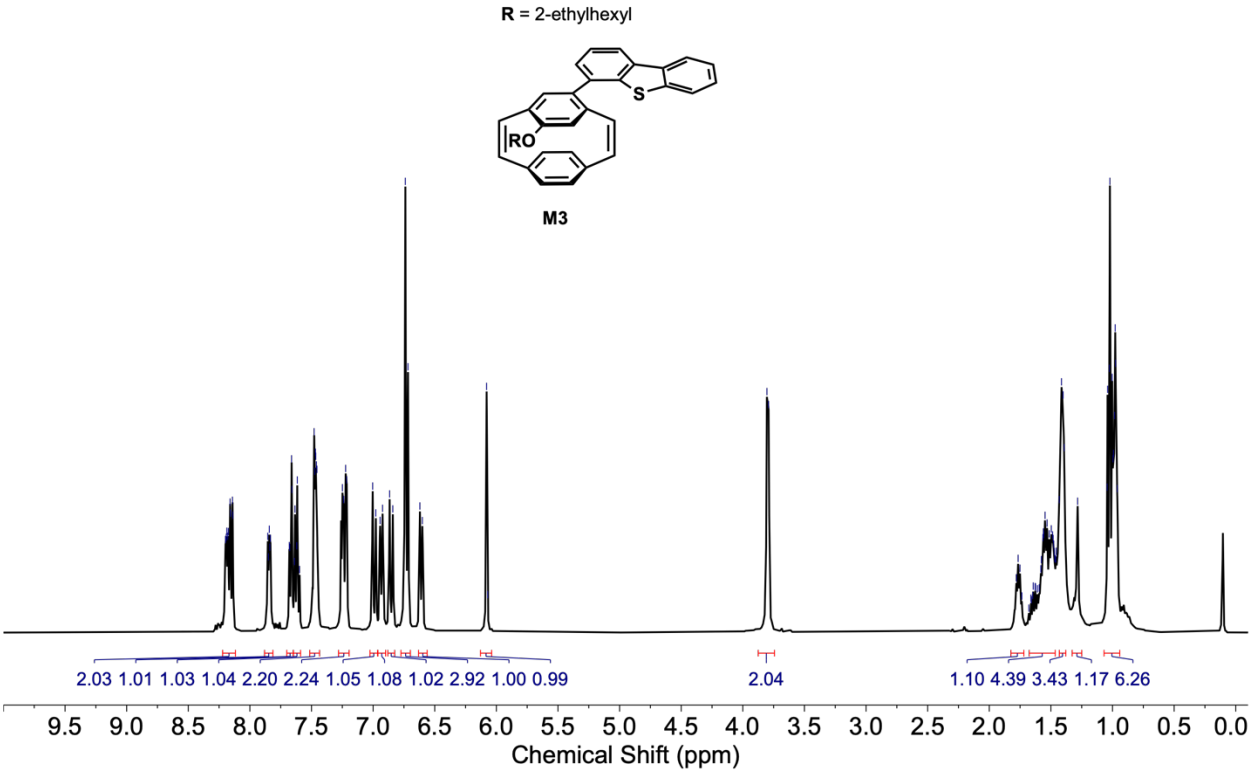

Figure S78. ^{1}H NMR (500 MHz, $CDCl_3$) spectrum of **M3**.

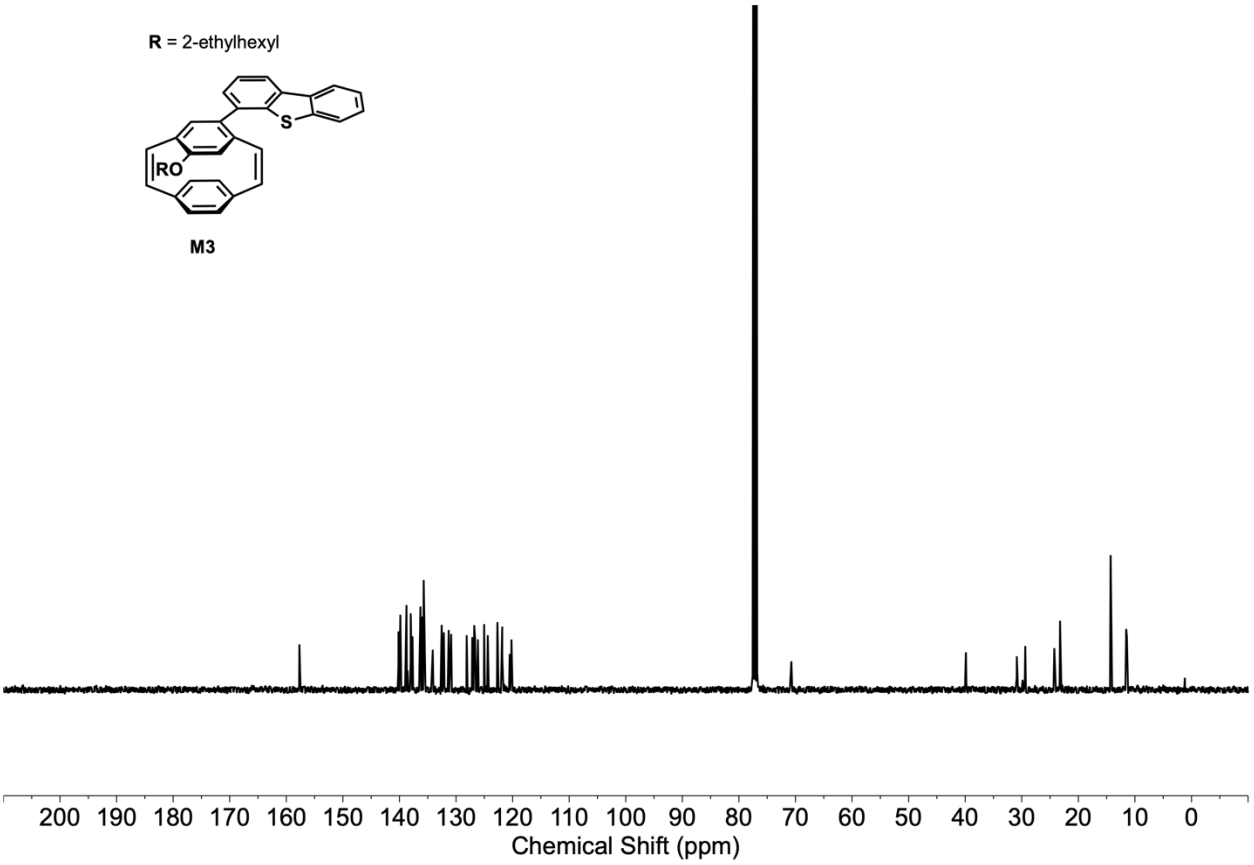

Figure S79. ^{13}C NMR (126 MHz, $CDCl_3$) spectrum of **M3**.

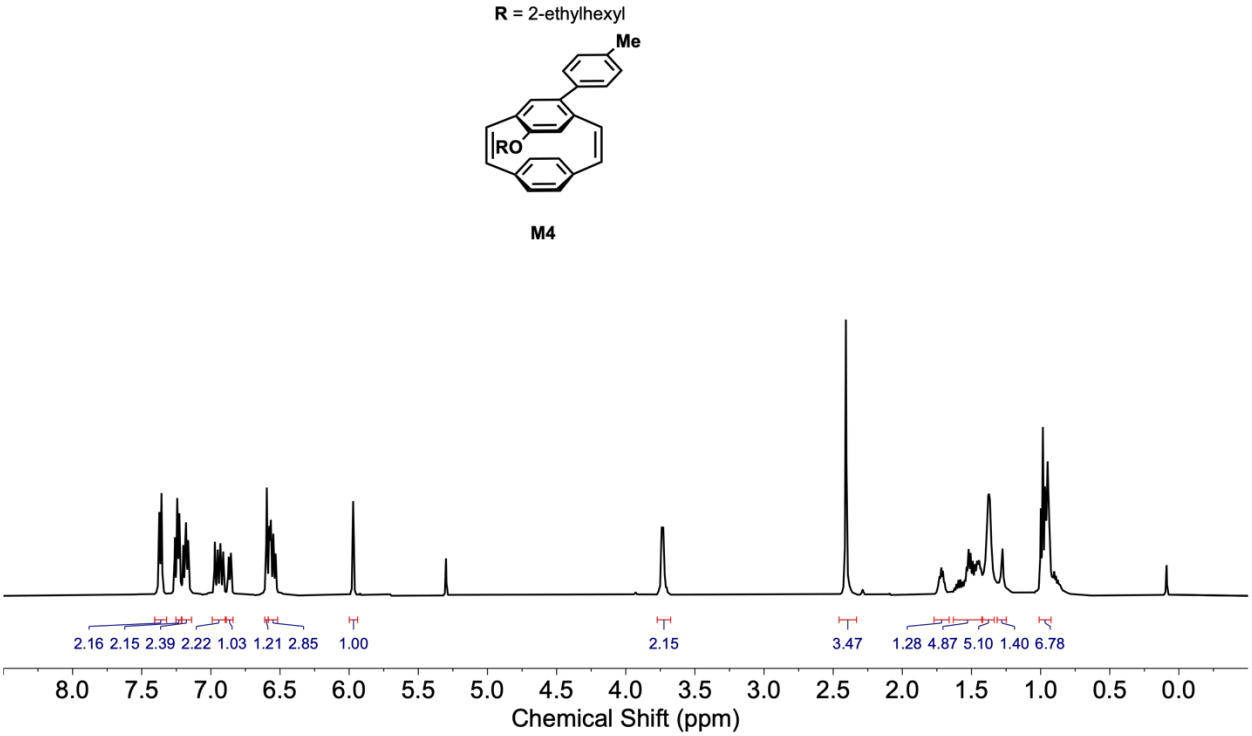

Figure S80. ^{1}H NMR (500 MHz, $CDCl_3$) spectrum of **M4**.

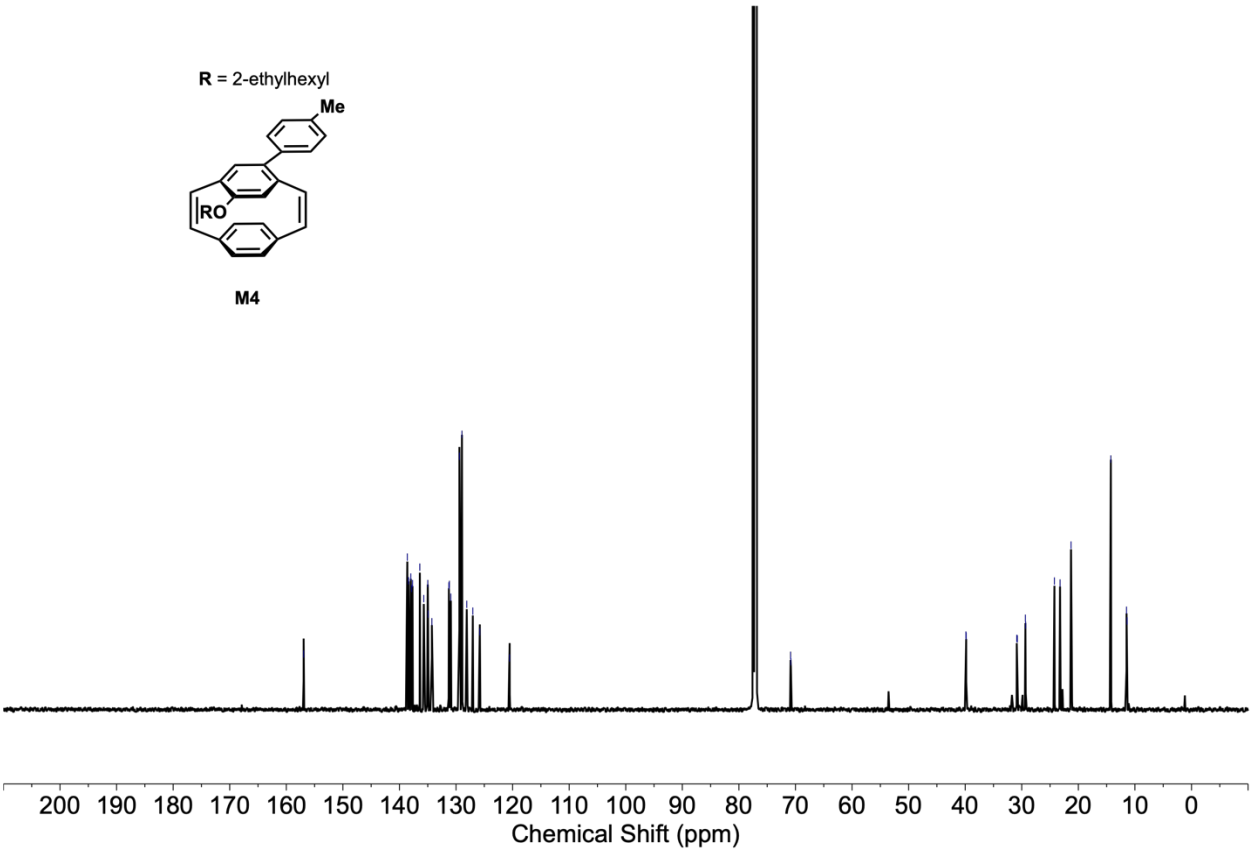

Figure S81. ^{13}C NMR (126 MHz, $CDCl_3$) spectrum of **M4**.

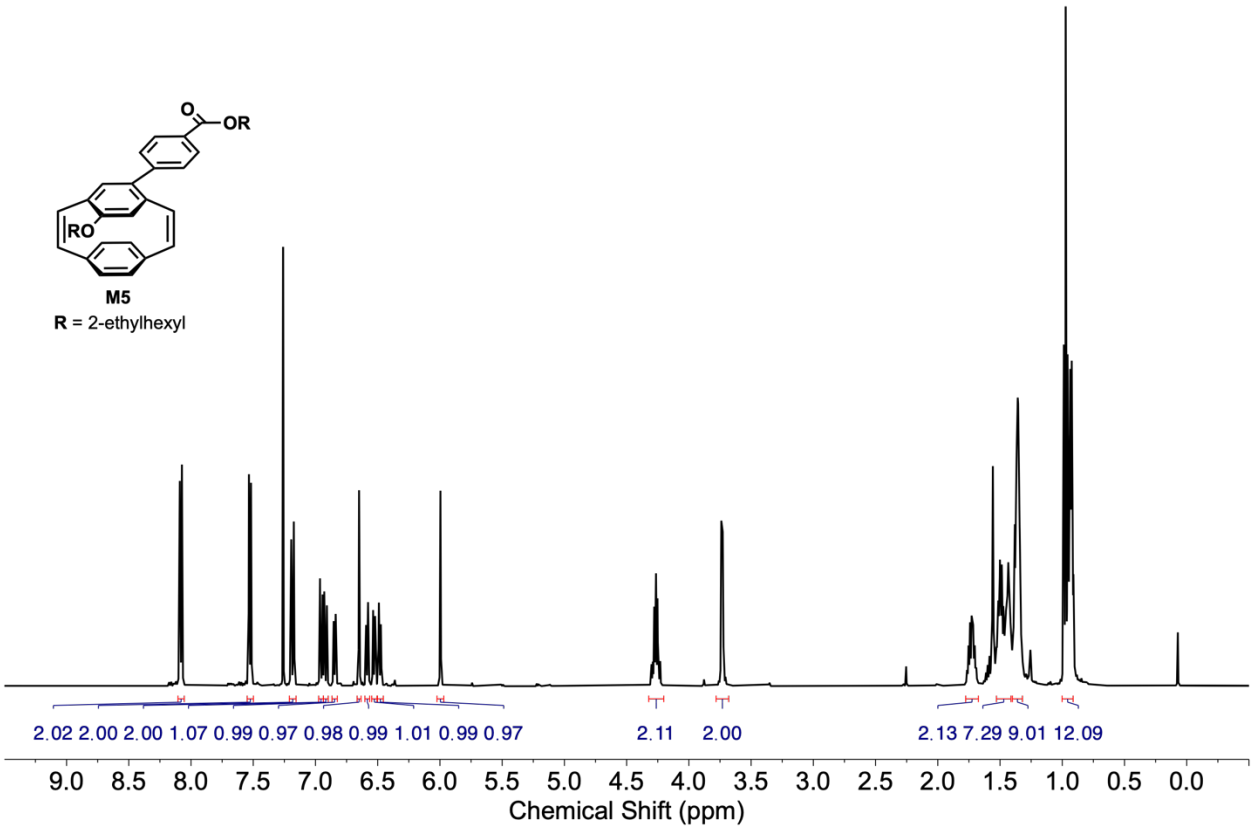

Figure S82. ^{1}H NMR (500 MHz, $CDCl_3$) spectrum of **M5**.

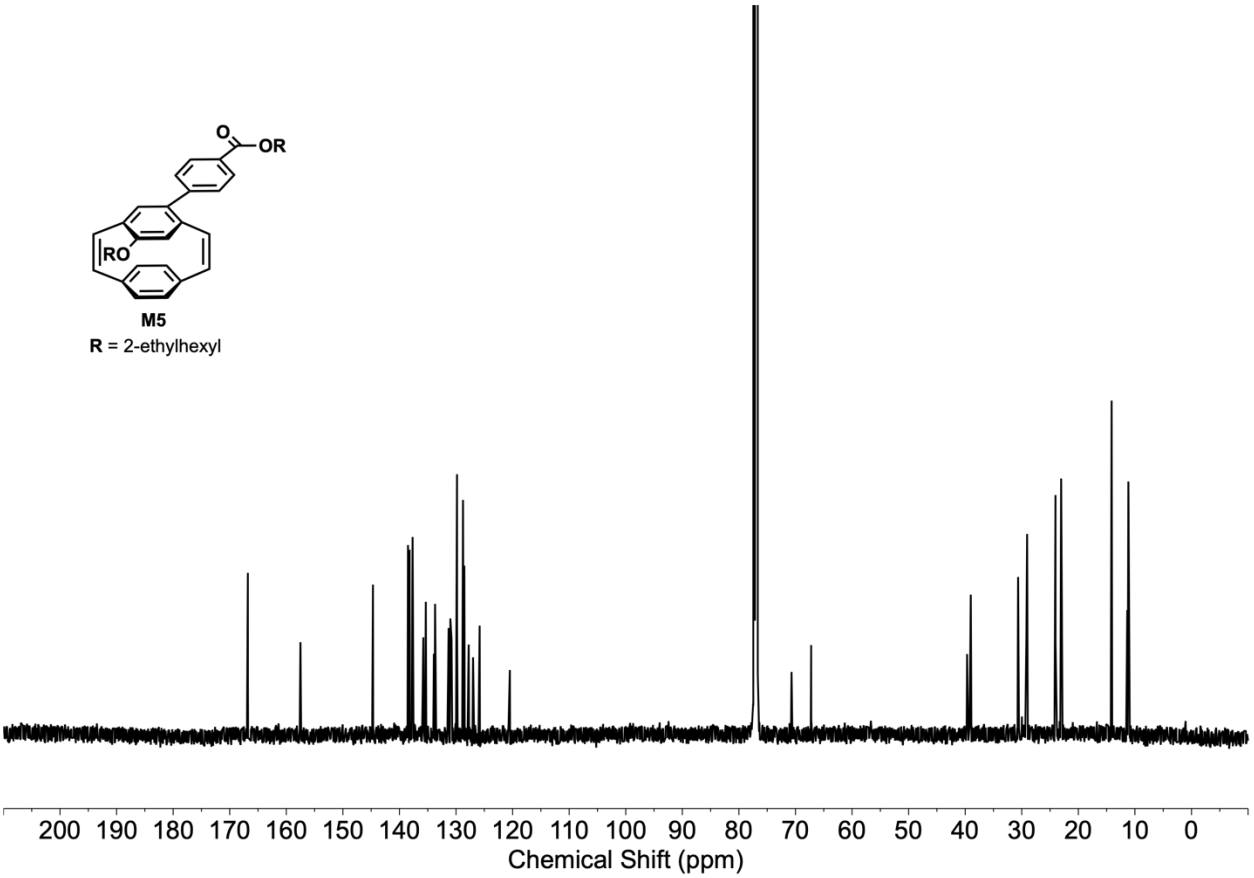

Figure S83. ^{13}C NMR (126 MHz, $CDCl_3$) spectrum of **M5**.

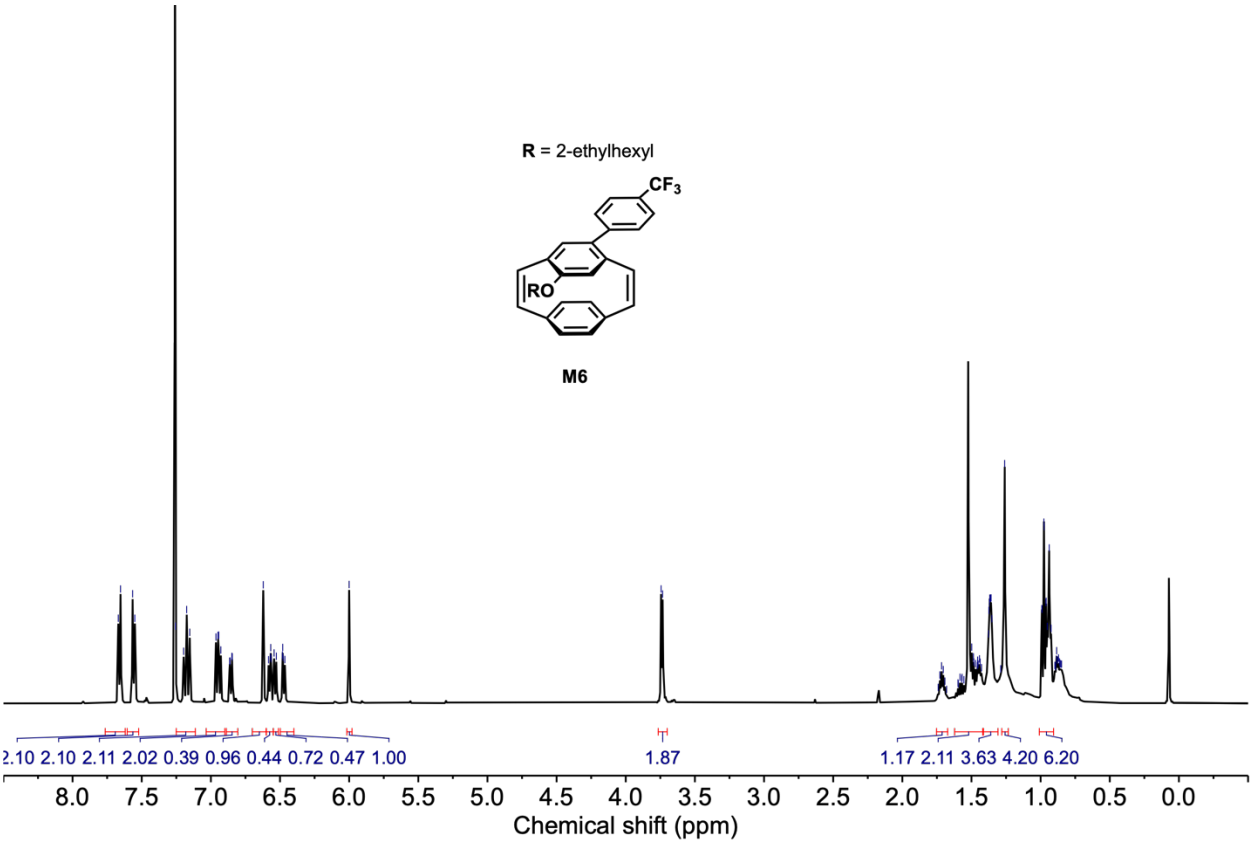

Figure S84. ^{1}H NMR (500 MHz, $CDCl_3$) spectrum of **M6.**

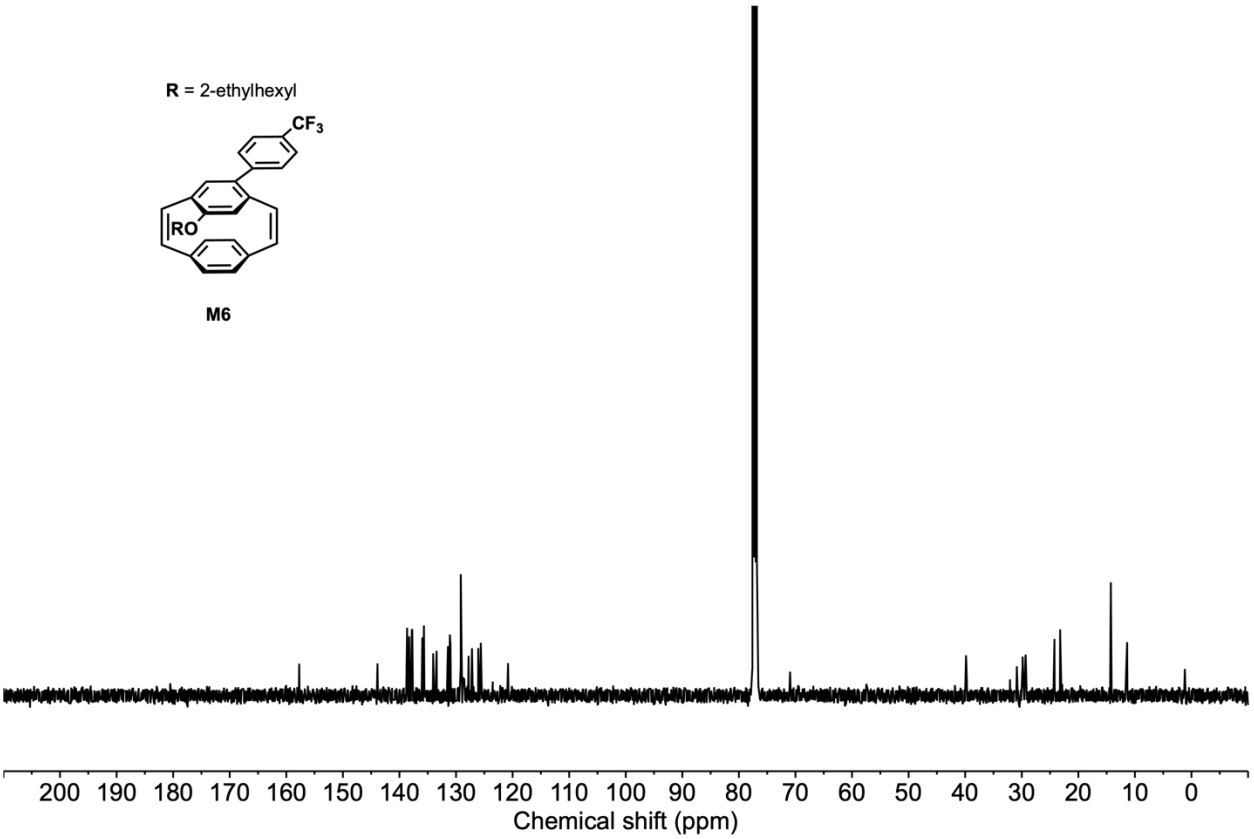

Figure S85. ^{13}C NMR (126 MHz, $CDCl_3$) spectrum of **M6**.

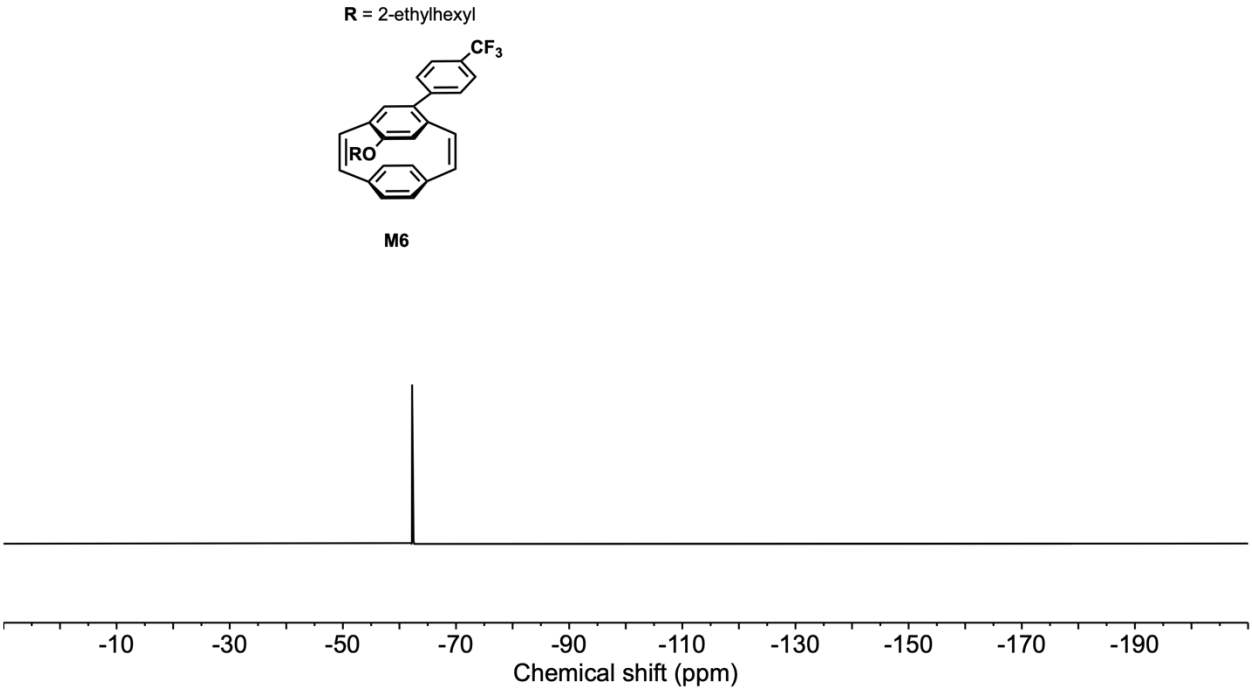

Figure S86. ^{19}F NMR (376 MHz, $CDCl_3$) spectrum of **M6**.

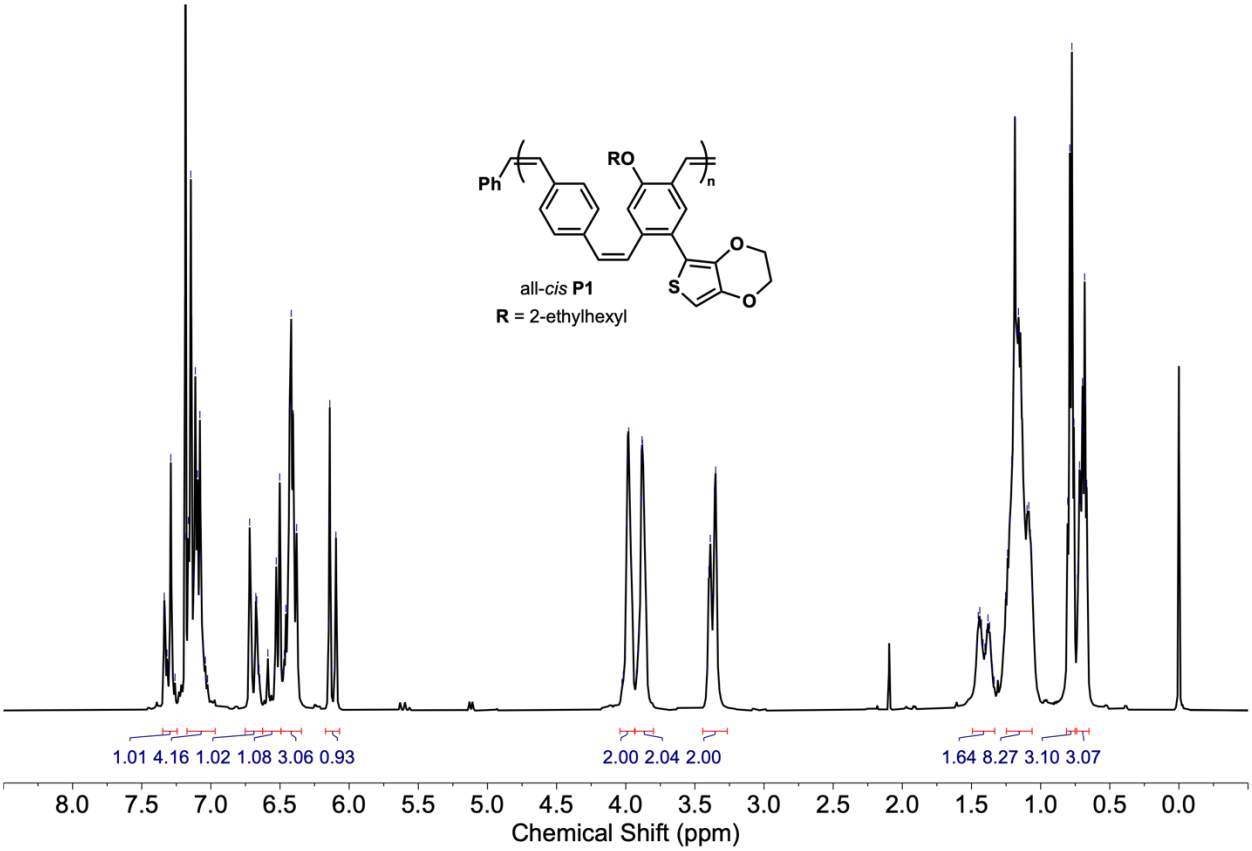

Figure S87. ^{1}H NMR (500 MHz, $CDCl_3$) spectrum of all-*cis* **P1**.

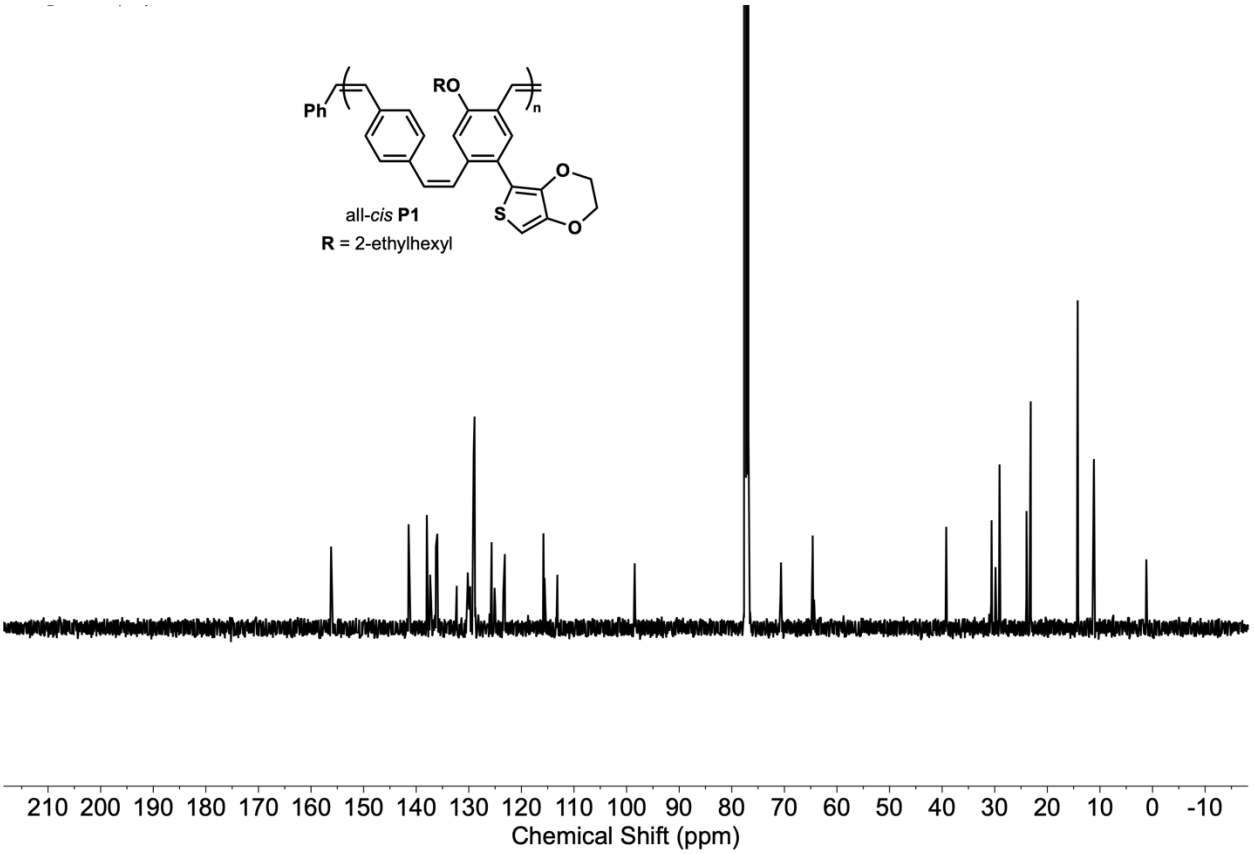

Figure S88. ^{13}C NMR (126 MHz, $CDCl_3$) spectrum of all-*cis* **P1.**

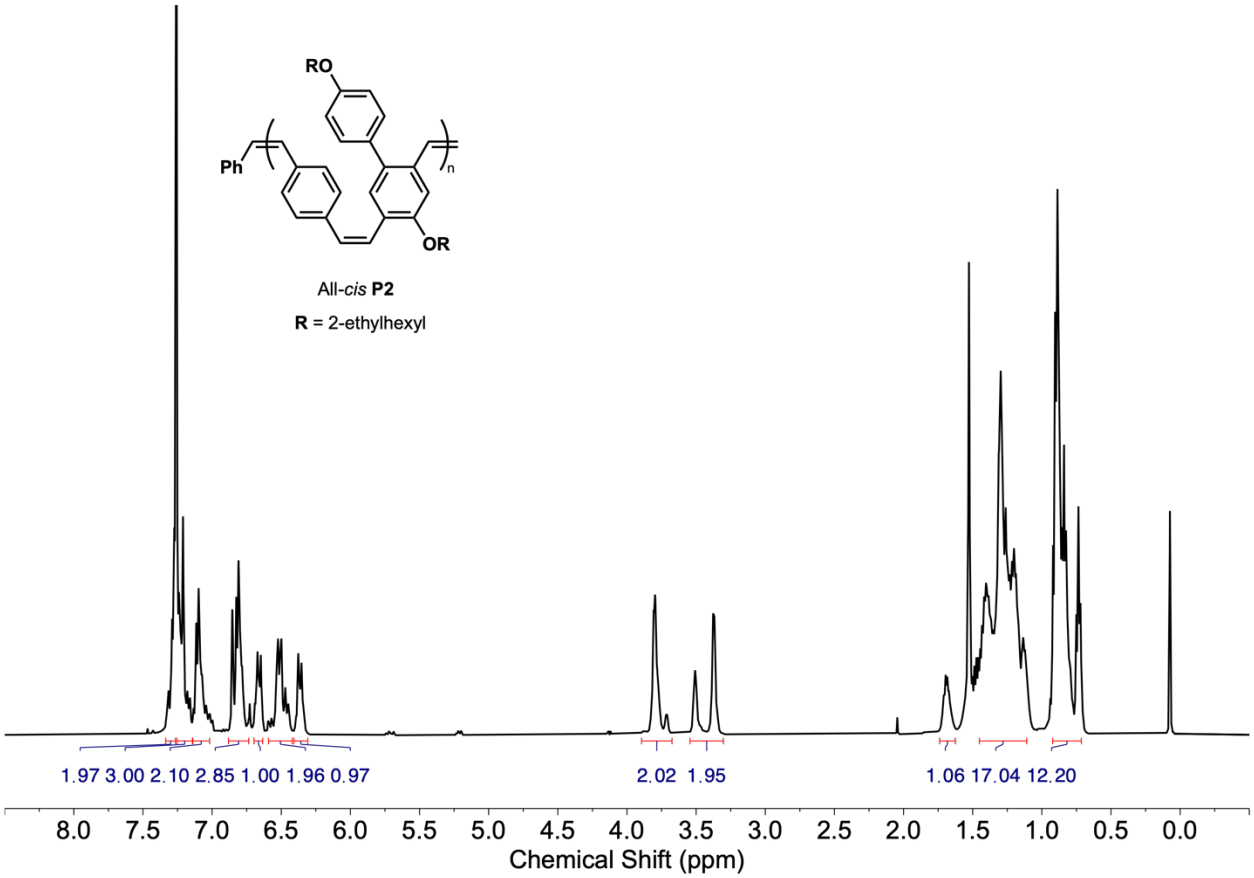

Figure S89. ^{1}H NMR (500 MHz, $CDCl_3$) spectrum of all-*cis* **P2**.

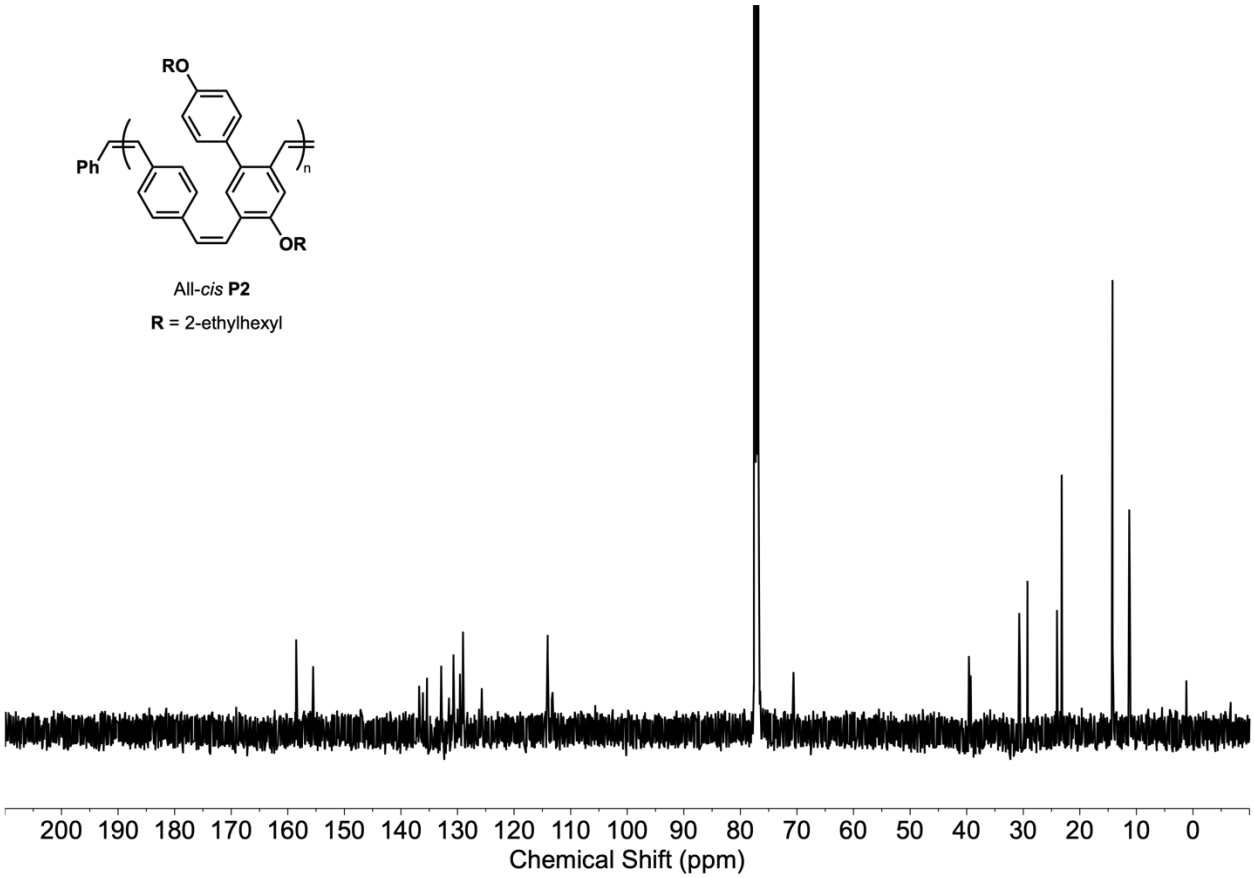

Figure S90. ^{13}C NMR (126 MHz, $CDCl_3$) spectrum of all-*cis* **P2.**

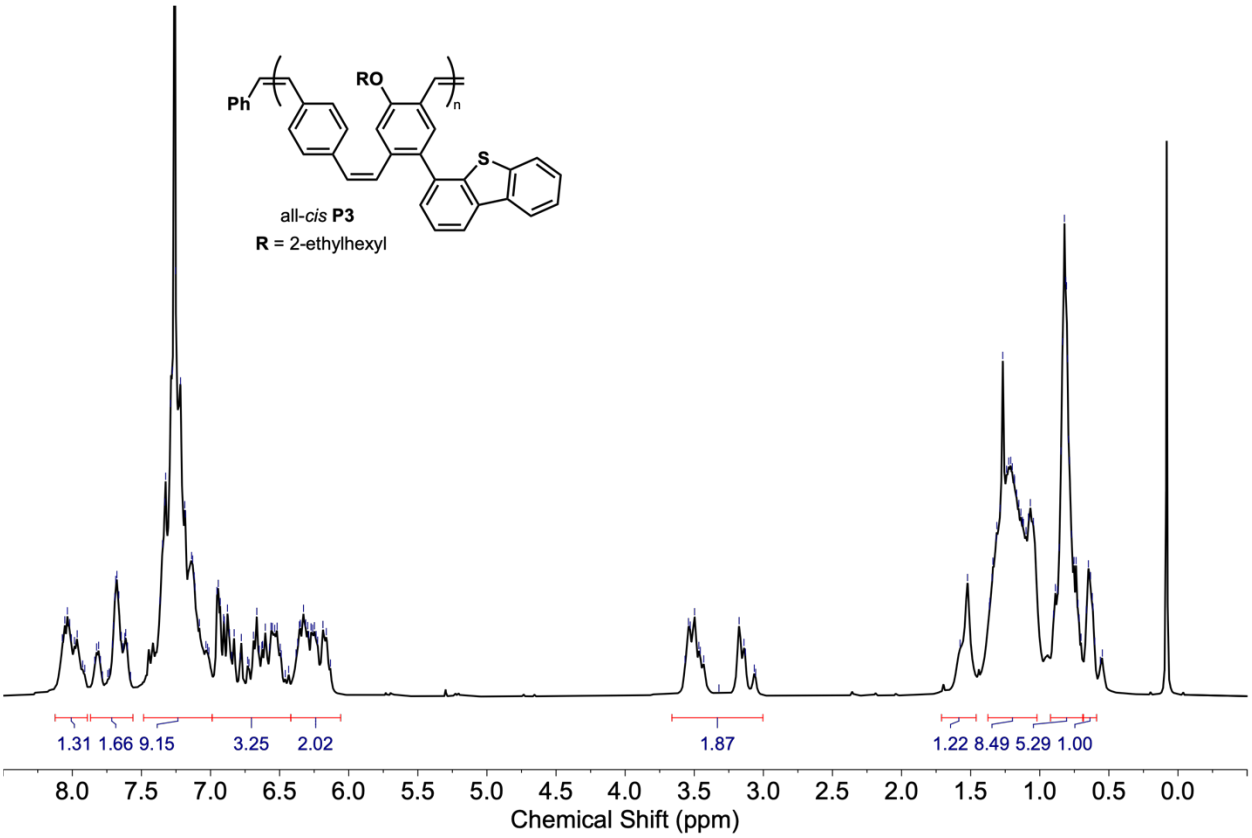

Figure S91. ^{1}H NMR (500 MHz, $CDCl_3$) spectrum of all-*cis* **P3**.

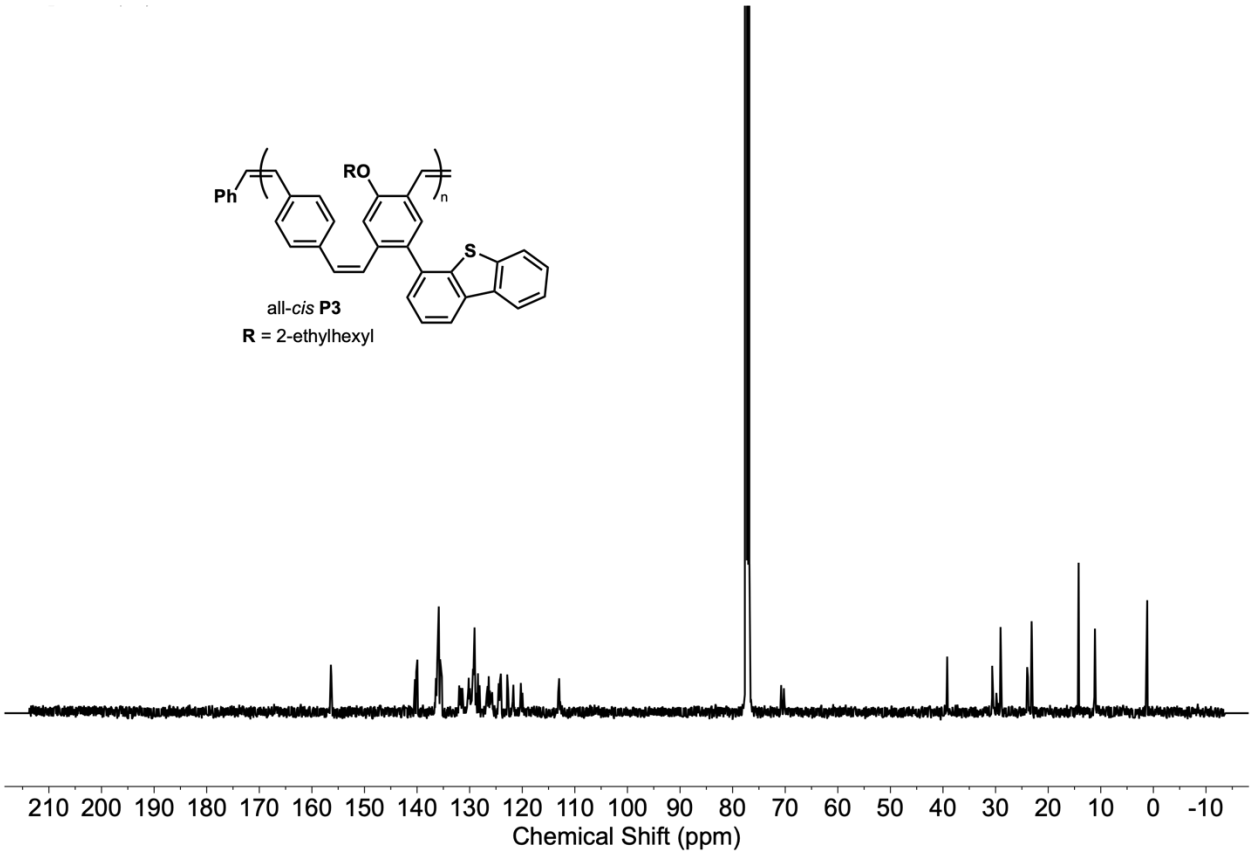

Figure S92. ^{13}C NMR (126 MHz, $CDCl_3$) spectrum of all-*cis* **P3**.

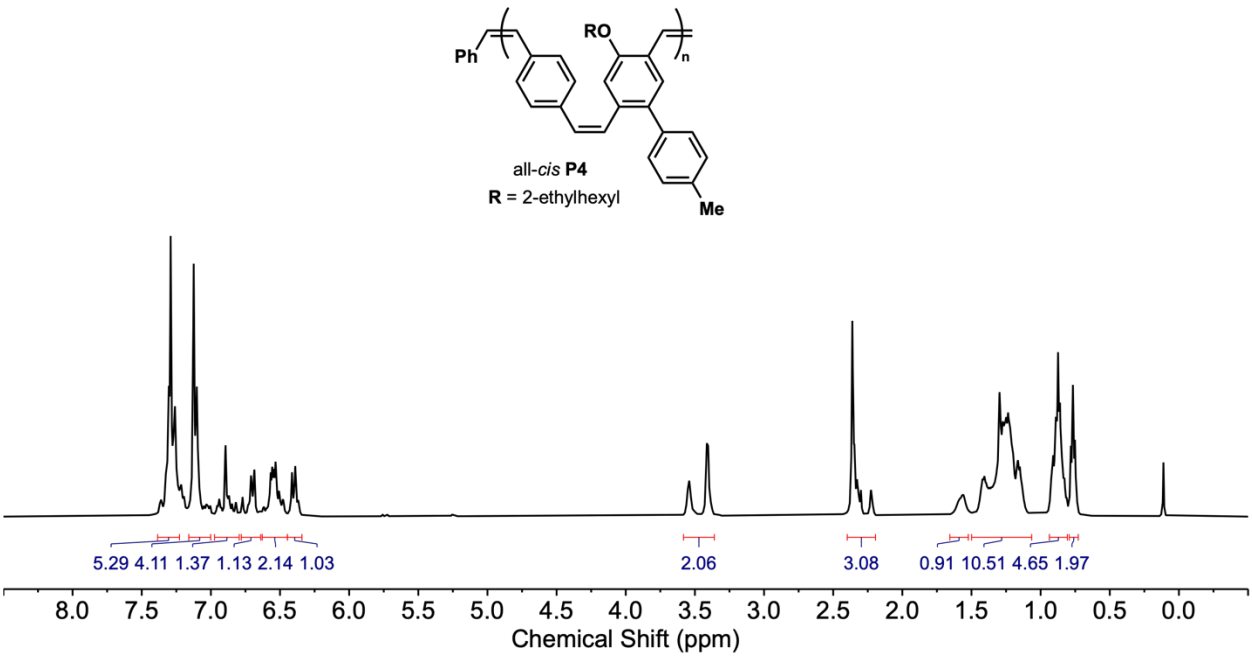

Figure S93. ^{1}H NMR (500 MHz, $CDCl_3$) spectrum of all-*cis* **P4**.

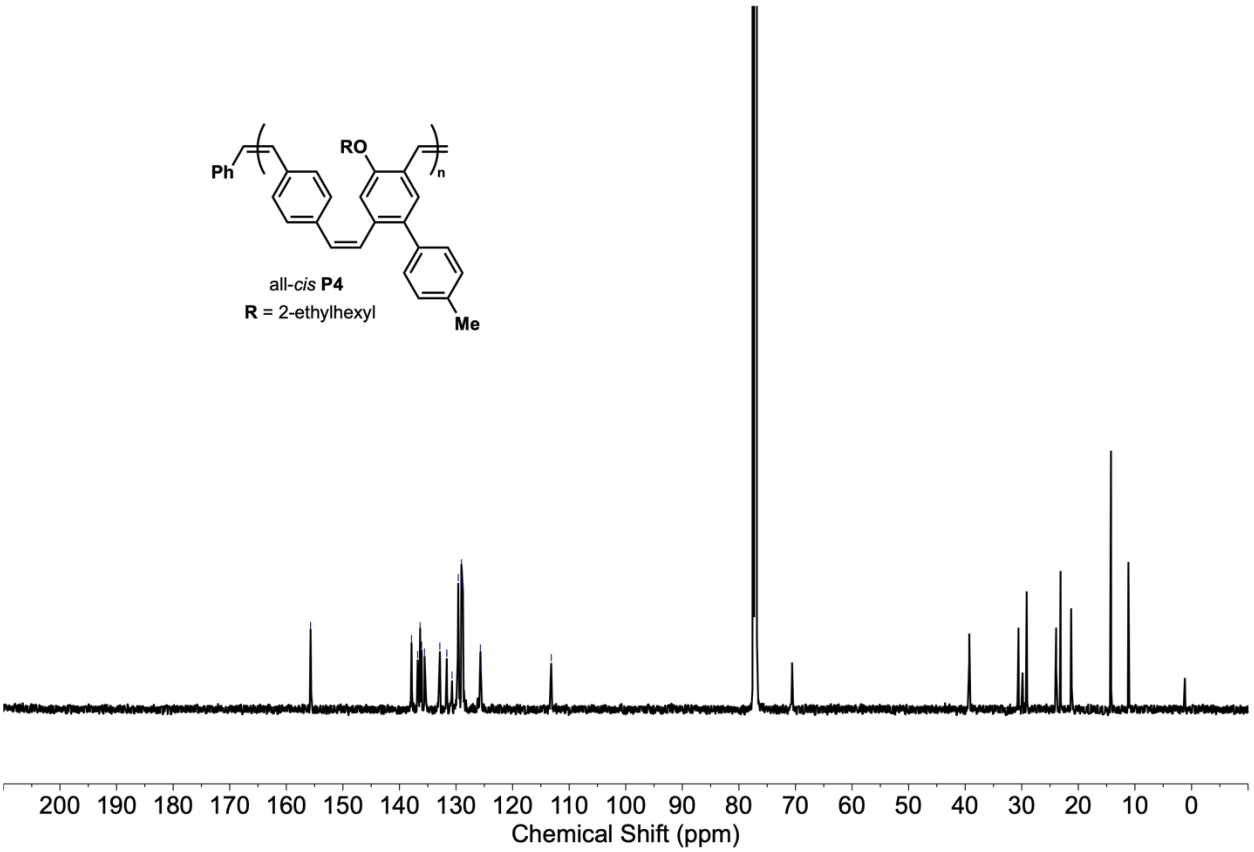

Figure S94. ^{13}C NMR (126 MHz, $CDCl_3$) spectrum of all-*cis* **P4**.

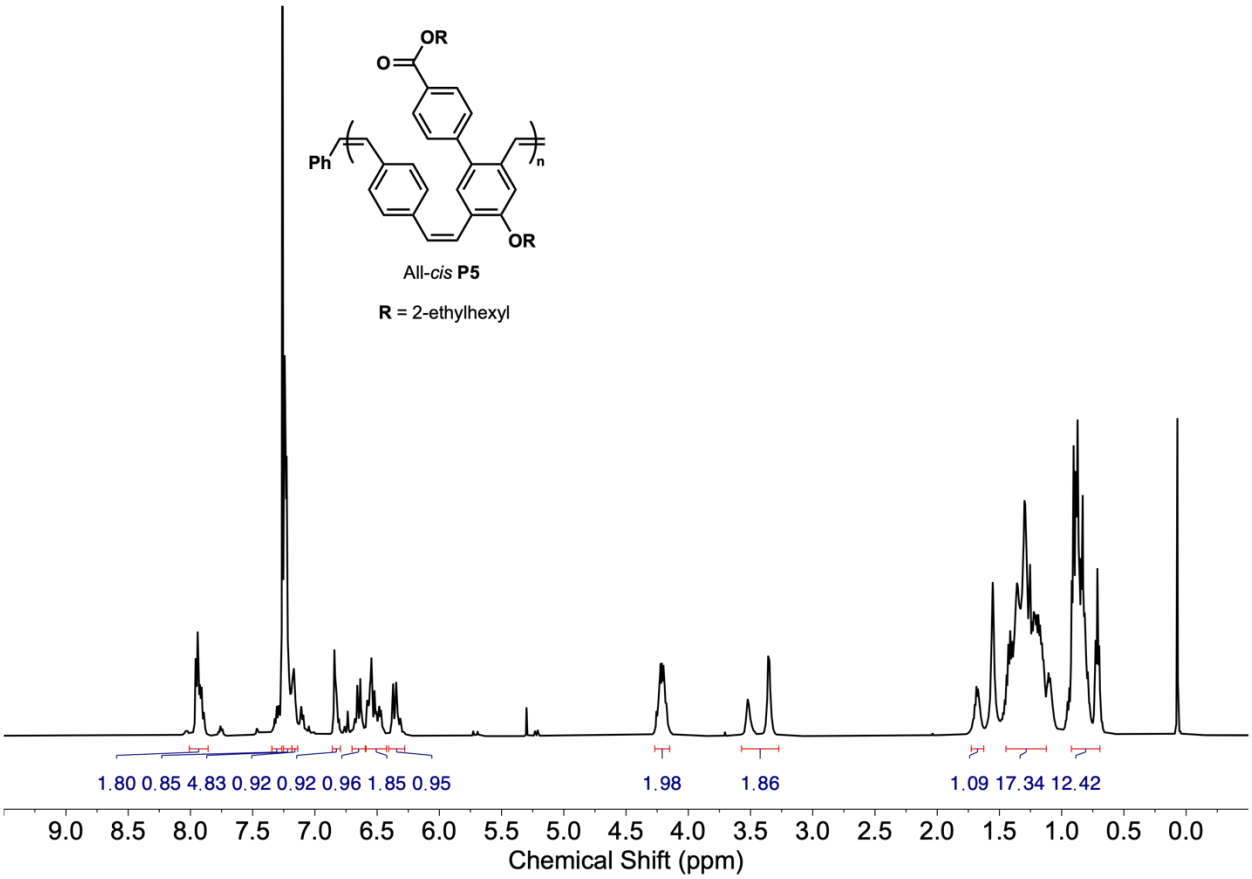

Figure S95. ^{1}H NMR (500 MHz, $CDCl_3$) spectrum of all-*cis* **P5**.

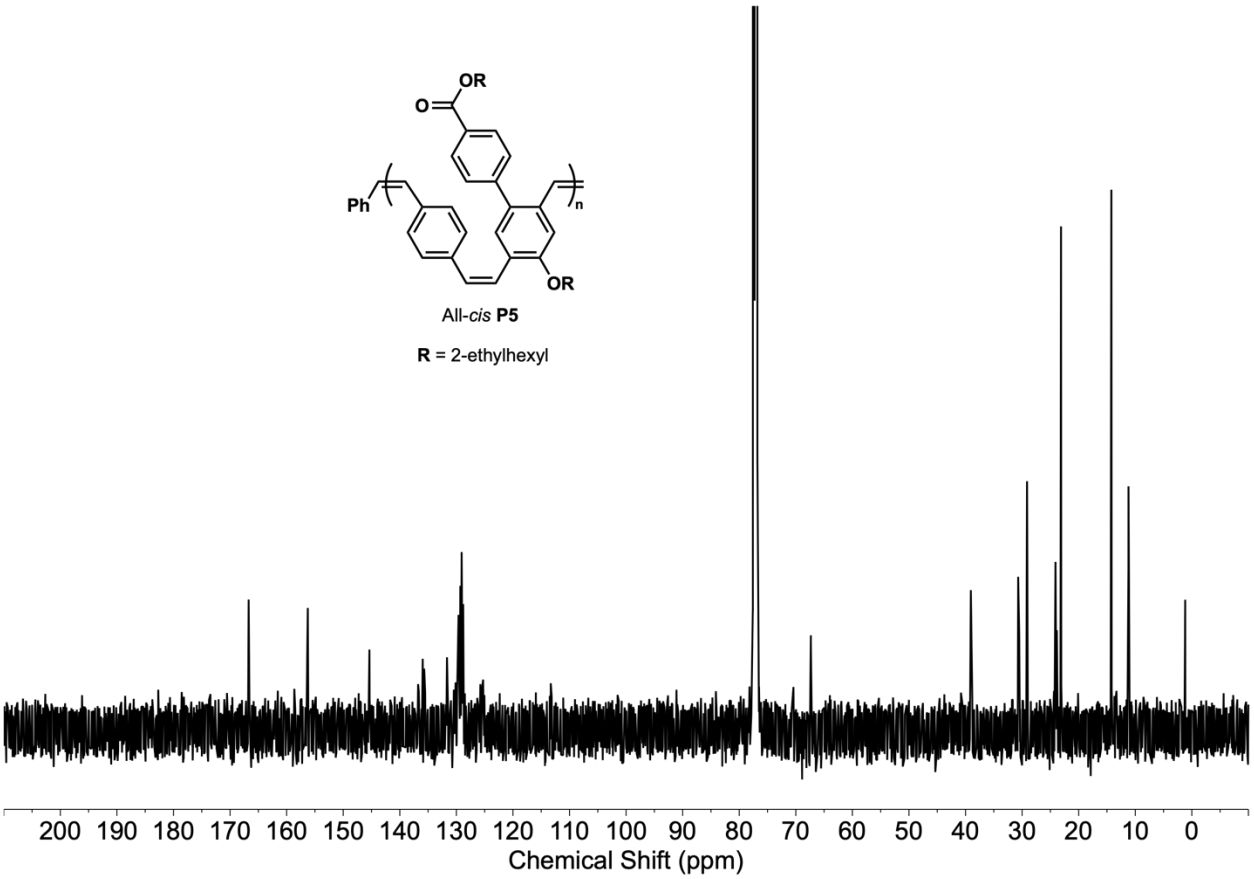

Figure S96. ^{13}C NMR (126 MHz, $CDCl_3$) spectrum of all-*cis* **P5**.

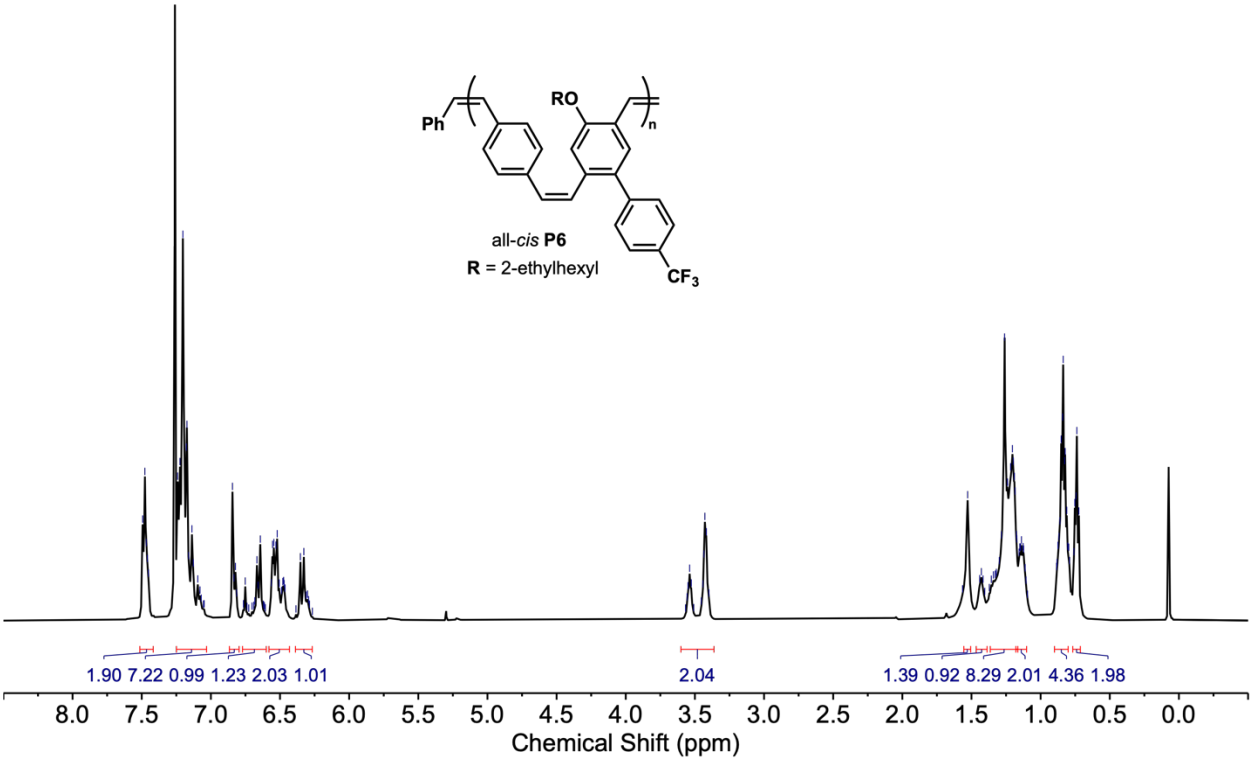

Figure S97. ^{1}H NMR (500 MHz, $CDCl_3$) spectrum of all-*cis* **P6**.

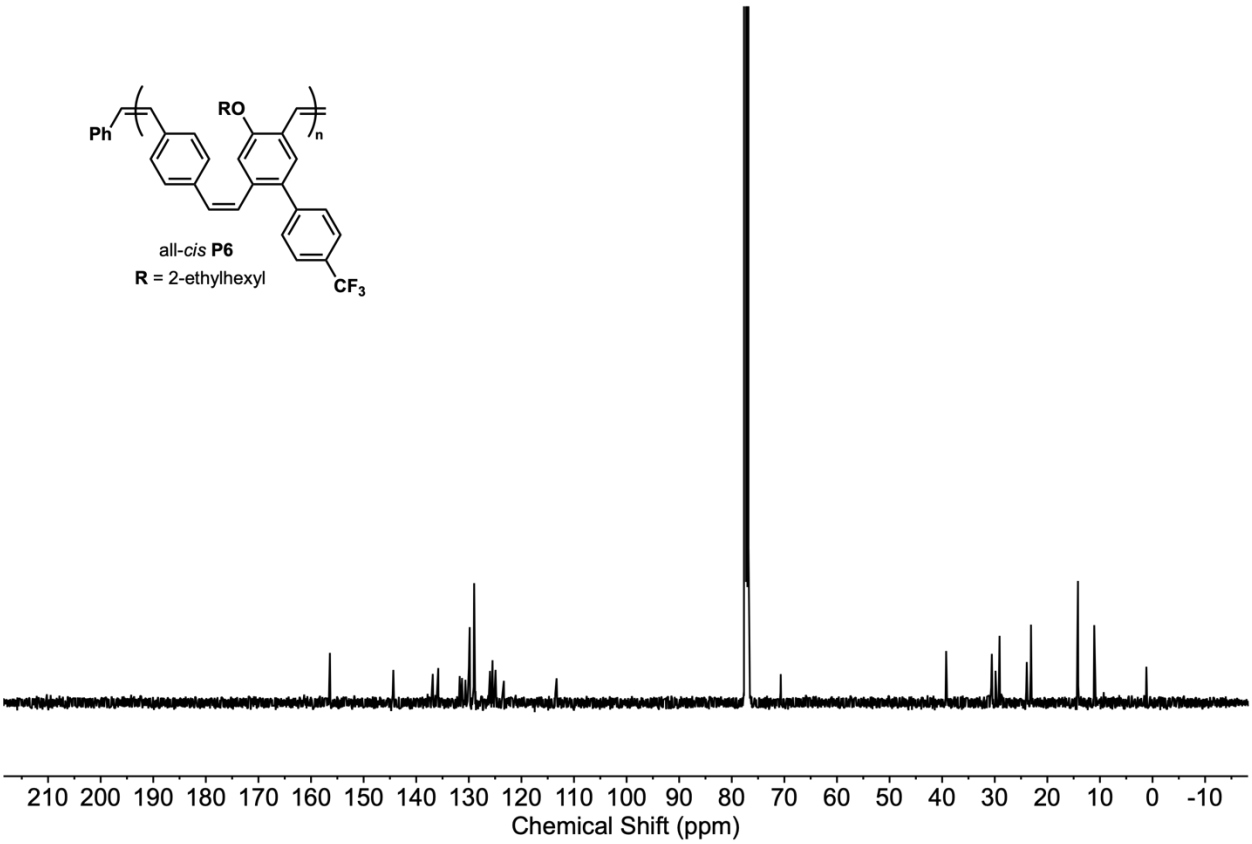

Figure S98. ^{13}C NMR (126 MHz, $CDCl_3$) spectrum of all-*cis* **P6**.

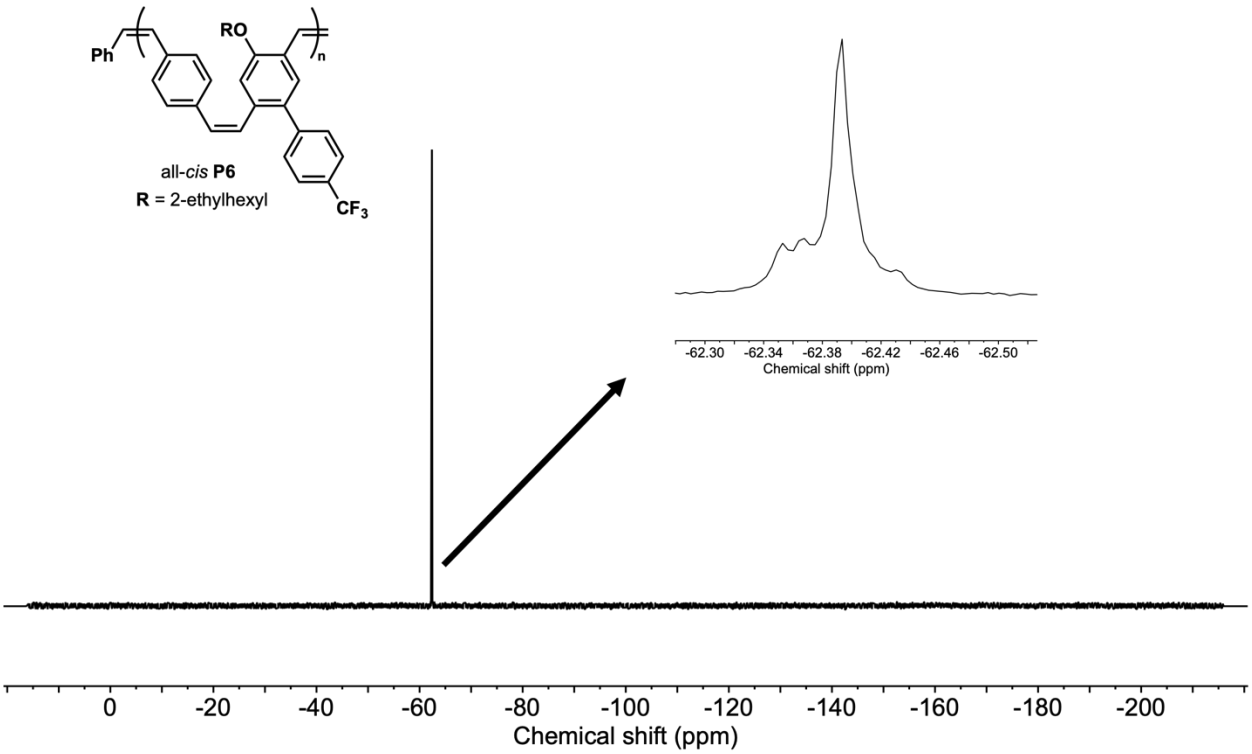

Figure S99. ^{19}F NMR (376 MHz, $CDCl_3$) spectrum of all-*cis* **P6**. Inset shows minor 19F NMR peaks indicating lack of full regioselectivity.

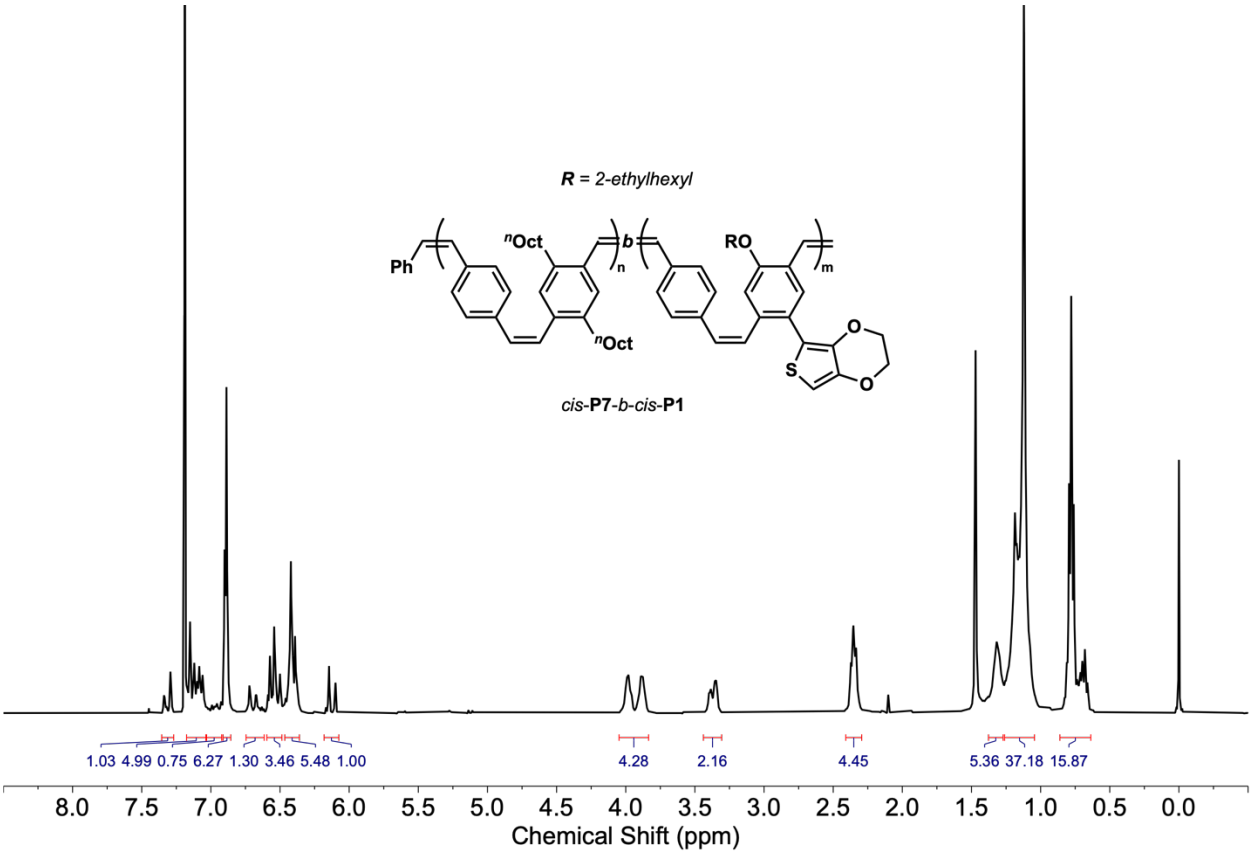

Figure S100. ^{1}H NMR (500 MHz, $CDCl_3$) spectrum of *cis*-**P7**-*b*-*cis*-**P1**.

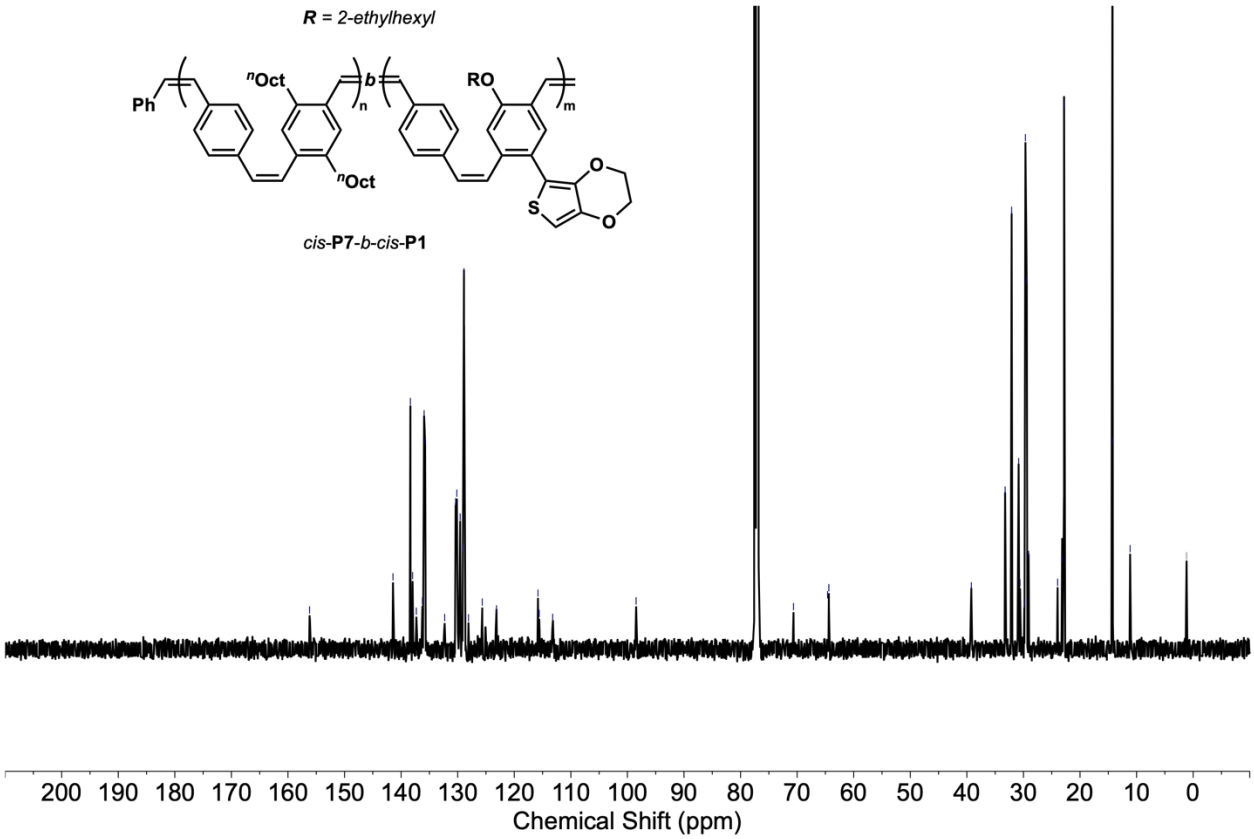

Figure S101. ^{13}C NMR (126 MHz, $CDCl_3$) spectrum of *cis*-**P7**-*b*-*cis*-**P1**.

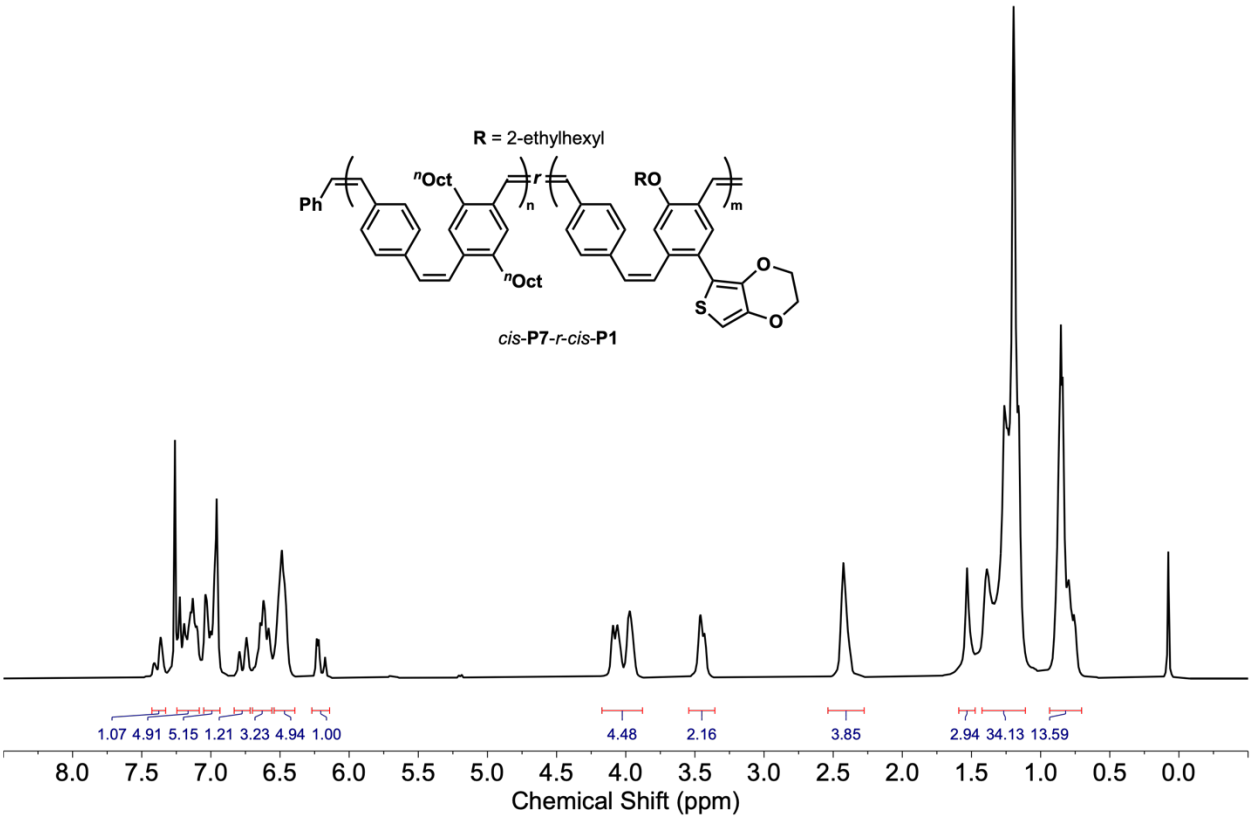

Figure S102. ^{1}H NMR (500 MHz, $CDCl_3$) spectrum of *cis*-**P7**-*r*-*cis*-**P1**.

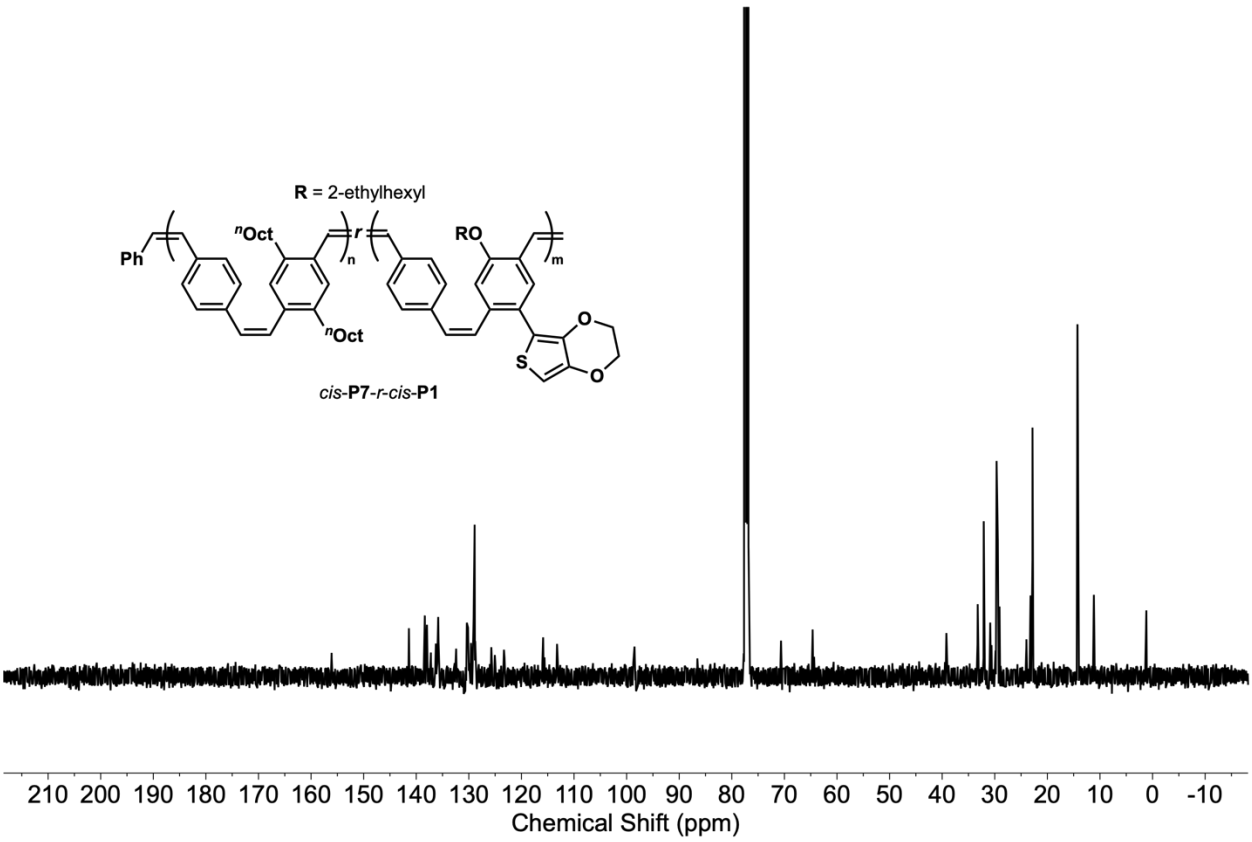

Figure S103. ^{13}C NMR (126 MHz, $CDCl_3$) spectrum of *cis*-**P7**-*r*-*cis*-**P1**.

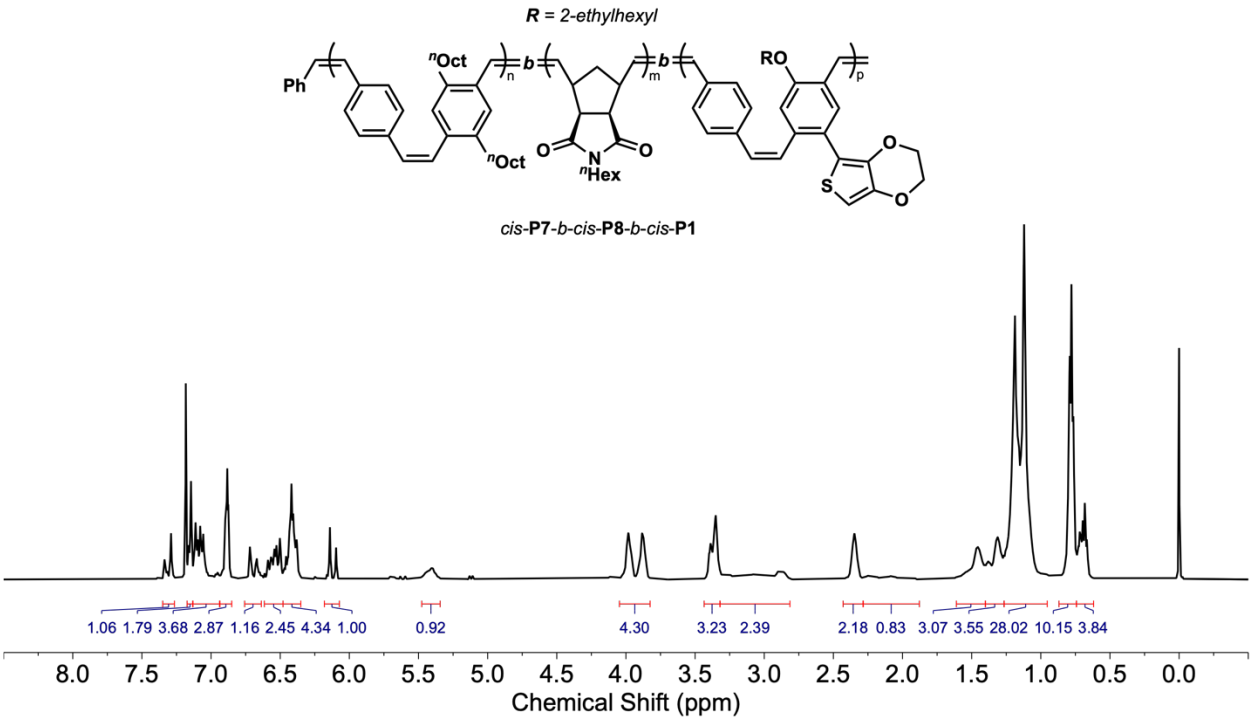

Figure S104. ^{1}H NMR (500 MHz, $CDCl_3$) spectrum of *cis*-**P7**-*b*-*cis*-**P8**-*b*-*cis*-**P1**.

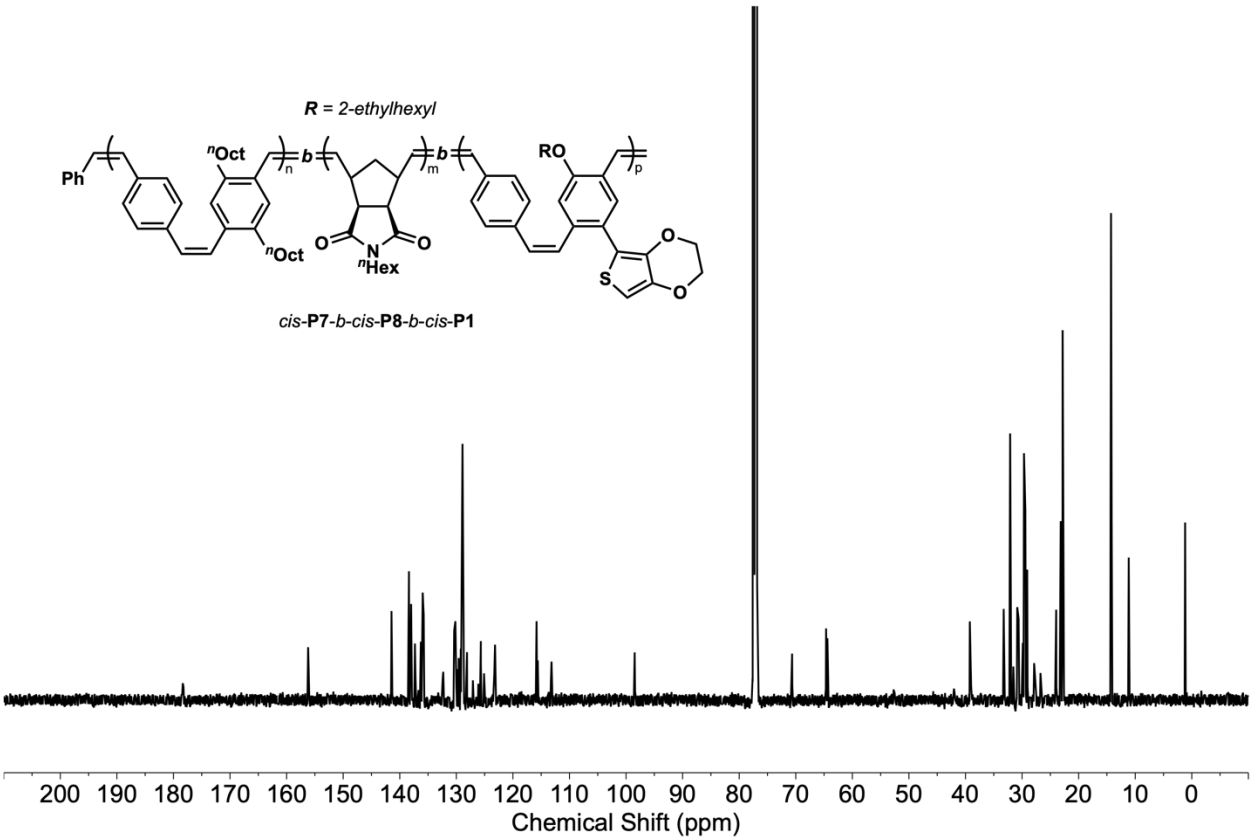

Figure S105. ^{13}C NMR (126 MHz, $CDCl_3$) spectrum of *cis*-**P1**-*b*-*cis*-**P8**-*b*-*cis*-**P1**.

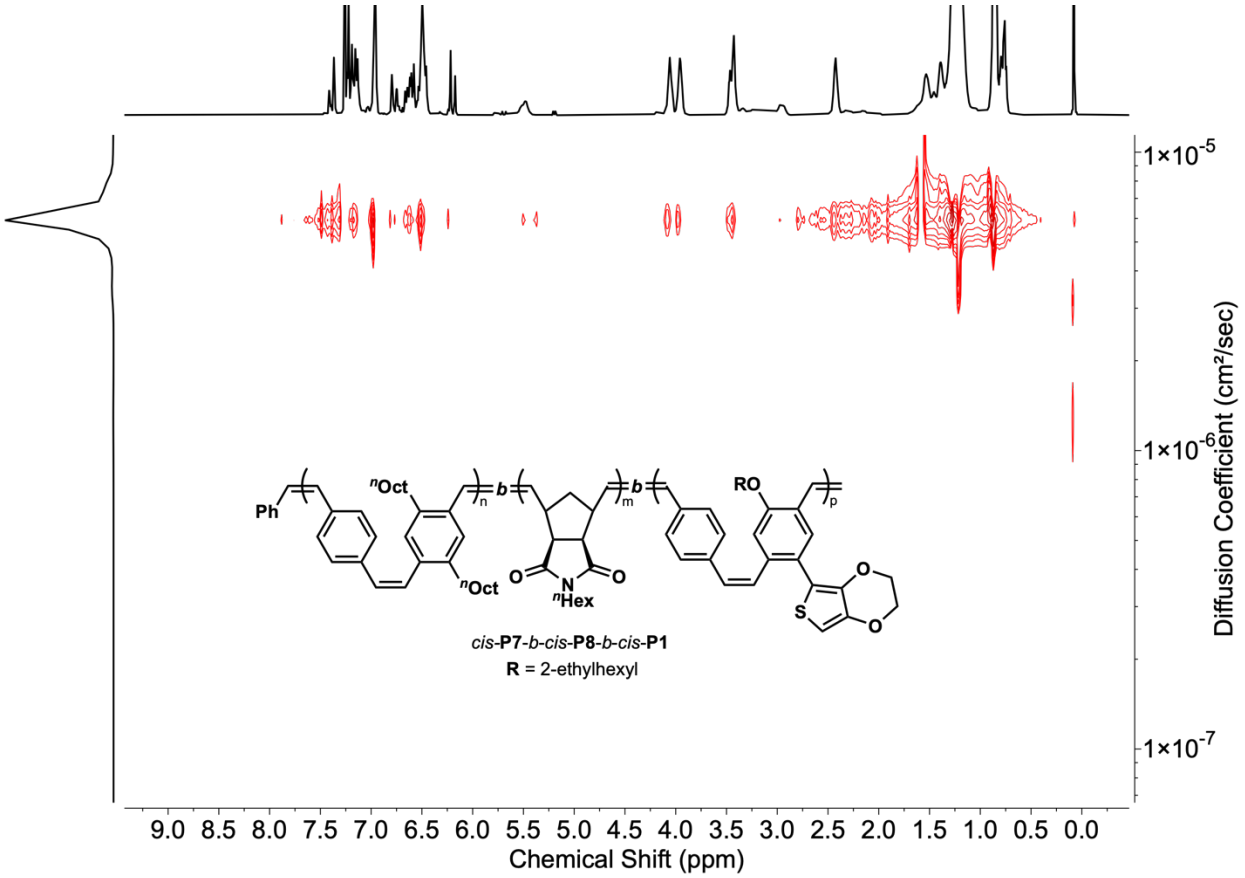

Figure S106. DOSY NMR (500 MHz, $CDCl_3$) spectrum of *cis*-**P1**-*b*-*cis*-**P8**-*b*-*cis*-**P1**.

References:

(1) Hsu, T. W.; Kim, C.; Michaudel, Q. Stereoretentive Ring-Opening Metathesis Polymerization to Access All-cis Poly(p-phenylenevinylene)s with Living Characteristics. *J. Am. Chem. Soc.* **2020**, *142* (28), 11983–11987.
(2) Mann, A.; Wang, C.; Dumlao, B. L.; Weck, M. Functionalized [2.2]Paracyclophanedienes as Monomers for Poly(p-phenylenevinylene)s. *ACS Macro Lett.* **2024**, *13* (2), 112–117.
(3) Yun Chi, H.; Bi-Hai Tong, M.; Tai-Nan Duan, C.; I-Jen Chen, H. Heteroleptic Ir(III) phosphors with bis-tridentate chelating architecture for high efficiency OLEDs. US9219237B1, 2015.
(4) Newsome, W. J.; Ayad, S.; Cordova, J.; Reinheimer, E. W.; Campiglia, A. D.; Harper, J. K.; Hanson, K.; Uribe-Romo, F. J. Solid State Multicolor Emission in Substitutional Solid Solutions of Metal–Organic Frameworks. *J. Am. Chem. Soc.* **2019**, *141* (28), 11298–11303.
(5) Hassan Omar, O.; la Gatta, S.; Tangorra, R. R.; Milano, F.; Ragni, R.; Operamolla, A.; Argazzi, R.; Chiorboli, C.; Agostiano, A.; Trotta, M.; et al. Synthetic Antenna Functioning As Light Harvester in the Whole Visible Region for Enhanced Hybrid Photosynthetic Reaction Centers. *Bioconjugate Chem.* **2016**, *27* (7), 1614–1623.
(6) Vilbrandt, N.; Gassmann, A.; von Seggern, H.; Rehahn, M. Blue-Greenish Electroluminescent Poly(p-phenylenevinylene) Developed for Organic Light-Emitting Diode Applications. *Macromolecules* **2016**, *49* (5), 1674–1680.
(7) Hsu, T.-W.; Kempel, S. J.; Michaudel, Q. All-cis poly(p-phenylene vinylene)s with high molar masses and fast photoisomerization rates obtained through stereoretentive ring-opening metathesis polymerization of [2,2]paracyclophane dienes with various aryl substituents. *J. Polym. Sci.* **2022**, *60* (3), 569–578.
(8) Hancock, S. N.; Yuntawattana, N.; Valdez, S. M.; Michaudel, Q. Expedient synthesis and ring-opening metathesis polymerization of pyridinonorbornenes. *Polym. Chem.* **2022**, *13* (39), 5530–5535.